

Slow Mg²⁺ unblock and inherent voltage dependence of NMDA receptors

by

Richard J. Clarke

Bachelor of Science, Allegheny College, 2000

Submitted to the Graduate Faculty of
Arts and Sciences in partial fulfillment
of the requirements for the degree of
Doctor of Philosophy

University of Pittsburgh

2006

UNIVERSITY OF PITTSBURGH

School of Arts and Sciences

This dissertation was presented

by

Richard J. Clarke

It was defended on

July 17, 2006

and approved by

Elias Aizenman, Ph.D.

Germán Barrionuevo, M.D.

Peter Drain, Ph.D.

Stephen Traynelis, Ph.D.

Nathan Urban, Ph.D.

Dissertation Advisor: Jon Johnson, Ph.D.

Copyright © by Richard J. Clarke

2006

Slow Mg^{2+} unblock and inherent voltage dependence of NMDA receptors

Richard J. Clarke, PhD

University of Pittsburgh, 2006

N-methyl-D-aspartate (NMDA) receptors are a subtype of ligand-gated ionotropic glutamate receptors that are involved in most fast, excitatory neuronal transmission in the mammalian central nervous system (CNS). NMDA receptor activity is crucial for normal brain function, and NMDA receptor dysregulation has been linked to a number of diseases of the CNS. There are several NMDA receptor subtypes. Each subtype has a unique temporal and spatial expression pattern, suggesting that different subtypes play different physiological roles in the CNS. Here, we have investigated how changes in membrane voltage impact the activity of various NMDA receptor subtypes in the absence and presence of the highly physiologically relevant channel blocker magnesium (Mg^{2+}). Mg^{2+} strongly blocks all NMDA receptor subtypes at, and near, typical resting membrane potentials. Only upon depolarization is Mg^{2+} block relieved. We found that, upon depolarization, NMDA receptors containing NR2C or NR2D subunits unblock Mg^{2+} very rapidly ($\tau < 1$ ms), while Mg^{2+} unblock from NMDA receptors containing the NR2A or NR2B subunit displays a prominent slow component (τ of several ms). We go on to show that the slow component of Mg^{2+} unblock from NR2A and NR2B containing NMDA receptors actually reflects inherent voltage-dependent alterations in NMDA receptor gating. In the absence of Mg^{2+} , NR2A and NR2B containing NMDA receptor currents are enhanced upon membrane depolarization. Utilizing data collected in the absence of Mg^{2+} , we developed kinetic models of NR2A and NR2B containing NMDA receptors that included inherent voltage sensitivity such that the receptors open more rapidly at positive membrane potentials. The NR2 subunit specific models reproduce experimentally recorded currents during changes in membrane voltage in both the absence and presence of Mg^{2+} . The models also reproduce several other previously described voltage-dependent characteristics of the NMDA receptor channel. Inherent voltage dependence further emphasizes the strong link between NMDA receptor activity and neuronal depolarization.

TABLE OF CONTENTS

PREFACE.....	XIII
1.0 INTRODUCTION.....	1
1.1 GLUTAMATE RECEPTOR SUBTYPE DIVERSITY	2
1.1.1 Subunit identification and genetic diversity	4
1.1.2 Subunit-dependent receptor properties.....	4
1.1.3 Regulation of subunit expression.....	5
1.1.4 Triheteromeric receptors	6
1.2 NMDA RECEPTOR STRUCTURE	7
1.2.1 Membrane topology	7
1.2.2 Extracellular domains	7
1.2.3 Transmembrane segments and ion permeation	8
1.2.4 Location of the activation gate.....	10
1.2.5 Intracellular segment.....	11
1.3 RECEPTOR ACTIVATION	12
1.3.1 Activation and deactivation of NMDA receptors.....	12
1.3.2 NMDA receptor desensitization.....	12
1.3.3 Modeling receptor activation.....	13
1.3.4 NMDA receptor gating models.....	14
1.4 VOLTAGE-DEPENDENT MODULATION OF LIGAND-GATED RECEPTORS.....	16
1.4.1 Membrane voltage and glutamate receptor activity.....	16
1.5 MAGNESIUM BLOCK AND UNBLOCK OF NMDA RECEPTORS.....	17
1.5.1 NR2 subunit differences in Mg²⁺ block.....	18
1.5.2 Kinetics of Mg²⁺ unblock	18

1.6	CHANNEL BLOCK AND NMDA RECEPTOR GATING	19
1.6.1	Interaction between blockers and gating machinery.....	19
1.6.2	Mg ²⁺ _o block and NMDA receptor gating	20
1.7	GOALS OF THIS DISSERTATION.....	21
1.7.1	NMDA receptor NR2 subunit dependence of the slow component of Mg ²⁺ _o unblock.....	21
1.7.2	Modulation of NR1/2B receptor activation by membrane voltage.	22
1.7.3	Voltage-dependent modulation of NMDA receptor activation: NR2 subunit dependence and slow Mg ²⁺ _o unblock.....	22
2.0	NMDA RECEPTOR NR2 SUBUNIT DEPENDENCE OF THE SLOW COMPONENT OF MAGNESIUM UNBLOCK.....	23
2.1	ABSTRACT.....	23
2.2	INTRODUCTION	24
2.3	MATERIALS AND METHODS	25
2.3.1	Cell culture and transfection.....	25
2.3.2	Solutions.....	26
2.3.3	Whole-cell recording.....	26
2.3.4	Data analysis and Curve Fitting	27
2.4	RESULTS	28
2.4.1	NR2 subunit identity controls Mg ²⁺ _o unblocking kinetics.....	28
2.4.2	Voltage Dependence of Slow Mg ²⁺ _o Unblock	33
2.4.3	Dependence of Mg ²⁺ _o unblocking kinetics on agonist concentration	39
2.4.4	Effect of the timing of membrane depolarization on Mg ²⁺ _o unblocking kinetics	42
2.4.5	Effect of varying the duration of depolarization on Mg ²⁺ _o unblock.....	45
2.5	DISCUSSION.....	49
2.5.1	Comparison with previous studies	49
2.5.2	Implications for synaptic plasticity	51
3.0	MODULATION OF NR1/2B RECEPTOR ACTIVATION BY MEMBRANE VOLTAGE.....	54
3.1	ABSTRACT.....	54

3.2	INTRODUCTION	54
3.3	MATERIALS AND METHODS	56
3.3.1	Cell culture and transfection.....	56
3.3.2	Solutions.....	56
3.3.3	Whole-cell recording.....	57
3.3.4	Data analysis and Curve Fitting.....	57
3.3.5	Kinetic Modeling.....	57
3.4	RESULTS	58
3.4.1	Slow development of outward currents persists in the absence of Mg^{2+}_o	58
3.4.2	Inherent voltage dependence of NR2 subunit gating.....	66
3.4.3	Voltage-dependent gating predicts slow Mg^{2+}_o unblock.....	74
3.4.4	NR1/2B currents during stimulation with AP waveforms	77
3.4.5	Voltage-dependent kinetics of NMDA-EPSCs	81
3.5	DISCUSSION.....	83
3.5.1	Voltage-dependent modulation of ligand-gated receptors	83
3.5.2	Interactions between Mg^{2+}_o and NR1/2B receptor gating.....	84
3.5.3	Impact of inherent voltage dependence on NMDA receptor mediated currents	85
4.0	INHERENCE OF NMDA RECEPTOR ACTIVATION: NR2 SUBUNIT DEPENDENCE AND SLOW MAGNESIUM UNBLOCK	87
4.1	ABSTRACT.....	87
4.2	INTRODUCTION	88
4.3	MATERIALS AND METHODS	89
4.3.1	Cell culture and transfection.....	89
4.3.2	Solutions.....	90
4.3.3	Whole-cell recording.....	90
4.3.4	Data analysis and Curve Fitting.....	90
4.3.5	Kinetic Modeling.....	91
4.4	RESULTS	91

4.4.1	NR1/2A receptor currents are enhanced at positive membrane potentials	91
4.4.2	Model of inherent voltage dependence of NR1/2A receptors.....	96
4.4.3	Kinetics of slow relaxation of NR1/2A currents.....	101
4.4.4	Mg ²⁺ _o unblock and desensitization	104
4.5	DISCUSSION.....	107
4.5.1	Inherent voltage dependence of NMDA receptors.....	107
4.5.2	Desensitization and Mg ²⁺ _o unblock.....	108
4.5.3	Functional implications for synaptic currents	109
5.0	GENERAL DISCUSSION	112
5.1	SLOW UNBLOCK VERSUS SLOW POTENTIALIAION.....	112
5.2	INTERACTIONS BETWEEN BLOCKERS AND CHANNEL GATING	114
5.3	MUTATIONS INFLUENCING VOLTAGE DEPENDENT CHARACTERISTICS	118
5.3.1	Voltage dependence and permeant ions.....	120
5.3.2	Gating associated movement of charged amino acids	121
5.4	VOLTAGE DEPENDENT ENHANCEMENT OF NMDA RECEPTOR CURRENTS	123
5.5	PHYSIOLOGICAL ROLES OF NMDA RECEPTOR SUBTYPES.....	126
5.5.1	The role of NMDA receptors as coincidence detectors.....	126
5.5.2	Differential roles of NR1/2A and NR1/2B receptors in synaptic plasticity	127
5.5.3	The physiological significance of low Mg ²⁺ _o affinity	130
5.6	SIGNALING VIA SYNAPTIC AND EXTRASYNAPTIC NMDA RECEPTORS.....	133
5.7	THE PESKY TRIHETEROMERIC CHANNELS	134
5.8	GENERAL CONCLUSIONS	136
	BIBLIOGRAPHY.....	138

LIST OF TABLES

Table 1. Depolarization induced current relaxations in the presence of 30 μM NMDA and 10 μM glycine in the absence and presence of Mg^{2+}	34
Table 2. Depolarization induced current relaxations in the presence of high agonist concentrations and the absence and presence of 1 mM Mg^{2+}	41
Table 3. Depolarization-induced current relaxations in the presence of 30 μM NMDA and 10 μM glycine in the absence and presence of Mg^{2+}	61
Table 4. Kinetics of depolarization induced current relaxations are not influence by changes in permeant ions	65
Table 5. Rates used for NR1/2B receptor model fitting and current simulations.....	67
Table 6. Depolarization induced current relaxations in 0 and 1 mM Mg^{2+}	95
Table 7. Rates used for NR1/2A receptor model fitting and current simulations.....	100
Table 8. Current relaxations following rapid depolarizing voltage steps.....	117

LIST OF FIGURES

Figure 1. Development of patch clamp recording techniques allowed visualization of single-channel currents.	3
Figure 2. Schematic of NMDA receptor subunit topology.....	9
Figure 3. Historical mechanisms proposed to describe ion channel activation.	15
Figure 4. Protocol used to investigate the kinetics of Mg^{2+} unblock from recombinant NMDA receptors during steady-state response.....	29
Figure 5. The kinetics of Mg^{2+} unblock are NR2 subunit dependent.....	32
Figure 6. Mg^{2+} unblocks rapidly from NR1/2D receptors even at high $[Mg^{2+}]_o$	35
Figure 7. Quantification of the subunit and voltage dependence of Mg^{2+} unblocking kinetics.	37
Figure 8. Slow reblock of Mg^{2+}	38
Figure 9. Kinetics of Mg^{2+} unblock in high agonist concentration.	40
Figure 10. Mg^{2+} unblock near the time of onset of NMDA receptor activity.	44
Figure 11. Brief depolarizations are more effective at stimulating Mg^{2+} unblock from NR1/2A than from NR1/2B receptors.....	48
Figure 12. NR1/2B receptor currents display a prominent slow relaxation in both the absence and presence of Mg^{2+} in response to membrane depolarization.....	60
Figure 13. Tail currents following repolarization are sensitive to the amplitude of the initial depolarization.....	62
Figure 14. NR1/2B receptor currents are equally sensitive to membrane voltage in normal and symmetric KCl solutions.....	64
Figure 15. Kinetic scheme used to model NR1/2B receptor activation.....	67

Figure 16. Models containing voltage dependence of the conformational change associated with either the NR1 or NR2 subunit predict a slow component of current relaxation in response to depolarization.....	69
Figure 17. Slow current relaxation in response to depolarization can be reproduced with a model containing voltage dependence of NR2B subunit gating.....	71
Figure 18. Voltage dependent modification of k_s predicts slightly slower kinetics of current relaxation in response to membrane depolarization.....	73
Figure 19. NR1/2B Model accurately predicts the kinetics of Mg^{2+}_o unblock in response to depolarization.....	76
Figure 20. The NR1/2B Model reproduced NR1/2B receptor currents during a complex voltage paradigm.	78
Figure 21. Inherent voltage dependence does not enhance NR1/2B receptor currents in response to depolarizations by AP waveforms.	80
Figure 22. The NR1/2B Model predicts a small increase in the decay of synaptic-like NR1/2B receptor currents at depolarized membrane potentials.....	82
Figure 23. NR1/2A receptor currents display a slow component of relaxation in response to depolarization in both 0 and 1 mM Mg^{2+}_o	94
Figure 24. Tail currents following return to -65 mV from several depolarized voltages.	97
Figure 25. Depolarization induced slow relaxation can be reproduced by a model containing inherent voltage dependence of NR1/2A receptor activation.	99
Figure 26. Slow Mg^{2+}_o unblock can be explained by voltage dependent gating of NR1/2A receptors.....	102
Figure 27. NR2 subunit specific gating kinetics lead to differences in Mg^{2+}_o unblocking kinetics.	103
Figure 28. Depolarization induced inward currents do not depend on the timing between receptor activation and membrane depolarization.	106
Figure 29. Decay of NR1//2A synaptic-like current simulations is only modestly influenced by membrane voltage.	111
Figure 30. NR1/2D receptor currents do not display a slow component in response to depolarization in 0 Mg^{2+}_o	113

Figure 31. Following a rapid depolarizing step, unblock of amantadine contains a prominent slow component.	116
Figure 32. Elimination of slow Mg^{2+}_o unblock by a single amino acid substitution.	119
Figure 33. Elimination of free extracellular Ca^{2+} does not have a large impact on NR1/2B receptor current response to depolarization.	122
Figure 34. NR1/2B Model simulations in response to AP waveforms of varying duration.	124
Figure 35. NR1/2A receptors are better equipped to act as coincidence detectors than NR1/2D receptors.	128
Figure 36. Voltage-dependent increase of simulated NMDA-EPSCs is NR2 subunit dependent.	131
Figure 37. Mg^{2+}_o unblocking kinetics may differ between synaptic and extrasynaptic NMDA receptors.	135

PREFACE

The Center for Neuroscience at the University of Pittsburgh has provided me with an incredibly rich and diverse training environment. Over the past 5 years I have had the pleasure of working within a large community of outstanding graduate students, faculty, and staff who have all enriched both my academic and person life. In particular, I would like to thank the members of the Johnson lab, past and present, for being generous with their time, advice and friendship.

I feel very fortunate to have been guided throughout my dissertation work by a tremendous committee. Elias Aizenman, Germán Barrionuevo, and Peter Drain have all provided me with excellent advice and guidance as I moved towards the end of my dissertation work. I would especially like to thank Nathan Urban, the chair of my committee. Nathan has provided me with many insightful and useful comments while working hard to make sure I was always moving forward in a positive direction.

I am, of course, most indebted to Jon Johnson, my thesis advisor. Jon is truly one of the most brilliant scientists that I have had the pleasure to work with and I hope to have many fruitful interactions with him during my post-doctoral work and beyond. I value his advice and friendship in the highest regard.

I would also like to thank my parents for their unwavering support and love. Finally, I would like to thank my wonderful wife Shauna. She has been my biggest supporter, fan, and sometimes motivational speaker. I am eternally indebted to her and I hope that she has learned from me a small fraction of that which I have learned from her over the past 5 years.

1.0 INTRODUCTION

Cell to cell communication within the central nervous system (CNS) drives such vast behaviors as a simple smile to the complex motions of a concert pianist. At the heart of neuronal communication lie ion channels. Ion channels are evolutionarily ancient proteins found throughout all life, from the simplest bacteria to humans. Through millions of years of evolution a dizzying array of ion channel subtypes have emerged, each shaped to serve specific physiological functions.

It is now well recognized that one of the key physiological functions of ion channels in vertebrates is to help mediate synaptic transmission in the CNS. However, many of the mechanisms underlying signaling between neurons were known in advance of any compelling evidence for the existence of ion channel proteins. In the late 1800's, Sydney Ringer performed a series of experiments which showed that various ions in solution, in particular calcium (Ca^{2+}) and potassium (K^+), are imperative in maintaining the normal rhythm of an isolated frog heart. A short time later, Julius Bernstein proposed the "membrane hypothesis", which explained membrane excitability by suggesting that during periods of activity, the cell membrane would breakdown, allowing ions to flow down their concentration gradients. Although Bernstein's membrane hypothesis explained both the resting membrane potential and the generation of action potentials (APs), it proved not to be entirely correct. In a series of classic experiments, Hodgkin and Huxley showed that APs were generated not by a breakdown of the cell membrane, but by changes in selective K^+ and sodium (Na^+) conductances (Hodgkin and Huxley, 1952c, 1952d, 1952b, 1952a). Although Hodgkin and Huxley had no direct evidence that these conductances were mediated by ion channels, they had the incredible foresight to describe the K^+ and Na^+ conductances in terms of voltage dependent gates.

Following the pioneering work of Hodgkin and Huxley, evidence continued to build in support of the existence of ion channels. For example, noise analysis provided estimates of the

single channel conductances underlying currents measured in response to application of acetylcholine to the neuromuscular junction (Katz and Miledi, 1972). However, it was not until the development of high resolution patch-clamp recordings by Erwin Neher and Bert Sakmann that currents through single ion channels could be measured directly (**Fig. 1**). The development, and further refinement, of patch-clamp recording techniques has led to the discovery and characterization of a multitude of channels types throughout the CNS.

Ion channels can be activated by a wide variety of stimuli, including changes in membrane voltage and binding of ligands. Ion channel activation leads to the opening of a pore extending across the cell membrane, which allows ions to flow down their electro-chemical gradient. Remarkably, ion passage through an open channel pore can reach rates of $>10^7$ ions per second.

The work presented in this dissertation focuses on one type of ion channel, the *N*-methyl-D-aspartate (NMDA) receptor. NMDA receptors are a subtype of glutamate receptor that are critically involved in a host of physiological processes, and NMDA receptor dysfunction has been implicated in several diseases (Dingledine et al., 1999; Cull-Candy et al., 2001). The research presented in this dissertation is intended to extend the knowledge of NMDA receptor activation and block, focusing on how these properties differ in a number of NMDA receptor subtypes.

1.1 GLUTAMATE RECEPTOR SUBTYPE DIVERSITY

In the late 1950's and early 1960's, the role of glutamate as a neurotransmitter was uncertain. It had been reported that application of glutamate produced neuronal excitation (Hayashi, 1954; Curtis et al., 1960), but it was unclear if glutamate acted via specific receptor systems or had a nonspecific effect on neurons. The development of specific agonists and antagonists finally provided compelling evidence that glutamate was indeed a neurotransmitter, and operated via recognition by multiple receptor types (McCulloch et al., 1974; Evans et al., 1979). Initially, the terms NMDA and non-NMDA receptors were suggested (Watkins and Evans, 1981), based on selective activation of a subset of glutamate receptors by the synthetic molecule NMDA. Later identification of additional subtype specific agonists led to the segmentation of the non-NMDA

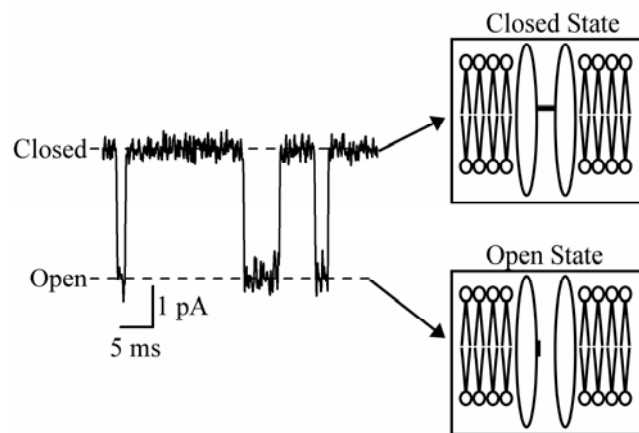


Figure 1. Development of patch clamp recording techniques allowed visualization of single-channel currents. Examples of NR1/2B receptor single-channel current traces (left) recorded at a membrane potential of -65 mV. Channel openings were elicited by application of 10 μ M glutamate and 30 μ M glycine in 0 Mg^{2+} . Downward current deflections reflect the channel moving from a closed state, in which the activation gate is closed, to an open state, in which the activation gate is open.

group into kainate and quisqualate (eventually α -amino-3-hydroxy-5-methyl-4-isoxazole propionate (AMPA)) types.

1.1.1 Subunit identification and genetic diversity

A new era of research on glutamate receptors began in the late 1980's and early 1990's with the cloning of the first glutamate receptor cDNAs (reviewed in Hollmann and Heinemann, 1994). The initial cloning results showed that the three glutamate receptor subtypes, previously classified based on subtype specific agonists (AMPA, NMDA, and kainate), were actually encoded by several gene families.

The NMDA receptor subtype alone is encoded by seven genes. The seven genes can be divided into three subunit classes, termed NR1, NR2, and NR3. In the CNS, functional NMDA receptors heteromeric proteins and must, at minimum, contain both NR1 and NR2 subunits (Moriyoshi et al., 1991; Kutsuwada et al., 1992; Ishii et al., 1993). The most recent evidence suggests that NMDA receptors are tetramers, containing two NR1 and two NR2 subunits (Schorge and Colquhoun, 2003; Furukawa et al., 2005).

The two NR3 subunit isoforms, NR3A and NR3B, have more recently been discovered (Ciabarra et al., 1995; Nishi et al., 2001). Incorporation of the NR3 subunit into a functional NMDA receptor reduces the single channel conductance and Ca^{2+} permeability of the receptor (Perez-Otano et al., 2001; Matsuda et al., 2002; Matsuda et al., 2003). There remains much to be learned about the physiological role of the NR3 subunit. However, the NR3 subunit will not be considered further in this dissertation.

1.1.2 Subunit-dependent receptor properties

The NR1 subunit is encoded by a single gene that displays extensive alternative splicing. One exon near the N-terminus (exon 5) and two exons near the C-terminus (exons 21 and 22) can be alternatively spliced. The alternative splicing leads to 8 NR1 subunit isoforms, termed NR1-1a through NR1-4b based on the nomenclature proposed by Hollmann and colleagues (Hollmann et al., 1993). Experiments utilizing heterologous expression of recombinant NMDA receptors have

shown that the identity of the NR1 subunit can influence many receptor properties, including sensitivity to inhibition by zinc (Zn^{2+}) and protons (Traynelis et al., 1995; Traynelis et al., 1998).

In contrast to the NR1 subunit, the NR2 subunit is encoded by 4 genes termed NR2A through NR2D. The identity of the NR2 subunit within a functional NMDA receptor has a profound influence on many receptor properties. The list of biophysical and pharmacological receptor properties that are NR2 subunit dependent is long and ranges from agonist affinity to Ca^{2+} permeability. In many cases, NMDA receptors containing

NR2 subunit confers unique characteristics to a functional NMDA receptor. However, there are several properties that are similar in NR2A and NR2B containing NMDA receptors (termed here NR1/2A and NR1/2B receptors, respectively). Likewise, NR1/2C and NR1/2D receptors share several similar properties, which differ significantly from those displayed by NR1/2A and NR1/2B receptors. For example, NR1/2A and NR1/2B receptors have a higher single channel conductance than NR1/2C and NR1/2D receptors (Stern et al., 1992; Wyllie et al., 1996). Ca^{2+} permeability of NR1/2A and NR1/2B receptors is indistinguishable, while Ca^{2+} permeability of NR1/2C receptors is significantly lower (Burnashev et al., 1995). Finally, NR1/2A and NR1/2B receptors have a higher affinity for extracellular magnesium (Mg^{2+}) than NR1/2C and NR1/2D receptors (Monyer et al., 1994; Kuner and Schoepfer, 1996; Qian et al., 2005).

1.1.3 Regulation of subunit expression

Given the important roles the various NR1 and NR2 subunits play in determining many receptor properties, it seems likely that NMDA receptors containing various combinations of NR1 and NR2 subunits have specialized roles within the CNS. This notion is supported by the tight spatial and temporal regulation of NR2 subunit expression. NR1 subunit isoforms also display some differential regional expression (Laurie and Seeburg, 1994; Laurie et al., 1995). However, much more attention has been paid to the physiological significance of both developmental and regional differences in NR2 subunit expression.

Early in development, expression of the NR2B and NR2D subunits is high throughout the CNS, while the NR2A and NR2C subunits show little to no expression (Ikeda et al., 1992; Monyer et al., 1994). As development proceeds, changes in NR2 subunit expression are brain-

region and cell-type specific. For example, NR2B subunit expression in the cortex decreases as the animal ages, while expression levels of the NR2A subunit rise sharply (Ikeda et al., 1992; Monyer et al., 1994). In the cerebellum, a switch in expression from NR2B to NR2C subunits in granule cells occurs several weeks after birth (Ikeda et al., 1992). NR2 subunit expression also differs in individual brain regions. Expression levels of NR2A and NR2B subunits are high in pyramidal cells in the hippocampus, while hippocampal interneurons have higher expression levels of the NR2C and NR2D subunits (Monyer et al., 1994; Standaert et al., 1996; Avignone et al., 2005).

Differential NR2 subunit expression has also been reported within individual cells. NMDA receptors on layer 5 cortical pyramidal neurons display NR2 subunit specific trafficking to synapses based on the origin of the presynaptic partner. Intracortical synapses are enriched in NR1/2B receptors, while synapses arising from commissural connections contain mostly NR1/2A receptors (Kumar and Huguenard, 2003). NR2 subunit specific trafficking of NR1/2A and NR1/2B receptors has also been reported in principal cells (Ito et al., 1997; Ito et al., 2000) and interneurons (Toth and McBain, 1998) of the hippocampus. Differential distribution of NR2 subunits has also been described between synaptic and extrasynaptic sites. In the mature hippocampus, NR1/2A receptors tend to cluster at sites of synaptic contact while NR1/2B receptors are more common at extrasynaptic sites (Li et al., 1998; Tovar and Westbrook, 1999).

1.1.4 Triheteromeric receptors

While it is easy to classify NMDA receptors as containing one type of NR1 subunit along with one type of NR2 subunit, this is probably not the case for all native NMDA receptors. There is ample evidence to suggest that many native NMDA receptors in the cortex and hippocampus are actually triheteromeric receptors, containing NR1, NR2A and NR2B subunit types (Sheng et al., 1994; Chazot and Stephenson, 1997; Luo et al., 1997; Tovar and Westbrook, 1999). Strong evidence also exists for the expression of NR1/2A/2C and NR1/2B/2C receptors in the cerebellum (Chazot et al., 1994; Cathala et al., 2000). Finally, NR1/2B/2D receptors have been found at extrasynaptic sites within cerebellar Golgi cells (Brickley et al., 2003) and are expressed by neurons of the substantia nigra (Jones and Gibb, 2005). Mixing of NR2 subunits, and

presumably NR1 subunit splice variants, in a single NMDA receptor greatly increases the potential number of receptor types and functional diversity. Even though this additional level of NMDA receptor diversity may be important for CNS physiology, little is known about the biophysical and pharmacological characteristics of triheteromeric NMDA receptors, although recent work has begun to characterize NR1/2A/2B triheteromeric receptors (Hatton and Paoletti, 2005).

1.2 NMDA RECEPTOR STRUCTURE

1.2.1 Membrane topology

NR1 and NR2 subunits share a common membrane topology. Starting with an extracellular N-terminus, there is a single membrane spanning domain (TM1), followed by a re-entrant P-loop, two additional membrane spanning domains (TM3 and TM4), and finally an intracellular C-terminus (**Fig. 2**). The membrane topology of NMDA receptors more closely resembles that of K⁺ channels as opposed to the cys-loop family of receptors, to which many ligand-gated ion channels belong. Substantial evidence exists to support an evolutionary link between glutamate receptors and K⁺ channels, including the characterization of GluR0, a glutamate-gated potassium selective channel (Chen et al., 1999a). The wealth of biophysical and structural information on K⁺ channels has proved very useful in directing the study of NMDA receptors.

1.2.2 Extracellular domains

Near the extracellular N-terminus, a section of the NMDA receptor protein shares significant homology with a bacterial periplasmic leucine/isoleucine/valine-binding protein (LIVBP) (O'Hara et al., 1993). The LIVBP-like domain binds extracellular modulators, which alter NMDA receptor function (**Fig. 2**). In NR1/2A receptors, the LIVBP-like domain binds Zn²⁺ with very high-affinity (Fayyazuddin et al., 2000; Low et al., 2000; Paoletti et al., 2000). In NR1/2B receptors, ifenprodil binds to the LIVBP-like domain with high-affinity (Zheng et al.,

2001). Once bound, Zn^{2+} and ifenprodil inhibit NR1/2A and NR1/2B receptors, respectively, via allosteric mechanisms (Kew and Kemp, 1998; Zheng et al., 2001; Erreger and Traynelis, 2005).

The ligand binding domain also lies within the extracellular space. The ligand binding domain is formed by two sections of the protein, termed S1 and S2 (**Fig. 2**). S1 is formed by a segment preceding TM1, while S2 is formed by a segment of the TM3-TM4 linker. Activation of NMDA receptors requires not only glutamate binding, but binding of the co-agonist glycine as well (Johnson and Ascher, 1987; Kleckner and Dingledine, 1988). Glycine binds to the NR1 subunit and glutamate binds to the NR2 subunit. Recent x-ray crystallography studies of AMPA (Armstrong et al., 1998) and NMDA (Furukawa and Gouaux, 2003; Furukawa et al., 2005) receptors have shown that the ligand binding domains adopt a clamshell like structure. In the unbound, or apo, state the clamshell is open, with a large degree of separation between the S1 and S2 domains. Ligand binding results in domain closure, bringing S1 and S2 closer together. In AMPA receptors the efficacy of the agonist correlates well with the degree of domain closure, with full agonists causing a greater degree of domain closure than partial agonists (Jin et al., 2003; Jin and Gouaux, 2003). However, binding of full and partial agonists at the NR1 glycine binding site all induce the same degree of domain closure (Inanobe et al., 2005), suggesting that a different mechanism leads to partial agonist action at NMDA as compared to AMPA receptors.

1.2.3 Transmembrane segments and ion permeation

Great strides in the understanding of ligand binding have been made using x-ray crystallographic techniques. Unfortunately, these techniques have yet to be successfully applied to the full length NMDA receptor, leaving the exact structure of the transmembrane segments unknown. Still, a wealth of biophysical data has provided information regarding the molecular determinants of channel activation and ion permeation.

The pore of NMDA receptors contains a large extracellular and a large intracellular vestibule, connected by a narrow constriction. The re-entrant P-loop is a critical component of the ion permeation pathway, lining the intracellular vestibule and forming the narrow constriction of the channel (Kuner et al., 1996). In contrast, the extracellular vestibule is composed of residues located on many parts of the protein, including M1, M3 and M4 (Beck et al., 1999).

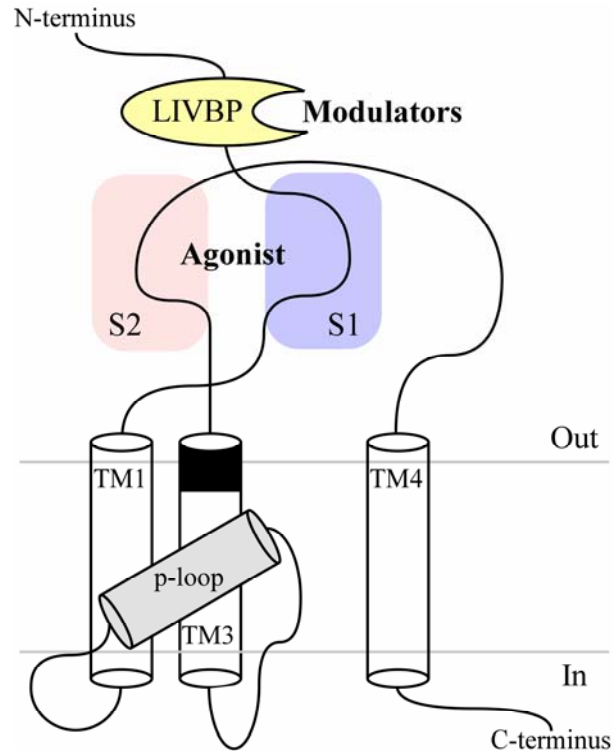


Figure 2. Schematic of NMDA receptor subunit topology. NR1 and NR2 subunits share a similar membrane topology. A region near the N-terminus in the extracellular space has been shown to share significant sequence homology with a bacterial periplasmic leucine/isoleucine/valine-binding protein (LIVBP). Allosteric modulators, such as Zn^{2+} (NR2A) and ifenprodil (NR2B), bind to the LIVBP-like domain (shown in yellow). Two domains (S1, blue and S2, pink) form a clamshell-like pocket which binds the endogenous ligands glycine (NR1) and glutamate (NR2). A re-entrant P-loop, often referred to as M2, connects the first and third transmembrane domains. The P-loop lines most of the NMDA receptor channel pore and combines with the P-loops from other subunits to create the site at which Mg^{2+} binds during channel block. The intracellular C-terminus varies in length depending on the subunit. In all subunits, the C-terminal tail mediates important interactions with many proteins, including signaling molecules such as CAMKII and scaffolding proteins such as PSD-95.

All glutamate receptors are permeable to cations and for the most part exclude anions from the pore. While the permeability of Na^+ and K^+ is thought to be nearly identical, one characteristic feature of NMDA receptors is an extremely high permeability to Ca^{2+} . Ca^{2+} is important for intracellular signaling and Ca^{2+} influx via NMDA receptors can activate a host of signaling pathways in neurons. All NMDA receptor subtypes have a much higher Ca^{2+} permeability than the AMPA or kainate subtypes of glutamate receptors (Burnashev et al., 1995; Wollmuth and Sakmann, 1998). However, Ca^{2+} permeability is not equivalent in all NMDA receptor subtypes: NR1/2A and NR1/2B receptors display higher fractional Ca^{2+} currents than NR1/2C receptors (Burnashev et al., 1995). The fractional Ca^{2+} current through NR1/2D receptors has not been measured, but based on many other receptor properties, it is likely to be close to that measured through NR1/2C receptors.

In NMDA receptors, an asparagine residue located at the tip of the P-loop, termed the N-site, plays a critical role in Ca^{2+} permeability. Mutation of the N-site asparagine greatly reduces the Ca^{2+} permeability of NMDA receptors (Burnashev et al., 1992). Although critical, the N-site is not the sole determinant of Ca^{2+} permeability. Evidence suggests that NMDA receptors contain several Ca^{2+} binding sites that cooperate to enhance Ca^{2+} flux through the receptor (Premkumar and Auerbach, 1996; Sharma and Stevens, 1996). The N-site probably contributes to a deep binding site for Ca^{2+} . A more external Ca^{2+} binding site is also formed by a string of charged amino acids (DRPEER) located at the C-terminal end of the NR1 subunit M3 segment (Watanabe et al., 2002). The multiple Ca^{2+} binding sites cause Ca^{2+} to pause in the channel as it permeates, resulting in a lower single channel conductance in the presence of high Ca^{2+} concentrations (Jahr and Stevens, 1987; Ascher and Nowak, 1988; Gibb and Colquhoun, 1992). There are also several other permeant ion binding sites located on the NMDA receptor. Occupation of these binding sites has been shown to greatly impact receptor characteristics, including block by Mg^{2+} (Antonov and Johnson, 1999; Zhu and Auerbach, 2001a, 2001b; Qian and Johnson, 2002).

1.2.4 Location of the activation gate

While many properties of the ion permeation pathway have been elucidated, the location of the activation gate remains a topic of controversy. Several lines of evidence suggest that the external

segments of the NMDA receptor channel undergo gating associated conformational changes (for review, see (Qian and Johnson, 2002)). However, these data do not remove the possibility that the conformational change that occludes ion flow occurs deep within the channel pore. Experiments utilizing the Substituted Cysteine Accessibility Method (SCAM) have placed the activation gate near the tip of the re-entrant P-loop (Wollmuth and Sobolevsky, 2004).

Regardless of the exact location of the activation gate, a linkage mechanism must be in place to translate ligand binding in the extracellular space to conformational changes leading to opening of the activation gate. The current working model of NMDA receptor activation proposes that closure of the ligand binding clamshell places tension on some portion of the protein which leads to opening of the activation gate (Mayer and Armstrong, 2004). Several lines of evidence suggest that a highly conserved motif (SYTANLAAF) near the external end of the M3 segment plays a critical role in linking agonist binding to channel gating (**Fig. 2**). Mutations within the SYTANLAAF region result in channels which can remain open after removal of agonist (Kashiwagi et al., 2002), or have altered deactivation kinetics (Kohda et al., 2000). Experiments utilizing SCAM have provided evidence that the SYTANLAAF region undergoes gating associated conformational changes (Jones et al., 2002; Yuan et al., 2005). These data support the hypothesis that the M3 domain is critically involved in linking agonist binding and channel activation.

1.2.5 Intracellular segment

NMDA receptor activation leads to Ca^{2+} influx, which in turn activates a host of intracellular signaling pathways. The intracellular C-terminus mediates interactions between the NMDA receptor and a large number of intracellular proteins (Husi et al., 2000). Several kinases have been shown to interact directly with the NMDA receptor C-terminus, including Src (Yu et al., 1997) and CAMKII (Strack and Colbran, 1998). The C-terminus of each NR2 subunit ends in a consensus sequence that binds PDZ containing proteins, such as PSD-95 and SAP-102 (Sheng, 2001). The interaction between the NMDA receptor and PDZ containing proteins is critical for both the synaptic clustering of NMDA receptors (Mori et al., 1998; Steigerwald et al., 2000) and the coupling of NMDA receptors with intracellular signaling pathways (Sprengel et al., 1998; Kohr et al., 2003).

1.3 RECEPTOR ACTIVATION

1.3.1 Activation and deactivation of NMDA receptors

Ligand-gated receptors are activated upon binding of agonists. As mentioned above, NMDA receptor activation requires binding of the co-agonists glutamate and glycine. The activation and deactivation kinetics of NMDA receptors are much slower than AMPA and kainate receptors. Across NMDA receptor subtypes, activation and deactivation kinetics are also NR2 subunit dependent. NR1/2A receptors display the fastest activation and deactivation kinetics, while NR1/2D receptors display the slowest (Monyer et al., 1992; Vicini et al., 1998; Wyllie et al., 1998; Erreger et al., 2005). Remarkably, the time constant of NR1/2D receptor deactivation is well over 1 second, while NR1/2A receptor deactivation occurs in tens of ms (Monyer et al., 1994; Vicini et al., 1998; Wyllie et al., 1998).

1.3.2 NMDA receptor desensitization

NMDA receptors display many forms of desensitization, which is defined as the reduction of current in the continuous presence of agonists (Dingledine et al., 1999). They include Ca^{2+} -dependent, glycine-dependent, and the ill-defined glycine-independent desensitization. Ca^{2+} -dependent desensitization, also termed Ca^{2+} -dependent inactivation, is due to elevation of intracellular Ca^{2+} (Clark et al., 1990; Legendre et al., 1993; Rosenmund and Westbrook, 1993b, 1993a). Elevation of intracellular Ca^{2+} causes dissociation of the NMDA receptor from the cytoskeleton (Rosenmund and Westbrook, 1993b), which, in turn, causes a reduction in the open probability (P_{open}) of the receptor (Legendre et al., 1993). The NR1 C-terminus mediates several interactions that are critical for Ca^{2+} -dependent inactivation (Zhang et al., 1998; Krupp et al., 1999). Ca^{2+} -dependent inactivation is also modulated by the NR2 subunit; Ca^{2+} -dependent inactivation is most prominent in NR1/2A receptors and absent in NR1/2C receptors (Krupp et al., 1996). Glycine-dependent desensitization occurs at sub-saturating concentrations of the co-agonist glycine and is due to a reduction in glycine affinity upon occupation of the glutamate binding site (Mayer et al., 1989; Benveniste et al., 1990).

Glycine-independent desensitization is a catch-all phrase used to describe any form of desensitization that cannot be accounted for by Ca^{2+} -dependent inactivation or glycine-dependent desensitization (Sather et al., 1990; Sather et al., 1992). A fast component of glycine-independent desensitization, which is present only in NR1/2A receptors, is due to inhibition of the receptor by Zn^{2+} (Chen et al., 1997; Krupp et al., 1998; Villarroel et al., 1998). Zn^{2+} binds to the LIVBP-like domain of NR1/2A receptors and enhances the affinity of the receptor for protons, which inhibit the receptor. Recent work has suggested that there is a positive allosteric interaction between the Zn^{2+} and glutamate binding sites, so that when glutamate is bound to the receptor, the affinity for Zn^{2+} is increased (Zheng et al., 2001; Erreger and Traynelis, 2005). A similar allosteric interaction may also exist between glutamate and ifenprodil on NR1/2B receptors (Zheng et al., 2001). A second, slower component of glycine-independent desensitization is also present in NR1/2A receptors. Originally, regions near the extracellular face of M1 were suggested to mediate this form of desensitization (Krupp et al., 1998; Villarroel et al., 1998), although recent data have questioned these conclusions (Hu and Zheng, 2005).

1.3.3 Modeling receptor activation

Receptor activation has long been a topic of heavy research. Del Castillo and Katz (1957) provided the first plausible mechanism to describe receptor activation (**Fig. 3a**). The model was developed to describe activation of nicotinic acetylcholine receptors at the neuromuscular junction (Del Castillo and Katz, 1957). In the Del Castillo and Katz model, the receptor in the closed state (R) binds a single agonist (A) molecule, which causes the receptor to undergo a conformation change and move into the open state (AR*). These steps are all described by rate constants that can be empirically derived. Through years of refinement, complex models of acetylcholine receptor activation have emerged. These recent models are able to account for many single channel characteristics and can explain the impact of mutations that lead to human diseases, such as congenital myasthenic syndromes (Hatton et al., 2003; Shelley and Colquhoun, 2005). The success of modeling acetylcholine receptor activation prompted application of similar techniques to many other receptor types, including NMDA receptors.

1.3.4 NMDA receptor gating models

One of the first widely used models of NMDA receptor function came from work by Lester and Jahr (1992) (**Fig. 3b**). The Lester and Jahr model reasonably reproduced macroscopic NMDA receptor mediated currents. However, the Lester and Jahr model could not account for many of the complex single channel characteristics of NMDA receptors. Further work, including a better understanding of the structure of NMDA receptors, has led to the development of more complete models of NMDA receptor activation. Several models have now been proposed which are able to, at least in part, explain the long and complex activations associated with NMDA receptor gating (Banke and Traynelis, 2003; Popescu et al., 2004; Auerbach and Zhou, 2005; Erreger et al., 2005; Schorge et al., 2005).

Several recently proposed models of NMDA receptor activation contain pre-gating states that represent independent conformational changes of the NR1 and NR2 subunits upon binding of glycine and glutamate, respectively (Banke and Traynelis, 2003; Erreger et al., 2005; Schorge et al., 2005). Using patches containing a single NR1/2B receptor, Banke and Traynelis (2003) were able to provide the first evidence suggesting that distinct conformational changes of the NR1 and NR2 subunits link glycine and glutamate binding, respectively, to NR1/2B receptor activation. In the Banke and Traynelis model (**Fig. 3c**), NR1 subunits undergo pre-gating conformational changes more rapidly than NR2B subunits. Using a similar approach, Erreger *et al.* (2005) developed a model to describe NR1/2A receptor activation. The NR1/2A and NR1/2B models differ in several respects. Most notably, the conformational change associated with the NR2 subunit proceeds more rapidly for NR2A than NR2B subunits (Erreger et al., 2005). Most recently, Schorge, Elenes & Colquhoun (2005) proposed a model that extends the Banke and Traynelis model to include glycine binding steps and an additional open state (Schorge et al., 2005). These recent models have been able to bring some order to the dauntingly complex activations of NMDA receptors.

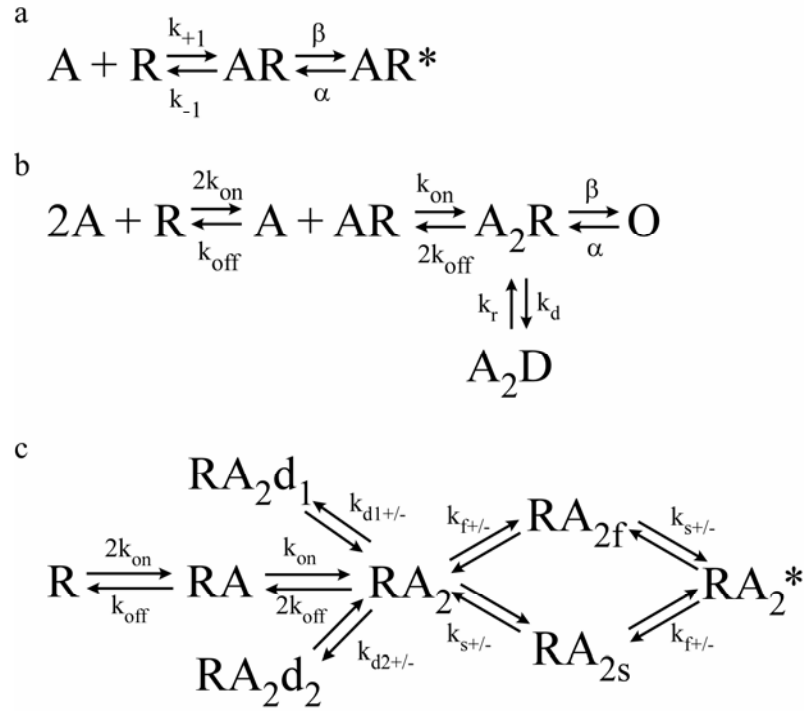


Figure 3. Historical mechanisms proposed to describe ion channel activation. (a) Mechanism first proposed by Del Castillo and Katz (1957) to describe activation of nicotinic acetylcholine receptors at the neuromuscular junction. A single agonist molecule (A) binds the closed receptor (R), inducing a conformational change of the receptor leading to activation (AR^*). (b) Lester and Jahr (1992) mechanism used to model macroscopic NMDA receptor currents. Experiments were performed in saturating glycine, which allowed the glycine binding site to be ignored. Two molecules of glutamate (A) must bind to the closed NMDA receptor (R). The doubly liganded receptor (A_2R) can then enter the open state (O), or enter a long-lived desensitized state (A_2D). Oscillations into and out of the A_2D state were proposed to contribute to the long activations exhibited by NMDA receptors. (c) Model proposed by Banke and Traynelis (2003) to describe NR1/2B receptor activation. Once the receptor reaches the doubly liganded state the Lester and Jahr (1992) and Banke and Traynelis (2003) models diverge. In the Banke and Traynelis (2003) model there are two desensitized state (RA_{2d1} and RA_{2d2}) as well as two additional states (RA_{2f} and RA_{2s}) linking the doubly liganded state (RA_2) to the open state (RA_2^*). The RA_{2f} and RA_{2s} states represent independent conformational changes of the NR1 and NR2 subunits, respectively.

1.4 VOLTAGE-DEPENDENT MODULATION OF LIGAND-GATED RECEPTORS

As mentioned above, ligand-gated receptors require binding of agonists to induce the conformational changes that lead to activation. However, activation of several ligand-gated receptors has been shown to be modulated by membrane voltage. Pioneering work by Magleby and Stevens (1972) on nicotinic acetylcholine receptors at the neuromuscular junction first described voltage-dependent modulation of a ligand gated receptor. Magleby and Stevens (1972) showed that the voltage-dependent decay of endplate potentials could be explained by assuming voltage-dependent alterations of nicotinic acetylcholine receptor gating. Specifically, they proposed that the closing rate of nicotinic acetylcholine receptors increases as the membrane is made progressively more positive (Magleby and Stevens, 1972). The closing rate of the inhibitory glycine receptor has also been proposed to be voltage-dependent, although the closing rate of the glycine receptor appears to decrease with depolarization (Legendre, 1999).

1.4.1 Membrane voltage and glutamate receptor activity

The activity of some glutamate receptor subtypes also displays voltage dependence. Certain AMPA receptor subtypes display strong inward rectification due to voltage dependent channel block by polyamines (Bowie and Mayer, 1995). In some preparations, the gating (Jonas and Sakmann, 1992; Raman and Trussell, 1995) and desensitization (Patneau et al., 1993) of AMPA receptors have been reported to display an inherent sensitivity to membrane voltage. However, in other preparations, AMPA receptor gating and desensitization appear insensitive to membrane voltage (Hestrin et al., 1990; Keller et al., 1991). AMPA receptors from invertebrate systems also display inherent voltage dependence (Dudel, 1974; Onodera and Takeuchi, 1978). Alterations in membrane potential affect the single channel conductance, open probability (P_{open}), and desensitization rates of invertebrate AMPA receptors (Tour et al., 1998).

NMDA receptor activity displays a steep dependence on membrane voltage due to open channel block by Mg^{2+} (Mayer et al., 1984; Nowak et al., 1984) (see below). However, several observations suggest that NMDA receptors display an additional sensitivity to membrane voltage, beyond that provided by Mg^{2+} block. At some synapses, the decay of NMDA receptor mediated excitatory post-synaptic currents (NMDA-EPSCs) is slower at depolarized membrane

potentials (Konnerth et al., 1990; Keller et al., 1991; D'Angelo et al., 1994), but see (Hestrin et al., 1990). A slow relaxation of NMDA receptor mediated currents in response to membrane depolarization has been attributed to voltage-dependent alterations of NMDA receptor channel properties (Benveniste and Mayer, 1995; Spruston et al., 1995). Several studies utilizing single channel recording techniques have shown that the mean open time of NMDA receptors increases with depolarization (Green and Gibb, 2001; Billups et al., 2002), but see (Gibb and Colquhoun, 1992). Finally, the P_{open} of NMDA receptors has been reported to be greater at positive membrane potentials (Nowak and Wright, 1992; Li-Smerin and Johnson, 1996; Li-Smerin et al., 2001). Taken together, these studies suggest that inherent voltage-dependent modulation may be a universal phenomenon, present in all ligand-gating ion channels.

1.5 MAGNESIUM BLOCK AND UNBLOCK OF NMDA RECEPTORS

One characteristic feature of NMDA receptors is powerful channel block by physiological concentrations of Mg^{2+} (Mayer et al., 1984; Nowak et al., 1984). Mg^{2+} block of NMDA receptors is strongly voltage dependent and increases with hyperpolarization. Due to block by Mg^{2+} , significant current flow through NMDA receptors only occurs upon coincident agonist binding and membrane depolarization.

Previous studies have provided evidence that the N-site asparagine, which is a key determinant of Ca^{2+} permeability, is also critical for Mg^{2+} block (Burnashev et al., 1992; Mori et al., 1992). Mutation of the NR2 subunit N-site drastically reduces block by Mg^{2+} , while mutation of the NR1 subunit N-site tends to have a larger affect on Ca^{2+} permeation (Burnashev et al., 1992). Within all NR2 subunits, a second asparagine adjacent to the N-site (termed the N+1 site) also strongly influences Mg^{2+} block (Wollmuth et al., 1998). These data suggest that the Mg^{2+} blocking site lies at the narrowest constriction of the channel.

1.5.1 NR2 subunit differences in Mg^{2+} block

Even though all NR2 subunits contain homologous asparagine residues at the N, and N+1 site, not all NMDA receptor subtypes display equivalent Mg^{2+} block. NR1/2A and NR1/2B receptors exhibit higher affinity Mg^{2+} block than NR1/2C and NR1/2D receptors (Monyer et al., 1992; Monyer et al., 1994; Kuner et al., 1996; Qian et al., 2005). The structural elements underlying the subunit differences in Mg^{2+} sensitivity are not completely clear, but they seem to be distributed over multiple sites within the NR2 subunit protein (Kuner and Schoepfer, 1996), although a single amino acid near the intracellular tip of M3 may play a particularly important role (Gao et al., 2004). Thus, despite sharing common structural elements, different NR2 subunits can confer unique Mg^{2+} blocking characteristics to functional NMDA receptors.

1.5.2 Kinetics of Mg^{2+} unblock

Early studies utilizing recordings at stationary membrane potentials provided evidence that both Mg^{2+} block and unblock occur extremely rapidly (Ascher and Nowak, 1988; Jahr and Stevens, 1990a, 1990b). Based on these experiments, depolarization induced Mg^{2+} unblock is often assumed to be effectively instantaneous (for review see (Koch, 1999)). However, more recent studies have showed that in response to rapid voltage jumps, Mg^{2+} unblock is multiphasic, containing at least a fast ($\tau < 1$ ms) and a slow (τ of many ms) component (Spruston et al., 1995; Vargas-Caballero and Robinson, 2003; Kampa et al., 2004). Slow Mg^{2+} unblock may alter the amount and kinetics of NMDA receptor mediated currents during physiological depolarizations (Vargas-Caballero and Robinson, 2003; Kampa et al., 2004; Vargas-Caballero and Robinson, 2004).

Although it is clear that the NR2 subunit identity can alter many NMDA receptor characteristics, it is not known if Mg^{2+} unblocking kinetics are also NR2 subunit dependent. Three recent studies describing a slow component of Mg^{2+} unblock in some detail utilized cortical slices containing native NMDA receptors of unknown subunit composition (Vargas-Caballero and Robinson, 2003; Kampa et al., 2004; Vargas-Caballero and Robinson, 2004). Based on previous expression studies (Monyer et al., 1994), native cortical NMDA receptors are likely to be composed of mostly NR1, NR2A and/or NR2B subunits. Slow Mg^{2+} unblock

persisted following application of ifenprodil, an NR2B subunit specific antagonist, suggesting that Mg^{2+}_o unblock from NR1/2A receptors contains a slow component (Vargas-Caballero and Robinson, 2004). However, it is not clear if Mg^{2+}_o unblock from NR1/2B receptors also displays a slow component and, if so, if slow Mg^{2+}_o unblock is equivalent from NR1/2A and NR1/2B receptors. Furthermore, it is not clear how the previous results describing slow Mg^{2+}_o unblock will translate, if at all, to native NMDA receptors in brain regions expressing high levels of the NR2C or NR2D subunits.

1.6 CHANNEL BLOCK AND NMDA RECEPTOR GATING

The most prominent NMDA receptor blocker is Mg^{2+}_o , as described above. However, many other compounds act as NMDA receptor channel blockers, including the dissociative anesthetics phencyclidine and ketamine (Anis et al., 1983; Honey et al., 1985) and the clinically useful drugs memantine and amantadine (Blanpied et al., 1997; Chen and Lipton, 1997). The study of NMDA receptor channel blockers provides not only information regarding the physiological role of NMDA receptors, but it can also help to further our understanding of NMDA receptor gating.

1.6.1 Interaction between blockers and gating machinery

Because channel gating involves structural changes in and around the pore, open channel blockers may perturb channel gating transitions. The most extreme examples of blocking molecules that perturb channel gating are sequential blockers, which prevent the channel activation gate from closing during block. 9-aminoacridine (Benveniste and Mayer, 1995), IEM-1857 (Antonov and Johnson, 1996) and tetrapentyl-ammonium (Sobolevsky et al., 1999) are all thought to act via sequential block of NMDA receptors. Other channel blockers do not prevent the activation gate from closing during block and can be “trapped” inside the channel. Once a blocker is trapped, the channel must move back to the open state for the blocker to exit the channel pore. Several examples of trapping blockers of NMDA receptors have been described, including MK-801 (Huettner and Bean, 1988), amantadine and memantine (Blanpied et al.,

1997; Chen and Lipton, 1997), ketamine and phencyclidine (MacDonald et al., 1991), and NEFA, a structural analogue of phencyclidine (Dilmore and Johnson, 1998). Although these trapping blockers do not affect channel gating as dramatically as sequential blockers, they still may alter gating transitions or agonist binding while trapped (Blanpied et al., 1997; Dilmore and Johnson, 1998; Sobolevsky et al., 1999; Sobolevsky and Yelshansky, 2000; Blanpied et al., 2005).

1.6.2 Mg^{2+} block and NMDA receptor gating

Noticeably absent from the discussion regarding interactions between blockers and channel gating is Mg^{2+} . The fast binding and unbinding kinetics of Mg^{2+} make it difficult to determine if Mg^{2+} can be trapped within the NMDA receptor pore. However, several studies have found that trapping block models can adequately reproduce many actions of Mg^{2+} (Ascher and Nowak, 1988; Jahr and Stevens, 1990a; Sobolevsky and Yelshansky, 2000; Vargas-Caballero and Robinson, 2004). The trapping of Mg^{2+} is further supported by the observation that Zn^{2+} , which is similar in size and valence to Mg^{2+} , is trapped by a NMDA receptor into which a high affinity Zn^{2+} binding site has been engineered by mutating the N-site amino acids to cysteine (Amar et al., 2001).

While there is evidence supporting a trapping block mechanism for Mg^{2+} , the influence of Mg^{2+} on channel gating is not yet clear. Data showing excellent agreement between the K_d and the IC_{50} of Mg^{2+} measured using single channel and whole-cell recordings, respectively, suggests blockade of NMDA receptors by Mg^{2+} does not influence channel gating (Johnson and Qian, 2002; Qian et al., 2002). A similar conclusion was reached in a study from Sobolevsky & Yelshansky (2000), in which it is reported that blockade by Mg^{2+} does not affect channel desensitization, channel closure, or agonist unbinding.

The hypothesis that block by Mg^{2+} does not alter NMDA receptor gating is in disagreement with the report of a reduction in single channel burst duration and frequency at hyperpolarized membrane potentials in the presence of Mg^{2+} (Ascher and Nowak, 1988). In addition, recent studies (Kampa et al., 2004; Vargas-Caballero and Robinson, 2004) have proposed models to describe slow Mg^{2+} unblock from native NMDA receptors in which Mg^{2+} block augments channel gating transitions alone, or along with alterations in agonist binding

kinetics. The Vargas-Caballero & Robinson model proposed that blockade by Mg^{2+} increases the channel closing rate roughly 3-fold. In the model proposed by Kampa *et al.* (2004), blockade by Mg^{2+} also increased channel closing rate, but in conjunction with an enhancement of receptor desensitization and a decrease in agonist affinity. The later model is in good agreement with previous data suggesting that NMDA receptor channel blockade by Mg^{2+} lowers the NMDA receptor's affinity for glutamate (Nahum-Levy *et al.*, 2002). Thus, the effects of Mg^{2+} block on NMDA receptor channel gating, agonist binding, and desensitization remains a topic of controversy.

1.7 GOALS OF THIS DISSERTATION

NMDA receptors play a critical role in both normal and pathological states in the CNS. The research in this dissertation is aimed at providing further insight into the relationship between membrane voltage and NMDA receptor activity. In addition, we were particularly interested in determining how expression of various NR2 subunit isoforms impacts the relationship between membrane voltage and NMDA receptor activity. The experimental results have several mechanistic and physiological implications for NMDA receptor activity. The results are outlined in the following three chapters:

1.7.1 NMDA receptor NR2 subunit dependence of the slow component of Mg^{2+} unblock.

In the series of experiments described in this chapter, we set out to characterize the kinetics of Mg^{2+} unblock from recombinant NR1/2A, NR1/2B, NR1/2C, and NR1/2D receptors. The results indicate that the kinetics of Mg^{2+} unblock are NR2 subunit dependent: Mg^{2+} unblock from NR1/2C and NR1/2D receptors is extremely rapid while Mg^{2+} unblock from NR1/2A and NR1/2B receptors displays a prominent slow component. Furthermore, the slow component of Mg^{2+} unblock from NR1/2B receptors is slower than from NR1/2A receptors.

1.7.2 Modulation of NR1/2B receptor activation by membrane voltage.

In this chapter we set out to determine if there was a relationship between slow current relaxations in response to depolarization in 0 Mg^{2+}_o and slow Mg^{2+}_o unblock. Utilizing whole-cell current recordings and kinetic modeling, we found that an NR1/2B model that incorporated inherent voltage-dependence of channel activation could account for NR1/2B receptor currents in both 0 and 1 mM Mg^{2+}_o . In addition, the NR1/2B model could at least partially reproduce previous reports of voltage-dependent decay of synaptic NMDA receptor currents.

1.7.3 Voltage-dependent modulation of NMDA receptor activation: NR2 subunit dependence and slow Mg^{2+}_o unblock.

The goal of this chapter was to determine if NR1/2A receptor activity displayed voltage dependence. We found that NR1/2A receptor activity was consistent with an enhancement of receptor P_{open} with depolarization. Using recently described subunit specific gating kinetics (Erreger et al., 2005), we adapted the NR1/2B model from Chapter 2 to describe NR1/2A receptors. Despite containing identical voltage sensitivity, the unique activation kinetics of NR1/2A receptors predicted the experimentally observed NR2 subunit differences in Mg^{2+}_o unblocking kinetics.

2.0 NMDA RECEPTOR NR2 SUBUNIT DEPENDENCE OF THE SLOW COMPONENT OF MAGNESIUM UNBLOCK

2.1 ABSTRACT

NMDA receptor activity is important for many physiological functions, including synapse formation and alterations in synaptic strength. NMDA receptors are most commonly composed of NR1 and NR2 subunits. There are four NR2 subunits (NR2A-D). NR2 subunit expression varies across both brain regions and developmental stages. The identity of the NR2 subunit within a functional NMDA receptor helps to determine many pharmacological and biophysical receptor properties, including strength of block by external Mg^{2+} (Mg^{2+}_o). Mg^{2+}_o block confers strong voltage dependence to NMDA receptor-mediated responses and is critically important for many functions that the NMDA receptor plays within the central nervous system. Here, we describe the NR2 subunit dependence of the kinetics of Mg^{2+}_o unblock following rapid depolarizations. We find that Mg^{2+}_o unblocks from NR1/2A and NR1/2B receptors with a prominent slow component similar to that previously described in native hippocampal and cortical NMDA receptors. Strikingly, this slow component of Mg^{2+}_o unblock is completely absent from NR1/2C and NR1/2D receptors. Thus, currents from NR1/2C and NR1/2D receptors respond more rapidly to fast depolarizations than currents from NR1/2A and NR1/2B receptors. In addition, the slow component of Mg^{2+}_o unblock from NR1/2B receptors was consistently slower than from NR1/2A receptors. This made rapid depolarizations, such as action potentials waveforms (APs), more efficacious at stimulating Mg^{2+}_o unblock from NR1/2A than from NR1/2B receptors. These NR2 subunit differences in the kinetics of Mg^{2+}_o unblock are likely to help determine the contribution of each NMDA receptor subtype to current flow during synaptic activity.

2.2 INTRODUCTION

Postsynaptic NMDA receptor responses are characterized by strong voltage-dependence, slow decay, and a large calcium (Ca^{2+}) conductance. Due in part to these unique characteristics, NMDA receptors are critically involved in synapse formation and modification during development (Bear and Colman, 1990; Cline and Constantine-Paton, 1990; Iwasato et al., 1997; Ramoa et al., 2001; Erisir and Harris, 2003), as well as changes in synaptic strength in adulthood (Bliss and Collingridge, 1993; Heynen et al., 2000; Lisman and McIntyre, 2001). NMDA receptor dysfunction has also been implicated in many diseases, such as epilepsy, schizophrenia, and several neurodegenerative disorders (Meldrum, 1992; Chapman, 2000; Cull-Candy et al., 2001; Tsai and Coyle, 2002; Zeron et al., 2002; Moghaddam, 2003).

Functional NMDA receptors are obligate heterotetramers, composed primarily of NR1 and NR2 subunits. The NR1 subunit has one gene product, but many splice variants, which are expressed ubiquitously (Laurie et al., 1995). In contrast, expression of the four NR2 subunit gene products (NR2A-NR2D) shows tight temporal and spatial regulation. For example, NR2B and NR2D subunits are expressed prenatally, while NR2A and NR2C subunit expression rises sharply after birth (Monyer et al., 1994; Wenzel et al., 1996). Differential NR2 subunit expression also occurs across brain regions. In adulthood, NR2A and NR2B subunits are predominant within the cortex, while NR2C and NR2D subunits are found within midbrain and hindbrain structures (Monyer et al., 1994; Wenzel et al., 1996). NR2 subunits even show differential expression within individual neurons; NR2A subunits cluster around synapses while NR2B subunits often occupy extrasynaptic sites (Tovar and Westbrook, 1999). NR2 subunit expression is tightly controlled because NR2 subunits help determine many pharmacological and biophysical receptor properties, including Mg^{2+} affinity (Dingledine et al., 1999).

Due to voltage-dependent channel block by Mg^{2+} (Mayer et al., 1984; Nowak et al., 1984; Ascher and Nowak, 1988), NMDA receptor mediated currents are prominent only during periods of coincident glutamate release and postsynaptic depolarization. Recent reports have shown that following rapid membrane depolarization, Mg^{2+} unblock from native NMDA receptors contains fast ($\tau < 1$ ms) and slow ($\tau = 3-20$ ms) components (Spruston et al., 1995; Vargas-Caballero and Robinson, 2003; Kampa et al., 2004). These findings are surprising because the kinetics of Mg^{2+} unblock at the single channel level (Nowak et al., 1984; Ascher

and Nowak, 1988) predict only rapid unblock. Instead, the slow component(s) account for as much as 50 % of the total current relaxation, which reduces NMDA receptor currents during the upstroke of action potentials (APs) (Vargas-Caballero and Robinson, 2003), and shortens the time window for spike-timing-dependent plasticity (STDP) (Kampa et al., 2004).

Previous studies describing slow Mg^{2+} unblock were performed on native NMDA receptors of an undefined subunit composition. Here, we set out to determine if the properties of Mg^{2+} unblock are NR2-subunit dependent. We find that the relative speed of Mg^{2+} unblock from NMDA receptor subtypes are: NR1/2C, NR1/2D >>> NR1/2A > NR1/2B. These NR2 subunit differences in Mg^{2+} unblock rendered brief depolarizations, such as APs, more effective at stimulating Mg^{2+} unblock from NR1/2A than from NR1/2B receptors.

2.3 MATERIALS AND METHODS

2.3.1 Cell culture and transfection

Human embryonic kidney (HEK) 293T cells were maintained as previously described (Qian et al., 2005). HEK 293T cells were plated onto untreated glass coverslips or onto glass coverslips pretreated with poly D-lysine (0.1 mg ml^{-1}) and rat-tail collagen (0.1 mg ml^{-1} , BD Biosciences, San Jose, CA) in 35-mm culture dishes at $1-2 \times 10^5$ cells per dish. 18-24 hours after plating, the cells were transiently transfected with cDNAs encoding the NR1-1a and one of the four NR2 subunits (NR2A-D) using a modified Ca^{2+} precipitation procedure (Qian et al., 2005). The cDNA for enhanced Green Fluorescent Protein (eGFP) was co-transfected as a marker of successful transfection. $0.7 \text{ }\mu\text{g}$ of eGFP, $1.3 \text{ }\mu\text{g}$ of NR1-1a, and $2-8 \text{ }\mu\text{g}$ of NR2A-D cDNA were used per dish. After incubation of cells with the transfection solution for 6-8 hours, precipitates were washed off with fresh culture medium that contained $200 - 1000 \text{ }\mu\text{M}$ APV and 2 mM Mg^{2+} . Experiments were performed 20 to 72 hours after transfection.

2.3.2 Solutions

Solutions were prepared daily from frozen stocks. Currents were activated by the indicated concentration of NMDA or glutamate either in the absence of Mg^{2+}_o or with 1 mM added Mg^{2+}_o . 10 μ M glycine was added to all solutions. We did not adjust for changes in osmolality that resulted from the addition of Mg^{2+}_o . The external solution contained (in mM): NaCl 140, $CaCl_2$ 1, KCl 2.8, and HEPES 10, pH 7.2 adjusted with NaOH, osmolality 290 ± 10 mmol/kg. The internal solutions contained (in mM): CsCl 125, EGTA 10 and HEPES 10, pH 7.2 adjusted with CsOH, osmolality 275 ± 10 mmol/kg. Sucrose was used as needed to adjust the osmolality of the external solution. The junction potential between the pipette and bath solution was 5 mV and all holding potentials were corrected for junction potentials. Ultrapure salts were used when available. All chemicals were from Sigma Chemical Co. (St Louis, MO).

2.3.3 Whole-cell recording

Whole-cell recordings from transfected HEK 293T cells were performed as described previously (Qian et al., 2005). Briefly, pipettes were pulled from borosilicate standard-walled glass with filaments (1.5 mm outer diameter; .86 mm inner diameter; Warner Instrument Corp., Portland, OR) and fire-polished to a resistance of 2-5 M Ω . Solutions were delivered using an in-house fabricated fast perfusion system (Qian et al., 2002) connected to an eight chamber gravity fed solution reservoir (AutoMate Scientific, San Francisco, CA). Solution exchanges were 90% complete within 20 ms for standard whole-cell experiments, or 90% complete within 1 ms for the lifted-cell experiments. Solution exchange measurements were made by recording whole-cell current from a transfected HEK 293T cell while moving between two barrels. Both barrels contained the same concentration of NMDA and glycine, but one barrel contained normal extracellular solution and the second barrel contained an extracellular solution with the impermeant ion NMDG in place of NaCl. The time course of current decrease upon movement into the NMDG extracellular solution was used to estimate solution exchange times.

In some experiments, the lifted-cell technique (Vicini et al., 1998) was used to permit faster solution exchange times. For these experiments, HEK 293T cells were plated onto untreated glass coverslips. Once whole-cell access was obtained negative pressure was re-

applied and the cell was slowly lifted into the solution flow. Small negative pressure was maintained throughout the experiment to prolong the duration of the experiment. The morphology of the cell was continuously monitored and if gross morphological changes occurred the experiment was terminated.

All currents were recorded with an Axopatch 200 amplifier (Axon Instruments, Foster City, CA) in voltage-clamp mode. The built-in series resistance correction and prediction circuitry were set to at least 80% in all experiments. Signals were low-pass filtered at 2.5 or 5 kHz (8-pole Bessel; Warner Instrument Corp, Hamden CT) and sampled at 10-50 kHz. Where indicated, signals were re-filtered at 1 kHz for display. All experiments were performed at room temperature.

2.3.4 Data analysis and Curve Fitting

NMDA receptor mediated current responses to depolarizing voltage jumps were corrected for leak and capacitive currents by subtracting the current response to an identical voltage jump in the absence of NMDA or glutamate using pClamp 9.2 (Axon Instruments, Foster City, CA). When multiple sweeps of the same amplitude voltage jump were obtained, responses in the absence of NMDA or glutamate were first averaged and then subtracted from the agonist-induced ensemble average. Leak- and capacitance- subtracted currents (I_{NMDA}) were then fit with multi-exponential equations of the form:

$$I_{\text{NMDA}} = C + \sum_{i=1}^n A_i (1 - \exp(-t/\tau_i))$$

where C is the current level prior to the voltage jump and A_i is the amplitude of the exponential component with time constant τ_i . n was adjusted between 1 and 3 as necessary to obtain quality fits. C , A_i , and τ_i were allowed to vary during fitting. The amplitudes were expressed as a percentage by dividing each A_i by the sum of the A_i 's of all the exponential components. In experiments where voltage jumps to 35 mV were applied shortly following agonist application (**Fig. 10**), the resulting currents were normalized to an averaged response to agonist application while the cell was held at 35 mV to remove the effects of desensitization. Prior to normalization, two 35 mV responses, pre- and post-voltage jump, were averaged to account for current run-

down. All curve fitting was performed using Clampfit 9.2 (Axon Instruments, Foster City, CA) or Origin 7.0 (OriginLab Corp., Northampton, MA). Data are expressed as means \pm S.E.M and statistical analysis was performed using Student's *t*-tests unless otherwise noted.

2.4 RESULTS

2.4.1 NR2 subunit identity controls Mg^{2+} unblocking kinetics

The rapid unblocking kinetics of Mg^{2+} at the single channel level (Nowak et al., 1984; Ascher and Nowak, 1988) predict that during whole-cell recordings, membrane depolarization would induce rapid Mg^{2+} unblock. However, recent data (Spruston et al., 1995; Vargas-Caballero and Robinson, 2003; Kampa et al., 2004) have shown that, following rapid membrane depolarization, Mg^{2+} unblock from native NMDA receptors of an undefined subunit composition actually contains both fast ($\tau < 1$ ms) and slow ($\tau = 3$ -20 ms) components. Because the identity of the NR2 subunit within a functional NMDA receptor influences many channel properties (Dingledine et al., 1999), we first investigated whether the kinetics of Mg^{2+} unblock are also NR2 subunit dependent. To obtain a homogenous population of NMDA receptors with a defined subunit composition, we co-transfected HEK 293T cells with the cDNA for the NR1-1a subunit and the cDNA for one of the four NR2 subunits (NR2A-D). HEK 293T cells are well suited for these experiments because the cells are electrotonically compact, which eliminates any slow changes in current due to poor space clamp as may be seen with neuronal cells (Vargas-Caballero and Robinson, 2003).

We first applied depolarizing voltage steps from -65 mV during long applications (15 s) of NMDA in the absence and presence of Mg^{2+} (**Fig. 4A, B**). Long applications of NMDA allowed whole-cell currents to reach a steady-state level despite varying degrees of desensitization between NMDA subtypes (Dingledine et al., 1999). In the presence of physiological concentrations of Mg^{2+} (1 mM), NR1/2A and NR1/2B receptor mediated currents were largely blocked at -65 mV ($94.7 \pm .6$ % and 96.1 ± 1.3 %, respectively), while NR2C and NR2D receptors showed substantially less block ($78.6 \pm .4$ % and 77.9 ± 2.0 %, respectively).

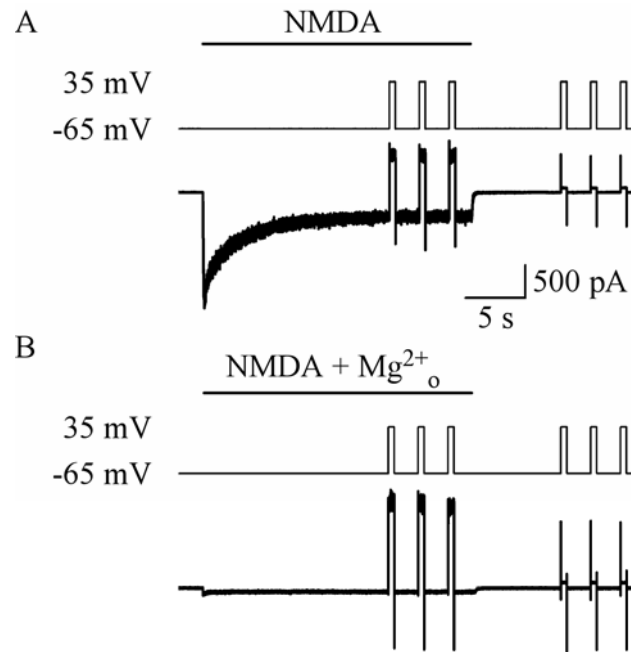


Figure 4. Protocol used to investigate the kinetics of Mg^{2+}_o unblock from recombinant NMDA receptors during steady-state response. 30 μ M NMDA and 10 μ M glycine (“NMDA”) was applied (top trace) in the absence (A) and presence (B) of 1 mM added Mg^{2+}_o during standard whole-cell recordings from an HEK 293T cell expressing NR1/2B receptors. Once the current (bottom trace) had reached a stationary level, three depolarizing voltage jumps (here, -65 to 35 mV) were applied (middle trace). Following termination of NMDA application, another identical set of depolarizing voltage jumps were applied to allow for off-line leak and capacitance subtraction. All 3 sweeps in the absence and presence of NMDA were averaged before subtraction. Current traces were re-filtered at 1 kHz for display.

This is consistent with previous reports (Monyer et al., 1994; Kuner and Schoepfer, 1996; Qian et al., 2005) showing that NR1/2C and NR1/2D receptors have a lower affinity for Mg^{2+}_o than NR1/2A and NR1/2B receptors.

A depolarizing voltage jump to 35 mV relieves the voltage-dependent block by Mg^{2+}_o from all receptor subtypes, and allows outward current flow. However, in response to a depolarizing voltage step, outward currents in the presence of 1 mM Mg^{2+}_o from both NR1/A and NR1/2B receptors developed with both fast and slow components (**Fig. 5A₂, B₂**). The observed slow component is predominately due to Mg^{2+}_o unblock because the same voltage jump performed in the absence of Mg^{2+}_o results in a more rapid relaxation of outward current (**Fig. 5A₁, 2B₁**). Strikingly, following an identical depolarizing voltage jump, Mg^{2+}_o unblocks from NR1/2C and NR1/2D receptors very rapidly, with no obvious slow component (**Fig. 5C₂, D₂**). The kinetics of outward currents from NR1/2C and NR1/2D receptors following a depolarizing voltage jump were also rapid in the absence of Mg^{2+}_o (**Fig. 5C₁, D₁**). Thus, unlike NR1/2A and NR1/2B receptors, under these experimental conditions there is no slow Mg^{2+}_o unblock from NR1/2C or NR1/2D receptors.

To quantify the kinetics of Mg^{2+}_o unblock, we fit currents in response to voltage jumps from -65 to 35 mV with a single or double exponential function (**Fig. 5**). In the absence of added Mg^{2+}_o , the current relaxation from all receptor subtypes was dominated by a single fast (sub-ms) component. However, we did observe a small slow component of outward current relaxation in the absence of added Mg^{2+}_o from both NR1/2A and NR1/2B receptors (**Fig. 5A₁, B₁**). Slow relaxation of NMDA mediated current following depolarizing voltage jumps in the absence of Mg^{2+}_o has been previously reported (Benveniste and Mayer, 1995; Spruston et al., 1995), but see (Vargas-Caballero and Robinson, 2003; Kampa et al., 2004). In our hands the kinetics of current relaxation following a depolarizing voltage jump to 35 mV with zero added Mg^{2+}_o are dominated by a fast (sub-ms) component, with the slow component having a small percent amplitude (< 15%) that in every case is significantly ($p < .01$) less than the amplitude of the slow component in the presence of Mg^{2+}_o (Supplemental Tables 1).

In the presence of Mg^{2+}_o , NR1/2A and NR1/2B receptor currents were well fit by a double exponential function, while a single exponential function provided excellent fits of currents from NR1/2C and NR1/2D receptors both in the presence and absence of Mg^{2+}_o (**Fig. 5**). The tau of the fast component (τ_1) did not differ significantly between any of the receptor

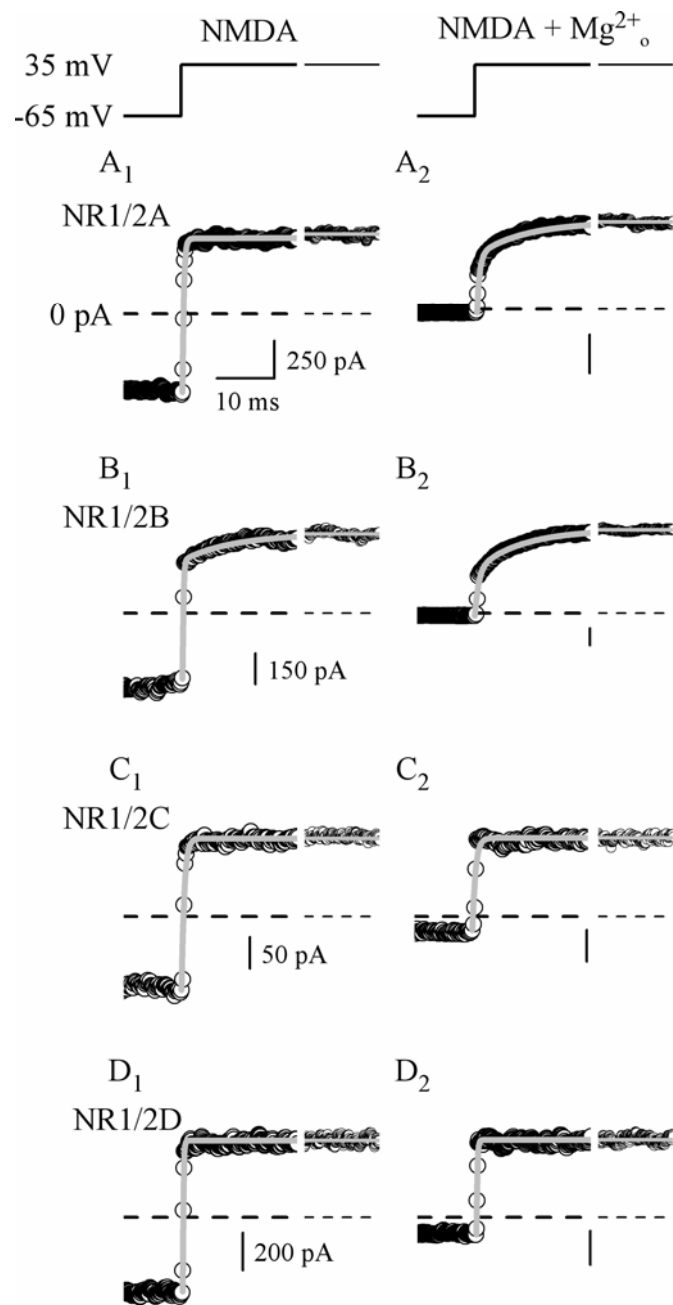


Figure 5. The kinetics of Mg^{2+}_o unblock are NR2 subunit dependent. Whole-cell currents are shown from NR1/2A (**A₁**, **A₂**), NR1/2B (**B₁**, **B₂**), NR1/2C (**C₁**, **C₂**), and NR1/2D (**D₁**, **D₂**) receptors during a 500 ms depolarizing voltage step from -65 to 35 mV. The voltage steps were applied either in the absence (**A₁** – **D₁**) or in the presence of 1 mM Mg^{2+}_o (**A₂** – **D₂**). A prominent slow relaxation of the outward current is present within records from NR1/2A and NR1/2B receptors when the depolarizing voltage jump is applied in the presence of 1 mM Mg^{2+}_o , indicating a slow component of Mg^{2+}_o unblock. In contrast, the outward current from NR1/2C and NR1/2D receptors in response to a depolarizing voltage jump relaxes with a single, fast component both in the absence and presence of Mg^{2+}_o . “NMDA” indicates that the currents are recorded in the presence of 30 μ M NMDA and 10 μ M glycine. The timing of the voltage jump is indicated by traces above **A₁** and **A₂** and the 0 current level is indicated by a dashed line. Double (**A₁** – **B₂**) or single (**C₁** – **D₂**) exponential fits are overlaid (grey lines). Note the different scale bars in panels **B₁** & **B₂** due to potentiation of NR1/2B receptors by Mg^{2+}_o (Paoletti et al., 1995).

subtypes, or depend on the presence of Mg^{2+}_o , with a value of ~ 5 ms under all conditions (**Table 1**). The tau of the slow component (τ_2) of Mg^{2+}_o unblock from NR1/2A and NR1/2B receptors was significantly ($p < .0001$) slower than τ_1 , with values of $4.80 \pm .39$ ms for NR1/2A ($n = 6$) and $9.15 \pm .83$ ms for NR1/2B receptors ($n = 8$). In addition, τ_2 was significantly ($p < .005$) slower from NR1/2B than from NR1/2A receptors (see below). In both NR1/2A and NR1/2B receptors the slow component accounted for ~ 40 % of the total current.

It is possible that we missed a small slow component of Mg^{2+}_o unblock from NR1/2C and NR1/2D receptors because they are less effectively blocked by 1 mM Mg^{2+}_o than NR1/2A and NR1/2B receptors (Monyer et al., 1994; Kuner and Schoepfer, 1996; Qian et al., 2005). To test this possibility, we raised Mg^{2+}_o to 5 mM, a concentration at which inhibition of NR1/2D receptor responses is comparable to inhibition of NR1/2B receptor responses by 1 mM Mg^{2+}_o . Even under these conditions there was no hint of a slow component of Mg^{2+}_o unblock from NR1/2D receptors (**Fig. 6**). The kinetics of Mg^{2+}_o unblock from NR1/2D receptors were similar in the presence of 1 and 5 mM Mg^{2+}_o , with time constants of 0.25 ± 0.01 ms and 0.30 ± 0.07 ms, respectively. The kinetics of Mg^{2+}_o unblock from NR1/2A and NR1/2B receptors in the presence of 5 mM also were similar to those observed in the presence of 1 mM Mg^{2+}_o (**Table 1**). Thus, the kinetics of Mg^{2+}_o unblock are determined by the identity of the NR2 subunit, with slow Mg^{2+}_o unblock only occurring from NMDA receptors that contain either the NR2A or NR2B subunit.

2.4.2 Voltage Dependence of Slow Mg^{2+}_o Unblock

To further characterize slow Mg^{2+}_o unblock from NR1/2A and NR1/2B receptors, we applied depolarizing voltage jumps from rest to test voltages from -45 to 35 mV using a protocol similar to that shown in **Figure 1**. The resulting currents were fit with single or double exponential equations. In the presence of 1 mM Mg^{2+}_o a double exponential equation was required for adequate fits of currents in response to voltage jumps to each of the tested voltages indicating slow Mg^{2+}_o unblock occurs throughout the physiological range of membrane voltages.

For both NR1/2B and NR1/2A receptors, τ_1 did not depend on the amplitude of the depolarization ($p > .05$, ANOVA), which enabled us to average the results across all test voltages. The averaged values for τ_1 did not significantly depend on NR2 subunit identity or the

Table 1. Depolarization induced current relaxations in the presence of 30 μ M NMDA and 10 μ M glycine in the absence and presence of Mg^{2+}_o

NR1/2A receptors	[Mg^{2+}_o]	τ_1 (ms)	τ_2 (ms)	A_{slow} (%)
-65 to -45 mV	0	0.27 ± 0.02	N/A	N/A
	1	0.19 ± 0.03	2.46 ± 0.58	19.4 ± 2.7
-65 to -25 mV	0	0.30 ± 0.05	N/A	N/A
	1	0.65 ± 0.09	3.58 ± 0.31 *	31.0 ± 4.4
-65 to 15 mV	0	0.28 ± 0.07	4.58 ± 1.60	5.52 ± 1.19
	1	0.30 ± 0.04	4.17 ± 0.21 *	33.0 ± 2.2
-65 to 35 mV	0	0.38 ± 0.13	4.34 ± 0.65 *	8.54 ± 2.02
	1	0.46 ± 0.07	4.80 ± 0.39 *	34.6 ± 3.0
	5	0.42 ± 0.04	4.56 ± 0.44 *	36.2 ± 2.8
NR1/2B receptors	[Mg^{2+}_o]	τ_1 (ms)	τ_2 (ms)	A_{slow} (%)
-65 to -45 mV	0	0.14 ± 0.06	N/A	N/A
	1	0.20 ± 0.06	3.79 ± 0.56	28.34 ± 5.84
-65 to -25 mV	0	0.38 ± 0.05	N/A	N/A
	1	0.61 ± 0.09	8.02 ± 0.52 *	36.83 ± 2.51
-65 to 15 mV	0	0.48 ± 0.21	5.62 ± 2.29	9.29 ± 3.35
	1	0.74 ± 0.24	7.81 ± 0.77 *	36.89 ± 0.62
-65 to 35 mV	0	0.54 ± 0.12	7.87 ± 0.72 *	15.53 ± 1.86
	1	0.69 ± 0.17	9.15 ± 0.93 *	44.74 ± 4.76
	5	0.43 ± 0.08	9.46 ± 1.23 *	40.75 ± 2.69
-65 to 35 mV (pH 8.2)	1	0.38 ± 0.01	3.93 ± 0.77	32.7 ± 1.3
NR1/2C receptors	[Mg^{2+}_o]	τ_1 (ms)	τ_2 (ms)	A_{slow} (%)
-65 to 35 mV	0	0.29 ± 0.04	N/A	N/A
	1	0.28 ± 0.20	N/A	N/A
NR1/2D receptors	[Mg^{2+}_o]	τ_1 (ms)	τ_2 (ms)	A_{slow} (%)
-65 to 35 mV	0	0.23 ± 0.04	N/A	N/A
	1	0.25 ± 0.01	N/A	N/A
	5	0.30 ± 0.07	N/A	N/A

Membrane voltage was changed during steady-state responses from HEK 293T cells expressing NR1 and the indicated NR2 subunit. * indicates a significant ($p > .01$) difference between the values from NR1/2A and the corresponding value from NR1/2B receptors. Values are shown as mean \pm SEM.

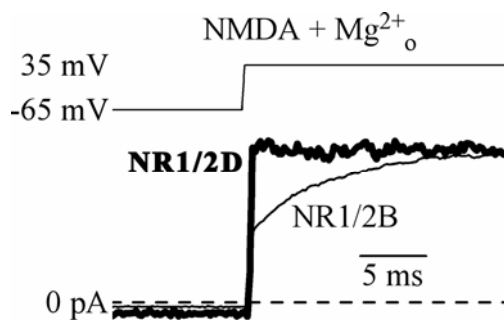


Figure 6. Mg²⁺_o unblocks rapidly from NR1/2D receptors even at high [Mg²⁺]_o. Superimposed whole-cell currents during a voltage jump from -65 to 35 mV from NR1/2B receptors in the presence of 30 μM NMDA, 10 μM glycine, and 1 mM Mg²⁺_o (thin trace), or NR1/2D receptors in the presence of 30 μM NMDA, 10 μM glycine, and 5 mM Mg²⁺_o (thick trace). Currents are normalized to the steady-state outward current at 35 mV. Note the comparable level of inward current mediated by each of the two receptor isoforms. Voltage change indicated by the top trace.

presence of Mg^{2+}_o , with values of $.40 \pm .11$ ms ($n = 16$) and $.31 \pm .02$ ms ($n = 19$) for NR1/2A receptors and $.52 \pm .23$ ms ($n = 19$) and $.38 \pm .13$ ms ($n = 15$) for NR1/2B receptors in the presence and absence of Mg^{2+}_o , respectively. In contrast, τ_2 from NR1/2B receptors was significantly slower than τ_2 from NR1/2A receptors at most test voltages (**Fig. 7A**). Only in response to the smallest amplitude voltage jump (-65 to -45 mV) was τ_2 not significantly different between NR1/2A and NR1/2B receptors. τ_2 from both NR1/2A and NR1/2B receptors did show weak voltage-dependence ($p < .05$, ANOVA), becoming slower as the amplitude of the depolarizing step increased (**Fig. 7**). The amplitudes of the slow component (A_{slow}) of Mg^{2+}_o unblock from NR1/2A and NR1/2B receptors was not significantly different (**Fig. 4B**), carrying roughly 40 % of the total depolarization-induced current relaxation at all test voltages. A_{slow} did not display any significant voltage dependence ($p > .05$, ANOVA) in either NR1/2A or NR1/2B receptors, although there was a trend for A_{slow} to increase as the amplitude of the voltage jump increased.

If the slow component of Mg^{2+}_o unblock resulted from slow unbinding of Mg^{2+}_o from open NMDA receptor channels, τ_2 should be strongly voltage dependent and become faster with depolarization. Instead, we found that slow Mg^{2+}_o unblock is only weakly voltage dependent and becomes slower with depolarization (**Fig. 7A**), in agreement with previous data from native NMDA receptors (Vargas-Caballero and Robinson, 2003). Thus, it is likely that the kinetics of slow Mg^{2+}_o unblock arise from slow exit of NMDA receptor channels from one or more closed block state(s) (see Discussion).

In the presence Mg^{2+}_o , returning the voltage to -65 mV caused rapid reblock of the channel (**Fig. 8A, B**). However, following depolarizations to -25, 15, and 35 mV a slow phase of Mg^{2+}_o block was also present (Fig. 8A, B). In cells with large enough responses to allow adequate signal to noise ratios, we fit the slow portion of Mg^{2+}_o reblock with a single exponential equation. The slow phase of Mg^{2+}_o reblock of NR1/2B receptors was significantly slower than the slow phase of Mg^{2+}_o reblock of NR1/2A receptors following repolarization to -65 mV from -25, 15, and 35 mV (**Fig. 8C**). In contrast, currents from NR1/2C and NR1/2D receptors showed very rapid reblock, which was well fit with a single exponential component with a τ of less than 1 ms (data not shown). Together, these data indicate that the kinetics of both Mg^{2+}_o unblock and reblock during rapid voltage changes are strongly dependent on the identity of the NR2 subunit.

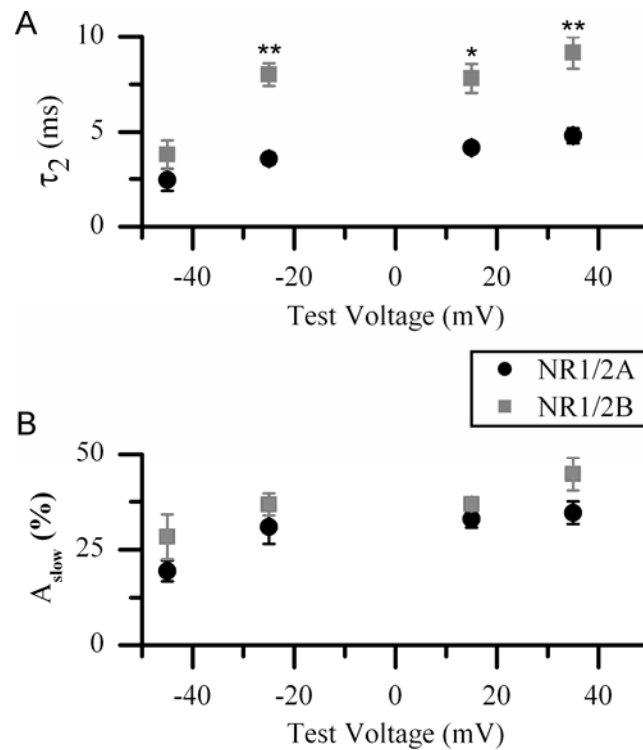


Figure 7. Quantification of the subunit and voltage dependence of Mg^{2+}_o unblocking kinetics. Results from double exponential fits to NR1/2A (black circles) and NR1/2B (grey squares) receptor currents in response to a depolarizing voltage jump from rest (-65 mV) to the indicated test voltages in the presence of 30 μ M NMDA, 10 μ M glycine, and 1 mM Mg^{2+}_o . **A.** Pooled results of τ_2 . τ_2 from fits to NR1/2B receptor currents was significantly slower than τ_2 from fits to NR1/2A receptor currents at all test voltages except -45 mV. τ_2 of both NR1/2A and NR1/2B receptors also showed weak voltage dependence, becoming significantly slower as the amplitude of the depolarizing voltage jump became larger. **B.** Pooled results of A_{slow} . A_{slow} did not differ significantly between NR1/2A and NR1/2B receptors and did not show any significant voltage dependence. * $p < .01$, ** $p < .005$.

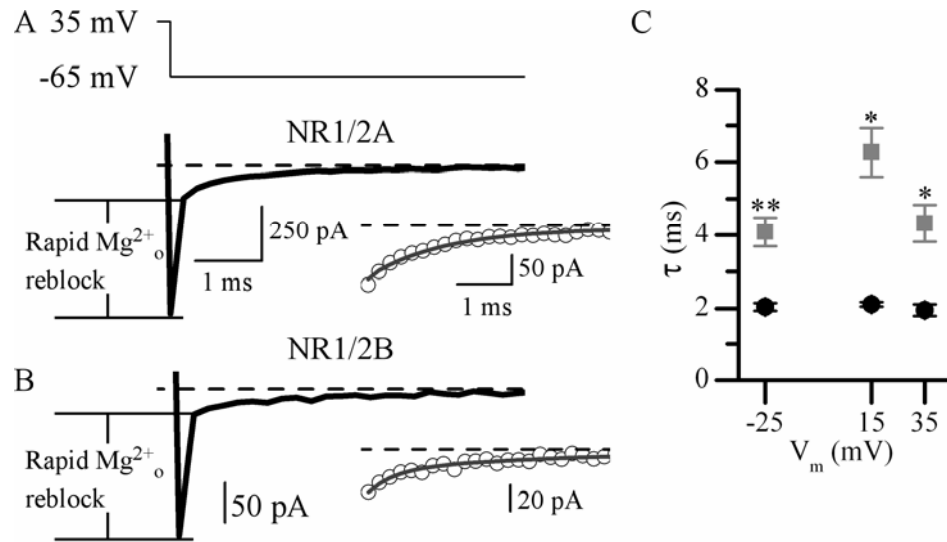


Figure 8. Slow reblock of Mg²⁺. Example traces from NR1/2A (**A**) and NR1/2B (**B**) receptors after the voltage was returned to -65 mV following a 500 ms depolarization to 35 mV in the presence of 30 μM NMDA, 10 μM glycine, and 1 mM Mg²⁺. The majority of Mg²⁺ reblock occurs in under 1 ms (indicated by rapid Mg²⁺ reblock). However, a slow phase of Mg²⁺ reblock is present, which delays the return to baseline current (indicated by dashed black line). *Insets.* Single exponential fits of the slow phase of Mg²⁺ reblock are overlaid as grey lines. **C.** Pooled results from fits to the slow phase of Mg²⁺ reblock. The time constant (τ) of slow of Mg²⁺ reblock of NR1/2B receptors (grey squares) is significantly slower than the τ of slow Mg²⁺ reblock of NR1/2A receptors (black circles) following repolarization to -65 mV from either -25, 15 or 35 mV. ** p < .01, * p < .05.

2.4.3 Dependence of Mg^{2+}_o unblocking kinetics on agonist concentration

Previous experiments investigating slow Mg^{2+}_o unblock have disagreed as to the time course of slow unblock, varying from a single slow component with a τ of 14-23 ms (Vargas-Caballero and Robinson, 2003) to two slow components, one with a τ of ~ 4 ms and one with a $\tau > 100$ ms (Kampa et al., 2004). One prominent difference between these previous studies is the concentration of agonist used to activate NMDA receptors; Vargas-Caballero & Robinson (2003) used 25 μM NMDA where as Kampa et al (2004) used 1 mM glutamate. To determine if the kinetics of Mg^{2+}_o unblock are dependent on the agonist concentration used to activate the receptors, we repeated the protocol described in Figure 1 using 1 mM glutamate or NMDA. Again, in response to a voltage step from -65 to 35 mV, currents from NR1/2A and NR1/2B receptors displayed a prominent slow component of Mg^{2+}_o unblock (**Fig. 9A, B**). In contrast, Mg^{2+}_o unblock from NR1/2C and NR1/2D receptors was dominated by a single fast component ($\tau < 1$ ms, **Table 2**), as observed previously in lower agonist conditions.

Unlike results using 30 μM NMDA, Mg^{2+}_o unblock from NR1/2A and NR1/2B receptors in these high agonist concentrations required a triple exponential equation for an adequate fit (**Fig. 9C**). The tau of the fast component (τ_1) of Mg^{2+}_o unblock did not differ significantly between NR1/2A and NR1/2B receptors (**Fig. 9D**), or depend on the agonist concentration. In contrast, the tau of the dominant slow component (τ_2) of Mg^{2+}_o unblock from NR1/2A receptors was significantly ($p < .005$) faster in 1 mM glutamate as compared to the corresponding τ_2 of Mg^{2+}_o unblock in the presence of 30 μM NMDA. This was also true for the τ_2 of Mg^{2+}_o unblock from NR1/2B receptors. It seems reasonable to compare these two components because the third component observed only in high agonist conditions was not NR2 subunit dependent, had a time constant (τ_3) of several hundred milliseconds, and had a small ($< 10\%$) amplitude (**Fig. 9 D, E**). Despite showing faster kinetics at high agonist concentrations, the τ_2 of Mg^{2+}_o unblock was still NR2 subunit dependent; NR1/2B receptor τ_2 was significantly slower and had a significantly larger amplitude than the corresponding τ_2 from NR1/2A receptors (**Fig. 9 D, E**).

For both NR1/2A and NR1/2B receptors, the main difference between the kinetics of Mg^{2+}_o unblock in 30 μM NMDA versus 1 mM glutamate was an acceleration of the prominent

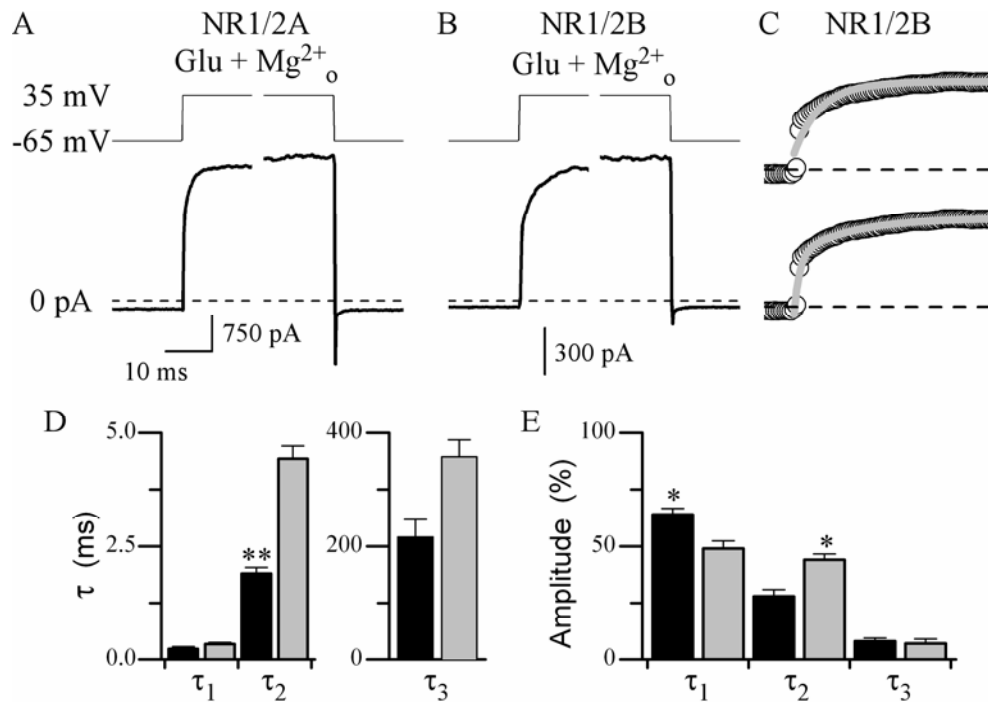


Figure 9. Kinetics of Mg^{2+}_o unblock in high agonist concentration. **A, B.** Examples of the current response to a depolarizing voltage jump (-65 to 35 mV) in the presence of 1 mM glutamate and 10 μ M glycine (termed “Glu”) and 1 mM Mg^{2+}_o from NR1/2A (**A**) or NR1/2B (**B**) receptors. **C.** Examples of double (top) and triple (bottom) exponential fits to NR1/2B receptor mediated currents in response to the voltage jump. A triple exponential equation was also required to obtain adequate fits of NR1/2A receptor mediated currents (data not shown). **D, E.** Pooled results from triple exponential fits of whole-cell current responses to a depolarizing voltage jump from NR1/2A (n = 4, black bars) and NR1/2B (n = 4, grey bars) receptors. The kinetics of the prominent, intermediate slow component (τ_2) of Mg^{2+}_o unblock is significantly slower and the relative amplitude significantly larger from NR1/2B than from NR1/2A receptors. *p < .01, **p < .0005.

Table 2. Depolarization induced current relaxations in the presence of high agonist concentrations and the absence and presence of 1 mM Mg²⁺_o

NR1/2A receptors; 1 mM NMDA, 10 μM glycine					
[Mg²⁺_o]	τ₁ (ms)	τ₂ (ms)	τ₃ (ms)	A_{slow} (%)	A_{slow2} (%)
0	0.21 ± 0.05	N/A	158.9 ± 30.3	N/A	2.6 ± 0.1
1	0.32 ± 0.05	1.87 ± 0.50 *	296.7 ± 134.2	28.1 ± 1.7 *	5.3 ± 1.2
NR1/2B receptors; 1 mM NMDA, 10 μM glycine					
[Mg²⁺_o]	τ₁ (ms)	τ₂ (ms)	τ₃ (ms)	A_{slow} (%)	A_{slow2} (%)
0	0.19 ± 0.04	3.46 ± 0.95	135.0 ± 11.4	15.3 ± 2.2	1.1 ± 1.0
1	0.30 ± 0.04	5.12 ± 0.30 *	114.2 ± 40.1	42.4 ± 3.6 *	2.9 ± 0.6
NR1/2A receptors; 1 mM glutamate, 10 μM glycine					
[Mg²⁺_o]	τ₁ (ms)	τ₂ (ms)	τ₃ (ms)	A_{slow} (%)	A_{slow2} (%)
0	0.19 ± 0.02	N/A	205.4 ± 49.0	N/A	6.4 ± 0.6 *
1	0.23 ± 0.05	1.89 ± 0.14 *	216.3 ± 30.7	28.0 ± 2.9 *	8.0 ± 1.5
NR1/2B receptors; 1 mM glutamate, 10 μM glycine					
[Mg²⁺_o]	τ₁ (ms)	τ₂ (ms)	τ₃ (ms)	A_{slow} (%)	A_{slow2} (%)
0	0.19 ± 0.02	4.31 ± 0.96	325.2 ± 172.2	10.4 ± 1.0	3.3 ± 0.7 *
1	0.34 ± 0.03	4.43 ± 0.28 *	357.8 ± 62.7	44.0 ± 2.5 *	7.0 ± 2.0

Membrane voltage was stepped from -65 to 35 mV during the steady-state response from HEK 293T cells expressing the NR1 and the indicated NR2 subunit. * indicates a significant ($p > .01$) difference between the values from NR1/2A and the corresponding value from NR1/2B receptors. Values are expressed as mean ± SEM.

slow component of unblock (termed τ_2 in both agonist conditions). This could be an agonist specific difference, but this is unlikely because similar results to those shown with 1 mM glutamate were obtained using 1 mM NMDA (**Table 2**). Instead, this difference may result from an increase in channel open probability (P_{open}) that results from increasing agonist concentration. The hypothesis that a larger P_{open} leads to a faster τ_2 of Mg^{2+}_o unblock is consistent with our observation that τ_2 is faster from NR1/2A than NR1/2B receptors (**Fig. 7**): NR1/2A receptors have a higher P_{open} than NR1/2B receptors (Chen et al., 1999b; Erreger et al., 2005).

Based on this hypothesis, any manipulation that raises the P_{open} of the receptor should accelerate the slow component of Mg^{2+}_o unblock. To test this hypothesis, we repeated the protocol in Figure 1 with NR1/2B receptors at pH 8.2, which reduces proton inhibition (Giffard et al., 1990; Tang et al., 1990; Traynelis and Cull-Candy, 1990) and hence raises P_{open} . Under these conditions τ_2 was significantly ($p = .02$) accelerated from $9.15 \pm .93$ ms at pH 7.2 to 3.93 ± 0.77 ms at pH 8.2. A_{slow} was also reduced from 44.7 ± 4.8 % at pH 7.2 to 32.7 ± 1.3 % at pH 8.2, although this difference did not reach statistical significance. These data support the hypothesis that the differences in Mg^{2+}_o unblock from NR1/2A and NR1/2B receptors are due to differences in P_{open} .

2.4.4 Effect of the timing of membrane depolarization on Mg^{2+}_o unblocking kinetics

The relative timing of synaptic NMDA receptor activation and postsynaptic depolarization plays a critical role in determining whether Ca^{2+} influx via NMDA receptors will lead to long term changes in synaptic strength (Magee and Johnston, 1997; Markram et al., 1997; Bi and Poo, 1998). Previous work has shown that the kinetics of Mg^{2+}_o unblock from native NMDA receptors also depend on the relative timing of receptor activation and postsynaptic depolarization; unblock was slower following prolonged receptor activation (Kampa et al., 2004). We next determined if the kinetics of Mg^{2+}_o unblock are NR2 subunit dependent when unblock is stimulated shortly following receptor activation.

For these experiments we used lifted HEK 293T cells, which allowed rapid exchange of the external solution (90 % complete in < 1 ms). To verify that glutamate application to lifted HEK 293T cells transfected with NR1/2A or NR1/2B receptors was rapid, we measured the rise

time of NMDA currents. The 10-90 % rise times of currents activated by 1 mM glutamate in the presence of 1 mM Mg^{2+}_o at a constant membrane potential of -65 mV was: NR1/2A receptors, $4.87 \pm .61$ ms ($n = 6$); NR1/2B receptors, 9.95 ± 1.39 ms ($n = 5$). These are similar to previously published values for the rise times of NR1/2A and NR1/2B receptor currents in the absence of Mg^{2+}_o (Chen et al., 1999b; Erreger et al., 2005).

In the presence of 1 mM Mg^{2+}_o , rapid glutamate applications at 35 mV resulted in large outward currents, while current responses to glutamate applications at -65 mV were largely blocked in both NR1/2A and NR1/2B receptors (**Fig. 10 A,B**). Voltage jumps from -65 to 35 mV applied after a ~15 ms delay following glutamate application resulted in outward currents which relaxed towards the current observed during glutamate application with the cell held at 35 mV. However, the current in response to the voltage jump did not immediately join the current during the glutamate application at 35 mV, indicating a slow component of Mg^{2+}_o unblock (**Fig. 10 A,B**). The voltage jump was time-locked to barrel movement signal, which resulted in some jitter between receptor activation and membrane depolarization due to variability in the distance between the barrels and the lifted cell. However, the average timing between receptor activation and membrane depolarization was similar in NR1/2A (15.0 ms) and NR1/2B (14.3 ms) receptors.

To quantify the kinetics of Mg^{2+}_o unblock, the current in response to the voltage jump was normalized to the current evoked by glutamate application while the cell was held at 35 mV. The normalized currents in response to these voltage jumps that occurred shortly after receptor activation were well fit with a double exponential equation. A triple exponential equation was not needed because a very slow component (τ of several hundred ms), which was observed when a prolonged application of 1 mM glutamate preceded the voltage jump, was absent. The time constant of the fast component (τ_1) of unblock did not differ significantly between NR1/2A and NR1/2B receptors with values of 0.22 ± 0.04 ms and 0.24 ± 0.06 ms, respectively. In contrast, the time constant of the slow component (τ_2) of Mg^{2+}_o unblock from NR1/2B receptors, $3.69 \pm .38$ ms, was significantly ($p < .01$) slower than from NR1/2A receptors, $2.13 \pm .27$ ms. In these experiments the amplitude of the slow component was similar for NR1/2A and NR1/2B receptors, with values of 32.2 ± 8.3 % and 44.1 ± 7.8 %, respectively. Thus, our data suggest that the kinetics of Mg^{2+}_o unblock depend slightly on the timing between receptor activation and membrane depolarization, with a very slow component ($\tau > 100$ ms) occurring only after prolonged receptor activation. However, in all situations Mg^{2+}_o unblock proceeds more rapidly

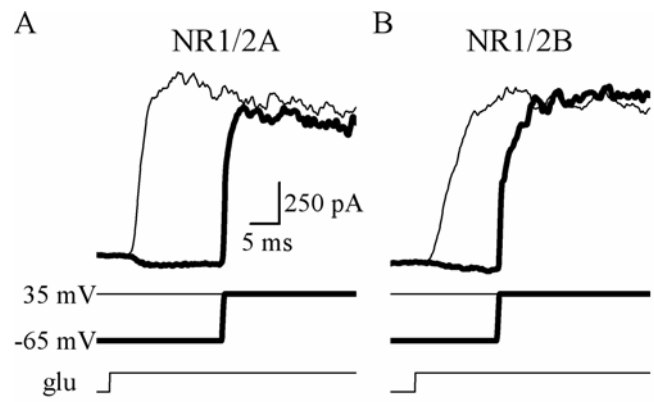


Figure 10. Mg^{2+}_o unblock near the time of onset of NMDA receptor activity. A, B. Example traces during a rapid application of 1 mM glutamate in the presence of 1 mM Mg^{2+}_o either while the cell was held at 35 mV (thin trace) or during a voltage-jump from -65 to 35 mV (thick trace) from NR1/2A receptors (**A**) and NR1/2B receptors (**B**). The timing of the voltage jump and the barrel movement are indicated by the middle and bottom traces respectively. Current traces were re-filtered at 1 kHz for display.

from NR1/2A than from NR1/2B receptors.

2.4.5 Effect of varying the duration of depolarization on Mg^{2+}_o unblock

Ca^{2+} influx through NMDA receptors plays a critical role in many physiological processes. The kinetics of Mg^{2+}_o unblock during membrane depolarization determines how many NMDA receptors become unblocked and hence available to pass inward current upon membrane repolarization. The repolarization-induced peak of inward current (I_{peak}) is of particular interest because it is the point at which the largest NMDA receptor-mediated Ca^{2+} influx occurs (Garaschuk et al., 1996). During brief depolarizations, slow Mg^{2+}_o unblock should reduce the fraction of NMDA receptors from which Mg^{2+}_o unblocks, and thus the fraction of receptors available to pass inward current during repolarization. In addition, brief depolarizations should be less effective at stimulating Mg^{2+}_o unblock from NR1/2B receptors (from which Mg^{2+}_o unblock occurs more slowly) than from NR1/2A receptors. Thus, the I_{peak} following brief depolarizations should be reduced compared to the I_{peak} following long depolarizations, and the reduction should be greater for NR1/2B than NR1/2A receptors. To test these hypotheses, we applied rapid voltage jumps from rest to 35 mV of varying duration (1, 2, 5, 10, 50 ms) in the presence of 1 mM glutamate and 1 mM Mg^{2+}_o . Because there is not a strong effect of the timing between receptor activation and membrane depolarization on the kinetics of Mg^{2+}_o unblock (see above), depolarizations were applied during prolonged agonist application (similar to **Fig. 4**). This allowed multiple voltage jumps to be applied during a single agonist application. Depolarizations were separated by 100 ms intervals, which is more than 10-fold longer than the τ of the slow component of Mg^{2+}_o reblock, allowing steady-state block to be reached between each depolarization.

As expected, longer duration depolarizations resulted in a larger I_{peak} (**Fig. 11A**). To quantify the relationship between depolarization duration and I_{peak} , all I_{peak} values were normalized to the I_{peak} following a 50 ms depolarization. In experiments from both NR1/2A and NR1/2B receptors, 1 ms depolarizations induced an I_{peak} that was less than 70 % of the I_{peak} following a 50 ms depolarization (**Fig. 11B**). Only after the depolarization duration was increased to 10 ms was the I_{peak} not significantly smaller than the I_{peak} following a 50 ms depolarization. In addition, following depolarizations of less than 10 ms, the normalized I_{peak}

from NR1/2A receptors were significantly larger than the normalized I_{peak} from NR1/2B receptors (**Fig. 11B**). Thus, slow Mg^{2+}_o unblock blunts inward currents through NR1/2A and NR1/2B receptors following brief depolarizations. However, brief depolarizations (< 10 ms) are able to stimulate more Mg^{2+}_o unblock from NR1/2A than from NR1/2B receptors.

Although square voltage jumps are easily applied experimentally, physiological voltage changes occur with slower rising and falling phases. Recently, there has been a strong interest in back-propagating APs (b-APs) invading the dendritic tree and providing the depolarization needed for Mg^{2+}_o unblock of NMDA receptors during synaptic activity (Magee and Johnston, 1997; Markram et al., 1997; Bi and Poo, 1998). Within dendrites near the soma b-APs are rapid, often having a half-width of less than 2 ms. Further out in the dendritic tree the b-AP half-width can be > 10 ms (Bernard and Johnston, 2003). In all instances the rising and falling phases of b-AP waveforms are slower than the square pulses we have employed above.

To test if the NR2 subunit-dependent differences in Mg^{2+}_o unblocking kinetics also impact NMDA receptor activity during physiological depolarizations, we voltage-clamped transfected HEK 293T cells to AP waveforms. Three waveforms were used: an unmodified AP recorded from the soma of a hippocampal CA1 pyramidal cell (termed somatic AP), and two APs that we modified so the duration at the most depolarized voltage was 5 ms (5 ms extended AP) or 25 ms (25 ms extended AP). The ability of each waveform to generate inward current through NMDA receptors following Mg^{2+}_o unblock was quantified by measuring the peak inward current during the repolarizing phase of the APs ($I_{\text{peak,AP}}$). The 25 ms extended AP should give maximum Mg^{2+}_o unblock from both NR1/2A and NR1/2B receptors. Thus, $I_{\text{peak,AP}}$ induced by the somatic AP and by the 5 ms extended AP were normalized to $I_{\text{peak,AP}}$ induced by the 25 ms extended AP. The normalized values of $I_{\text{peak,AP}}$ for the 5 ms AP were close to 1 for both NR1/2A and NR1/2B receptors (**Fig. 11C,D**). This suggests that the 5 ms and 25 ms extended APs induced a similar amount of Mg^{2+}_o unblock. In contrast, the normalized values of $I_{\text{peak,AP}}$ for the somatic AP were significantly ($p < .001$) less than 1 for both NR1/2A and NR1/2B receptors (**Fig. 11C,D**). Thus, the somatic AP was too brief to stimulate full Mg^{2+}_o unblock from either NR1/2A or NR1/2B receptors. The normalized value of $I_{\text{peak,AP}}$ for the somatic AP was also significantly smaller for NR1/2A than for NR1/2B receptors (**Fig. 11D**). This suggests that somatic APs are more effective at stimulating Mg^{2+}_o unblock from NR1/2A than from NR1/2B receptors. Thus, during synaptic activity, postsynaptic APs coincident with presynaptic

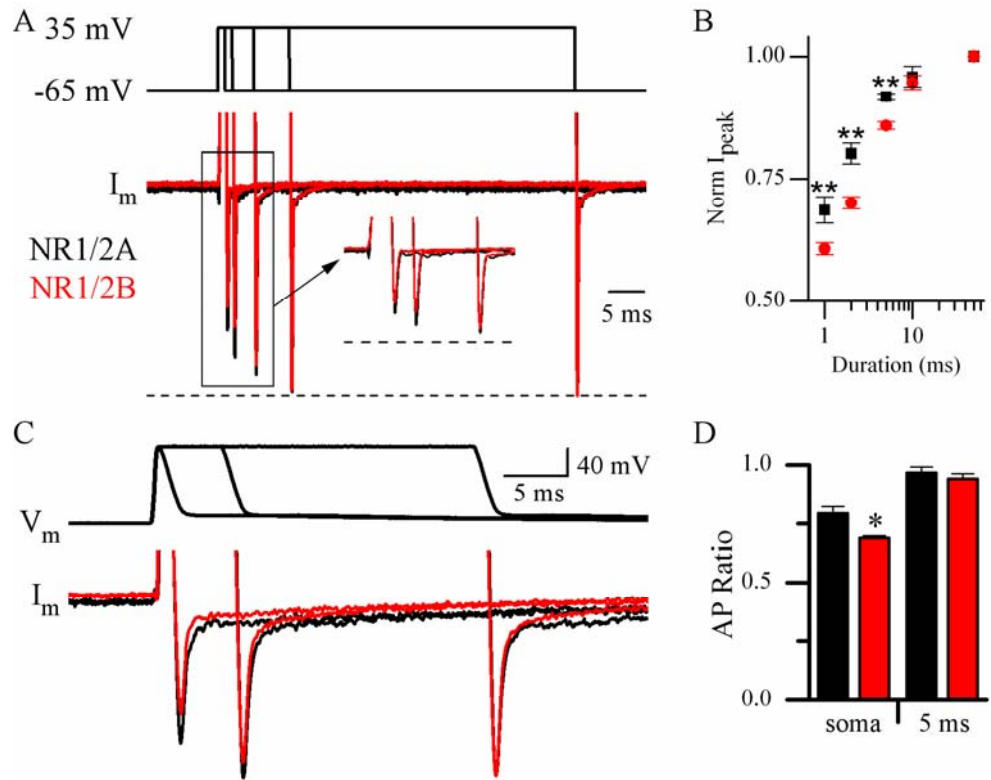


Figure 11. Brief depolarizations are more effective at stimulating Mg^{2+} o, unblock from NR1/2A than from NR1/2B receptors. **A.** Superimposed currents from NR1/2A (black) and NR1/2B (red) receptors (lower traces) during depolarizations of varying duration (1, 2, 5, 10, and 50 ms; indicated by top traces) in the presence of 1 mM glutamate, 10 μ M glycine, and 1 mM Mg^{2+} o. Currents are normalized to the I_{peak} value following a 50 ms depolarization. The value of $I_{B_{peak}}$ following the 50 ms depolarization is indicated by a dotted line. *Inset.* Blow-up of the normalized inward peaks in response to the briefest depolarizations (1, 2, and 5 ms). **B.** Comparison of the I_{peak} values following depolarizations of varying duration. Results are from NR1/2A (n = 5, black) and from NR1/2B (n = 4, red) receptors. I_{peak} values were normalized to the I_{peak} following a 50 ms depolarization. **C.** Superimposed currents (lower traces) from NR1/2A (black) and NR1/2B (red) receptors during three APs (somatic, 5 ms extended, and 25 ms extended; upper traces) in the presence of 1 mM glutamate, 10 μ M glycine, and 1 mM Mg^{2+} o. Traces are normalized to the I_{peak} , AP induced by the 25 ms extended AP. **D.** Pooled ratios of I_{peak} , AP values in response to the somatic or 5 ms extended APs normalized to the I_{peak} , AP value in response to the 25 ms extended AP. Results are from NR1/2A (black bars) and NR1/2B (red bars) receptors. **p < .0005, *p < .01.

glutamate release are more effective at stimulating Mg^{2+}_o unblock from NR1/2A than from NR1/2B receptors.

2.5 DISCUSSION

Many pharmacological and biophysical properties of NMDA receptors are, at least in part, determined by the identity of the NR2 subunit (Dingledine et al., 1999). Our results show that Mg^{2+}_o unblocking kinetics are also NR2 subunit dependent. Mg^{2+}_o unblocks from NR1/2A and NR1/2B receptors with a prominent slow component that is not present when Mg^{2+}_o unblocks from NR1/2C or NR1/2D receptors (Fig. 5). In addition, the slow component of Mg^{2+}_o unblock from NR1/2A and NR1/2B receptors is not equivalent; Mg^{2+}_o unblocks from NR1/2B receptors more slowly than from NR1/2A receptors (Fig. 7). These NR2 subunit differences in Mg^{2+}_o unblock render brief depolarizations, including APs, more effective at stimulating Mg^{2+}_o unblock from NR1/2A than from NR1/2B receptors (Fig. 11).

2.5.1 Comparison with previous studies

Our data are consistent with previous studies describing slow Mg^{2+}_o unblock from native hippocampal and cortical NMDA receptors (Spruston et al., 1995; Vargas-Caballero and Robinson, 2003; Kampa et al., 2004) in that the hippocampus and cortex predominantly express the NR2A and NR2B subunits (Monyer et al., 1994). Our data also provide potential explanations for discrepancies between previous studies of the kinetics of Mg^{2+}_o unblock. When depolarizations occurred during prolonged receptor activation, Vargas-Caballero and Robinson (2003) reported that slow Mg^{2+}_o unblock had a single component ($\tau_{s1} > 10$ ms), while Kampa et al. (2004) reported that slow Mg^{2+}_o unblock contained two components ($\tau_{s1} \sim 4$ ms and $\tau_{s2} \sim 300$ ms). One experimental difference between these two studies is the concentration of agonists used to activate NMDA receptors. Vargas-Caballero and Robinson (2003) used 25 μ M NMDA whereas Kampa et al (2004) used 1 mM glutamate. We find that at high agonist concentrations the main component of slow Mg^{2+}_o unblock is accelerated (from τ_2 between 5-9 ms to a τ_2

between 2-5 ms) and an additional very slow component ($\tau = 200-400$ ms) is discernable (Fig. 9). It is also likely that the τ_{s1} reported by Vargas-Caballero and Robinson (2003) was slower than the τ_{s1} reported by Kampa et al (2004) because Vargas-Caballero and Robinson (2003) used younger animals than Kampa et al (2004), which should express a higher percentage of NR1/2B receptors.

The additional very slow component of Mg^{2+}_o unblock is not present when depolarizations occur shortly after agonist application (Fig. 40). This is in agreement with Kampa et al (2004) and shows that the kinetics of Mg^{2+}_o unblock depend on the relative timing of receptor activation and membrane depolarization. However, following prolonged glutamate application, we find that the very slow component of Mg^{2+}_o unblock accounts for less than 10% of the total outward current relaxation, rather than $\sim 30\%$ of the total outward current relaxation reported previously (Kampa et al., 2004). The source of this discrepancy is not clear. Resolution of this conflict is important because changes in the kinetics of Mg^{2+}_o unblock with prolonged receptor activation influences the time window for STDP induction (Kampa et al., 2004).

Several previously published models of NMDA receptor function (Jahr and Stevens, 1990a; Antonov and Johnson, 1999; Sobolevsky and Yelshansky, 2000) do not predict a slow component of Mg^{2+}_o unblock in response to a depolarizing voltage jump (data not shown). To explain the surprising observation of slow Mg^{2+}_o unblock, two models have been proposed (Kampa et al., 2004; Vargas-Caballero and Robinson, 2004). These models suggest that occupation of the channel by Mg^{2+}_o moderately accelerates only the rate of channel closure (Vargas-Caballero and Robinson, 2004), or accelerates the rates of channel closure and agonist unbinding, along with increasing the occupancy of desensitized states (Kampa et al., 2004). These models predict accurately the appearance of slow component(s) of Mg^{2+}_o unblock. They also are supported by the observed reduction in single-channel burst duration of cortical NMDA receptors in the presence of Mg^{2+}_o (Ascher and Nowak, 1988), as would be predicted if Mg^{2+}_o accelerates channel closure. These models, however, are not fully consistent with other observations. If Mg^{2+}_o accelerates channel closure, the IC_{50} for Mg^{2+}_o inhibition of whole-cell currents should be lower than the $Mg^{2+}_o K_d$ calculated from single-channel measurements, a prediction that disagrees with previous measurements (Qian et al., 2002). Additional relevant data involve the organic NMDA receptor channel blocker amantadine, which unblocks from open channels even faster than Mg^{2+}_o . Burst analysis demonstrated that amantadine does

moderately accelerate channel closure (Blanpied et al., 2005). Following a depolarizing voltage step, amantadine, like Mg^{2+}_o , exhibits a slow component of channel unblock. However, the slow component of unblock is much slower for amantadine than for Mg^{2+}_o (Blanpied et al., 2005). These data suggest that a complete understanding of the mechanistic basis of the slow component of Mg^{2+}_o unblock awaits further research.

We have also described here a slow component of Mg^{2+}_o reblock of NR1/2A and NR1/2B receptors (Fig. 8). This contrasts with previous studies (Spruston et al., 1995; Vargas-Caballero and Robinson, 2003; Kampa et al., 2004), which report near instantaneous Mg^{2+}_o reblock of native NMDA receptors. Because the slow phase of Mg^{2+}_o reblock observed here is small, it is possible that it was not observed in previous studies using nucleated patches (Spruston et al., 1995; Vargas-Caballero and Robinson, 2003; Kampa et al., 2004), which typically yield relatively small currents. We were able to quantify slow Mg^{2+}_o reblock only from whole-cell records that had large currents (> 100 pA) at -65 mV in the presence of 1 mM Mg^{2+}_o . Although of small amplitude, the slow phase of Mg^{2+}_o reblock provides a relatively long window during which highly significant Ca^{2+} influx could occur following a postsynaptic AP that coincides with synaptic input.

We have studied NMDA receptors containing one of the four NR2 subunits. However, there is evidence that triheteromeric receptors, which contain more than one type of NR2 subunit, exist within many brain regions, including the cortex (Sheng et al., 1994; Chazot and Stephenson, 1997; Luo et al., 1997), cerebellum (Chazot et al., 1994; Cathala et al., 2000; Brickley et al., 2003), and substantia nigra (Jones and Gibb, 2005). Co-expression of the NR1, NR2A, and NR2D subunits in *Xenopus* oocytes yields a receptor with many characteristics intermediate between NR1/2A and NR1/2D receptors (Cheffings and Colquhoun, 2000). It is tempting to speculate that triheteromeric receptors would show intermediate Mg^{2+}_o unblocking kinetics. However, testing this hypothesis would be challenging because presently it is difficult to isolate triheteromeric receptors within heterologous systems (Vicini et al., 1998).

2.5.2 Implications for synaptic plasticity

Ca^{2+} influx through NMDA receptors during coincident synaptic activity and postsynaptic depolarization underlies long-term changes in synaptic strength at many synapses (Bliss and

Collingridge, 1993). However, not all NMDA receptors are equivalent. Because NR1/2C and NR1/2D receptors have a lower affinity for Mg^{2+} (Monyer et al., 1994; Kuner and Schoepfer, 1996; Qian et al., 2005), they allow significant Ca^{2+} influx near typical resting membrane potentials where NR1/2A and NR1/2B receptors are more than 95% blocked. In addition, we show here that the relatively weak Mg^{2+} block of NR1/2C and NR1/2D receptor currents is more rapidly relieved upon depolarization than Mg^{2+} block of NR1/2A and NR1/2B receptor currents (Fig. 5). Thus, Mg^{2+} block has a stronger influence on NR1/2A and NR1/2B receptor currents than NR1/2C and NR1/2D receptor currents, rendering NR1/2A and NR1/2B receptors are more effective coincidence detectors.

Several recent studies have suggested that selective NR1/2A receptor activation leads preferentially to long-term potentiation (LTP), while selective NR1/2B receptor activation leads to long-term depression (LTD) (Liu et al., 2004; Massey et al., 2004; Kim et al., 2005; Mallon et al., 2005). Based on proposed differences in the Ca^{2+} threshold for LTP and LTD induction (Bienenstock et al., 1982; Cormier et al., 2001), our data suggest a mechanism that could help differentiate the physiological impact of NR1/2A and NR1/2B receptor activation. In response to brief membrane depolarizations, the relatively faster unblock of Mg^{2+} from NR1/2A receptors would result in greater Ca^{2+} influx (Fig. 41), favoring LTP, while the relatively slower unblock of Mg^{2+} from NR1/2B receptors would result in lower Ca^{2+} influx, favoring LTD. It should be noted, however, that it is unlikely that there is an exclusive association of NR1/2A receptors with LTP and of NR1/2B receptors with LTD (Tang et al., 1999; Berberich et al., 2005; Toyoda et al., 2005; Weitlauf et al., 2005; Neyton and Paoletti, 2006).

In many studies of the NR2 subunit dependence of synaptic plasticity, induction protocols that involve pairing of presynaptic stimulation with prolonged postsynaptic depolarization are used. Such induction protocols reduce the relevance of the kinetics of Mg^{2+} unblock. We also expect slow Mg^{2+} unblock to have limited impact during relatively small synaptic depolarizations: slow unblock time constants are faster, amplitudes are smaller, and NR2 subunit-dependent differences are smaller at more hyperpolarized potentials (Fig. 7). The kinetics of Mg^{2+} unblock are most clearly of critical importance when plasticity is induced with STDP protocols, which pair synaptic input with postsynaptic APs (Magee and Johnston, 1997; Markram et al., 1997; Bi and Poo, 1998). The NR2 subunit differences in Mg^{2+} unblock

kinetics reported here should help determine the magnitude of Ca^{2+} influx mediated by NR1/2A and NR1/2B receptors in response to brief, large amplitude depolarizations such as APs.

3.0 MODULATION OF NR1/2B RECEPTOR ACTIVATION BY MEMBRANE VOLTAGE

3.1 ABSTRACT

Ligand-gated ion channels, such as NMDA receptors, are activated by binding of agonists. However, previous work has suggested that the gating of some ligand-gated channels is also modulated by membrane voltage. Here we demonstrate a depolarization-induced enhancement of NR1/2B receptor-mediated currents. Potentiation of NR1/2B receptor currents at depolarized voltages is manifested by a slow component of current relaxation in response to membrane depolarization. In addition, stepping the cell membrane from a positive to a negative potential induces a tail current that increases as the starting voltage is made increasingly more positive. Based on experiments in 0 Mg^{2+}_o , we develop a kinetic model of NR1/2B receptor activation which incorporates weak inherent voltage dependence of gating. This model not only accurately predicts current relaxations in response to membrane depolarization in 0 Mg^{2+}_o , but the model also accounts for the previously described slow component of Mg^{2+}_o unblock. The voltage dependence of NR1/2B receptor gating is not strong enough to result in significant enhancement of NR1/2B receptor currents during rapid, or small, depolarizations such as AP waveforms. However, the NR1/2B Model can partially reproduce the voltage dependence of NMDA-EPSC decay previously reported at several synapses.

3.2 INTRODUCTION

NMDA receptors are a subtype of ligand-gated, ionotropic glutamate receptors that participate in fast excitatory synaptic transmission throughout the mammalian CNS. Functional NMDA

receptors are heterotetramers, most commonly composed of NR1 and NR2 subunits. There are eight NR1 subunit isoforms that arise due to alternative splicing and four NR2 subunit gene products (NR2A-D). The NR2 subunit helps to determine many biophysical and pharmacological receptor properties (Cull-Candy et al., 1998; Dingledine et al., 1999; Cull-Candy and Leszkiewicz, 2004). NMDA receptors are critically involved in a number of physiological processes, including synapse formation (Li et al., 1994; Iwasato et al., 1997) and many forms of synaptic plasticity (Bliss and Collingridge, 1993; Bear and Abraham, 1996; Malenka and Bear, 2004). NMDA receptor dysfunction has also been implicated in neuronal death following stroke, as well as several diseases, including schizophrenia, Parkinson's, and Alzheimer's (Meldrum, 1992; Cull-Candy et al., 2001; Moghaddam, 2003; Hynd et al., 2004; Sonkusare et al., 2005).

NMDA receptors have several unusual properties, including high Ca^{2+} permeability (Mayer et al., 1987; Schneggenburger et al., 1993) and strong voltage-dependent block by Mg^{2+} (Mayer et al., 1984; Nowak et al., 1984). Mg^{2+} block of NMDA receptors is nearly complete at typical resting membrane potentials, and is only relieved upon membrane depolarization (Mayer et al., 1984; Nowak et al., 1984). Thus, significant NMDA receptor mediated current occurs only during periods of coincident presynaptic glutamate release and postsynaptic depolarization.

Although voltage-dependent block by Mg^{2+} is a hallmark of NMDA receptors, several observations suggest that NMDA receptors display an additional, inherent, sensitivity to membrane voltage. These observations include voltage-dependent decay of NMDA receptor mediated excitatory postsynaptic currents (NMDA-EPSCs) (Konnerth et al., 1990; Keller et al., 1991; D'Angelo et al., 1994), slow relaxation kinetics of NMDA receptor mediated currents in response to membrane depolarization (Benveniste and Mayer, 1995; Spruston et al., 1995), and an enhancement of channel open probability upon membrane depolarization (Nowak and Wright, 1992; Li-Smerin and Johnson, 1996; Li-Smerin et al., 2001). Voltage-dependent modulation of ligand-gated ion channels is not without precedent. Responses mediated by acetylcholine (Magleby and Stevens, 1972), AMPA (Raman and Trussell, 1995), and invertebrate glutamate (Dudel, 1974; Onodera and Takeuchi, 1978; Tour et al., 1998) receptors have all been shown to be augmented by membrane voltage due to voltage-dependent changes of channel gating.

Previous studies utilizing rapid membrane depolarizations have described a slow component of Mg^{2+} unblock from native NMDA receptors (Vargas-Caballero and Robinson,

2003; Kampa et al., 2004) and recombinant NR1/2A and NR1/2B receptors (Clarke and Johnson, 2006). Although most prominent in the presence of Mg^{2+}_o , a slow component of NR1/2B receptor current relaxation was also observed in the absence of Mg^{2+}_o (Clarke and Johnson, 2006). Here, we set out to determine if a relationship exists between inherent voltage dependence of NR1/2B receptor activation, slow current relaxations in 0 Mg^{2+}_o , and the slow component of Mg^{2+}_o unblock.

We find that NR1/2B receptor currents are enhanced upon depolarization. To account for the depolarization-induced current potentiation, we developed a model of NR1/2B receptor activation which includes weak voltage dependence of channel gating. The voltage dependence was such that, upon depolarization, the channel opens more rapidly. We go on to show that without any additional modifications, the NR1/2B model is able to account for the slow component of Mg^{2+}_o unblock. Finally, we show that the NR1/2B model can partially account for the voltage-dependent decay of NMDA-EPSCs described at many central synapses (Konnerth et al., 1990; Keller et al., 1991; D'Angelo et al., 1994).

3.3 MATERIALS AND METHODS

3.3.1 Cell culture and transfection

The culture and transfection methods used in this study are described in section 2.3.1.

3.3.2 Solutions

Solutions were prepared and applied according to the procedures described in section 2.3.2. Two external solutions were used in these studies (in mM): normal external solution, NaCl 140, $CaCl_2$ 1, KCl 2.8, and HEPES 10 and symmetric KCl solution, KCl 150 and HEPES 10. Both external solutions were adjusted to a pH of 7.2 with NaOH and the osmolality was adjusted to 290 mmol/kg with sucrose. The junction potential between the pipette and bath solution was 5 mV

and 0 mV for normal and symmetric KCl solutions, respectively. All holding potentials were corrected for junction potentials.

3.3.3 Whole-cell recording

Whole-cell recordings were performed as described in section 2.3.3.

3.3.4 Data analysis and Curve Fitting

Whole-cell currents were leak and capacitance corrected as described in section 2.3.4. NR1/2B receptor currents were then fit with multi-exponential equations as described in section 2.3.4. The number of exponential components was adjusted as necessary to provide high quality fits, as determined visually. NR1/2B receptor currents during I-V curve measurements (**Fig. 17a**) were fit with a double exponential equation. The current amplitudes of the fast (I_{fast}) and slow (I_{slow}) components were converted to conductances (g_{fast} and g_{slow} , respectively) using the following equations:

$$g_{fast} = I_{fast} / (\text{End}V_m - (-100\text{mV})) \quad (1)$$

$$g_{slow} = I_{slow} / (\text{End}V_m - V_{rev}) \quad (2)$$

where $\text{End}V_m$ is the voltage to which the membrane was depolarized and V_{rev} is the reversal potential, which was set to -5 mV as determined from voltage-ramps in 3 cells.

NR1/2B receptors containing the NR1-1a subunit are potentiated by Mg^{2+}_o (Paoletti et al., 1995). Where indicated, NR1/2B receptor currents were normalized to the steady-state outward current level to remove effects of Mg^{2+}_o potentiation and allow comparisons with depolarization induced currents recorded in 0 Mg^{2+}_o .

3.3.5 Kinetic Modeling

All model fitting and current simulations were done using SCoP 4.0 (Simulation Resources, Inc., Berrien Springs, MI). Current simulations in response to membrane depolarizations were run

with zero free parameters. Most parameters were set as described in Erreger *et al.* (2005) (see **Table 5**). The only rates that differed from Erreger *et al.* (2005) were the forward rate of the NR2B subunit pre-gating conformational change (k_{s+}) and the entry into and recovery from desensitized states (**Fig. 15**). The rate k_{s+} depended exponentially on membrane voltage (Hille, 2001). The strength (e-fold per 175 mV) of the voltage sensitivity was determined as described in **Figure 17**. Because desensitization rates and channel number vary from cell to cell, these parameters were determined by fitting the NR1/2B Model to experimental data. With desensitization rates and receptor number as free parameters, the NR1/2B model was fitted to at minimum a 4-s whole-cell current response to application of 1 mM glutamate in the continuous presence of 10 μ M glycine +/- 1 mM Mg^{2+}_o at -65 mV using SCoP (**Fig. 17-19**)

After determination of receptor number and desensitization rates, all rates were fixed and model simulations were run in response to depolarizations from -65 mV to both 35 and 95 mV (0 Mg^{2+}_o) or -65 mV to -25, 35, and 95 mV (1 mM Mg^{2+}_o) (**Fig. 17-19**). The kinetics of the depolarization induced current relaxation from simulations were determined as described in the Data analysis and Curve Fitting section. Due to the complexity of the models, simulated current relaxations contained several exponential components. The depolarization induced relaxation of current simulations in 0 Mg^{2+}_o contained three exponential components and in 1 mM Mg^{2+}_o four exponential components. The amplitudes of all the exponential components of current simulations with τ 's > 1 ms were summed for comparisons with experimental data (**Fig. 19d**). The amplitude of the exponential components of current simulations were summed because each component was only separated by a few ms and would not have been easily isolated by fits of experimental data.

3.4 RESULTS

3.4.1 Slow development of outward currents persists in the absence of Mg^{2+}_o

Whole-cell currents from HEK 293T cells expressing NR1/2B receptors were elicited by application of 30 μ M NMDA in the continuous presence of 10 μ M glycine and 0 or 1 mM

Mg²⁺_o. Once the whole-cell current had reached a steady-state level, the cell was depolarized from -65 mV to one of several positive voltages for 500 ms (**Fig. 12a**). In 1 mM Mg²⁺_o, current relaxations in response to depolarization displayed slow as well as fast components, reflecting the slow component of Mg²⁺_o unblock (Vargas-Caballero and Robinson, 2003; Kampa et al., 2004; Vargas-Caballero and Robinson, 2004; Clarke and Johnson, 2006). In response to large depolarizations (-65 to 95 mV), current relaxations in 0 Mg²⁺_o also displayed a prominent slow component (**Fig. 12b**).

We fit current relaxations in 0 and 1 mM Mg²⁺_o with a double exponential equation (**Fig. 12b**). The time constants of the fast (τ_{fast}) and slow (τ_{slow}) components did not depend significantly on the presence of Mg²⁺_o, or on the size of the depolarization (**Table 3**). In contrast, the amplitude of the slow component (A_{slow}) was significantly larger in 1 mM than in 0 Mg²⁺_o in response to all depolarizations (**Fig. 12c**). In both the presence and absence of Mg²⁺_o, increasing the amplitude of the depolarization resulted in a concomitant increase in A_{slow} (**Fig. 12c**). It is unlikely that the slow relaxation in 0 Mg²⁺_o was due to contaminating Mg²⁺_o, because residual Mg²⁺_o in our solutions was previously estimated to be less than 2 μM (Antonov and Johnson, 1996). In addition, unblock of residual Mg²⁺_o would not be consistent with the observed voltage dependence of the slow component (**Fig 12c**).

Slow current relaxation in response to depolarization in 0 Mg²⁺_o would be consistent with the NMDA receptor channel moving slowly into a higher P_{open} mode at depolarized membrane potentials. The NMDA receptor P_{open} has previously been reported to be greater at positive membrane potentials (Nowak and Wright, 1992; Li-Smerin and Johnson, 1996; Li-Smerin et al., 2001). To test the hypothesis that the P_{open} of the NMDA receptor channel is enhanced at depolarized voltages, we examined the current response to repolarization to -65 mV from a depolarized voltage. Upon repolarization to -65 mV, a tail current was observed which surpassed the subsequent steady-state current level at -65 mV (**Fig. 13a**). The repolarization induced peak of inward current (I_{peak}) depended significantly on the amplitude of the previous depolarization, becoming larger following repolarization from more positive voltages (**Fig. 13b**). After the initial peak, the tail current slowly returned to the baseline current level. The return to baseline was well fit by a single exponential equation with τ 's of 6.4 ± 2.2 , 5.3 ± 0.8 , 3.0 ± 0.2 , and 4.8 ± 0.3 ms following repolarization to -65 from 15, 35, 55 and 95 mV, respectively. These results are consistent with the hypothesis that the P_{open} of the NMDA receptor channel is slowly

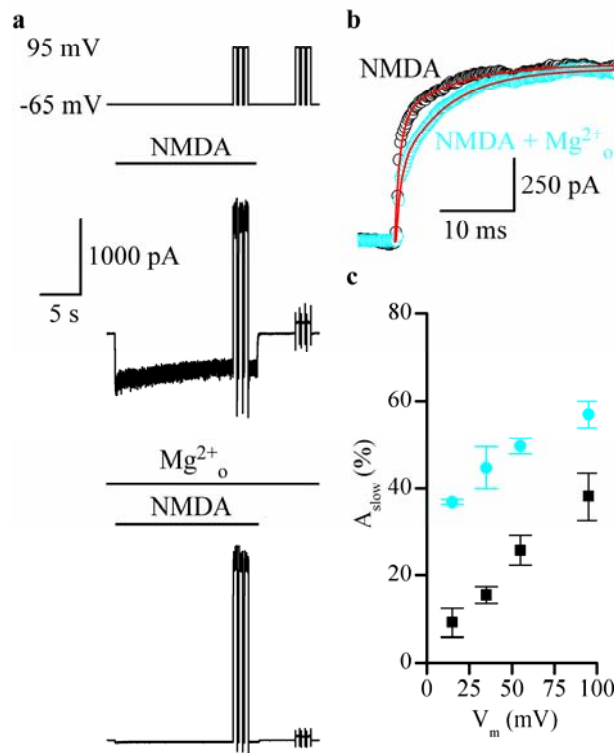


Figure 12. NR1/2B receptor currents display a prominent slow relaxation in both the absence and presence of Mg^{2+}_o in response to membrane depolarization. (a) Current traces during application of 30 μ M NMDA and 10 μ M glycine (termed NMDA) in the absence (top current trace) and presence (bottom current trace) of 1 mM Mg^{2+}_o . 500 ms depolarizing voltage jumps (-65 mV to 95 mV, top trace) were applied in both the presence and absence of NMDA. Voltage jumps applied in the absence of NMDA were used for leak and capacitance subtraction. (b) Currents in response to a voltage jump from -65 to 95 mV in the absence (black) and presence (cyan) of 1 mM Mg^{2+}_o . Double exponential fits are overlaid in red. Currents are normalized to the steady-state outward current response at 95 mV to account for Mg^{2+}_o potentiation (Paoletti et al., 1995) (c) The percentage of the total current relaxation carried by the slow component (A_{slow}) was determined from double exponential fits. A_{slow} was significantly larger ($p < .005$) in the presence (cyan) than in the absence (black) of 1 mM Mg^{2+}_o in response to voltage jumps from -65 mV to 15, 35, 55, and 95 mV. Experiments utilizing voltage jumps from -65 to 15 and 35 mV were reported previously in Clarke & Johnson (2006).

Table 3. Depolarization-induced current relaxations in the presence of 30 μ M NMDA and 10 μ M glycine in the absence and presence of Mg^{2+}_o

0 Mg^{2+}_o	τ_{fast} (ms)	τ_{slow} (ms)
-65 to 15 mV	.480 \pm .215	5.62 \pm 2.29
-65 to 35 mV	.542 \pm .120	7.87 \pm .721
-65 to 55 mV	.456 \pm .180	6.46 \pm 1.06
-65 to 95 mV	.367 \pm .179	7.30 \pm .950
1 mM Mg^{2+}_o	τ_{fast} (ms)	τ_{slow} (ms)
-65 to 15 mV	.737 \pm .238	7.81 \pm .771
-65 to 35 mV	.689 \pm .172	9.15 \pm .926
-65 to 55 mV	.491 \pm .085	8.03 \pm .750
-65 to 95 mV	.701 \pm .131	7.43 \pm 1.54

Depolarizing voltage jumps were applied after the NR1/2B receptor current response had reached a steady-state level. Results from fits of current responses to voltage jumps from -65 to 15 and 35 mV were reported previously in Clarke & Johnson (2006). Amplitudes of the slow components (A_{slow}) are reported in **Fig. 12c**. Values are expressed as mean \pm SEM.

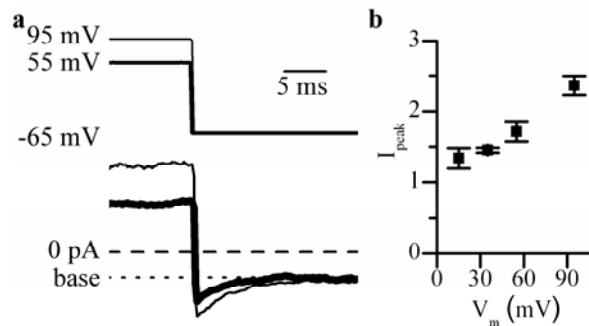


Figure 13. Tail currents following repolarization are sensitive to the amplitude of the initial depolarization. (a) Current traces (bottom traces) during repolarization from 55 mV (thick) or 95 mV (thin) to -65 mV. Immediately following repolarization the whole-cell current exceeds the steady-state current measured at -65 mV (base, dotted line). Membrane voltage is indicated by the top trace. *Inset.* Expanded view of the inward peaks induced by repolarization. Currents are normalized to the steady-state current level measured at -65 mV. (b) I_{peak} values depend significantly on the amplitude of the initial membrane depolarization (ANOVA, $p < .01$), increasing as the starting voltage was made more positive.

modulated by membrane voltage, with the NMDA receptor channel displaying a higher P_{open} at depolarized membrane potentials.

One of the most studied examples of voltage dependent modulation of a ligand-gated ion channel gating is the effect of membrane voltage on the closing rate of nicotinic acetylcholine receptors; the closing rate of nicotinic acetylcholine receptors becomes more rapid with hyperpolarization (Magleby and Stevens, 1972). Voltage dependent occupation of a permeant ion binding site has been suggested to underlie the voltage dependence of nicotinic acetylcholine receptor channel closure (Ascher et al., 1978; Marchais and Marty, 1979). The NMDA receptor also contains several permeant ion binding sites, including multiple Ca^{2+} binding sites which coordinate to endow the NMDA receptor with high Ca^{2+} permeability (Sharma and Stevens, 1996; Premkumar et al., 1997; Antonov and Johnson, 1999; Zhu and Auerbach, 2001a, 2001b; Qian et al., 2002). It is plausible that occupation of a permeant ion binding site could lead to a slow, voltage-dependent augmentation of P_{open} . To determine if changes in permeant ions impact the kinetics of NR1/2B receptor current in response to depolarization, recordings were performed with symmetric 150 mM KCl internal and external solutions (symmetric KCl).

Voltage jumps were applied as in **Figure 12**, except in these experiments currents were elicited by application of 1 mM glutamate instead of 30 μM NMDA. In response to a depolarization to 95 mV, currents recorded in symmetric KCl and 0 Mg^{2+} displayed a prominent slow relaxation that was indistinguishable from that observed in experiments using normal internal and external solutions (**Fig. 14a**). The τ_{fast} and τ_{slow} from double exponential fits did not depend significantly on the composition of the internal and external solutions, or the size of the depolarization (**Table 4**). A_{slow} was also not statistically different between experiments using symmetric KCl and experiments using normal internal and external solutions (**Fig. 14b**). In both solutions, A_{slow} was significantly larger in response to depolarizations to 95 than to 35 mV (**Fig. 14b**). Upon repolarization to -65 mV, a tail current that surpassed the -65 mV steady-state current level was also observed in symmetric KCl experiments. I_{peak} was again sensitive to the voltage of the previous depolarization, having a significantly larger value following repolarization from 95 than from 35 mV (**Fig. 14c**). Thus, even in symmetric KCl solutions, NR1/2B receptor currents are modulated by the membrane voltage, becoming larger with depolarization. These results suggest that permeant ions, in particular Ca^{2+} , do not play a critical role in the inherent voltage sensitivity of NR1/2B receptors.

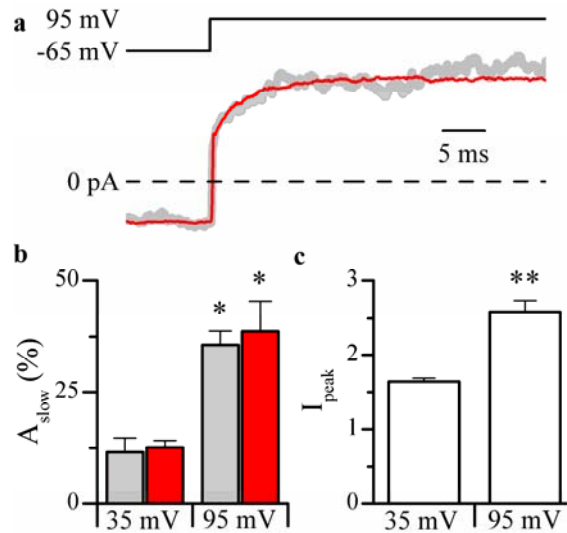


Figure 14. NR1/2B receptor currents are equally sensitive to membrane voltage in normal and symmetric KCl solutions. (a) Current traces (bottom) in response to a voltage step from -65 to 95 mV in normal internal and external solutions (grey) or symmetric KCl solutions (red). Membrane voltage is indicated by top trace. Currents are normalized to the steady-state outward current response at 95 mV. (b) Pooled results of the amplitude of the slow component (A_{slow}) from multi-exponential fits of current responses to voltage jumps from -65 mV to either 35 or 95 mV in normal internal and external solutions (grey) or symmetric KCl solutions (red). In both recording conditions, increasing the depolarization voltage jump from 35 to 95 mV results in a significant (*, $p < .01$) increase in A_{slow} . (c) I_{peak} values are significantly (**, $p < .005$) larger following repolarization from 95 mV than 55 mV in experiments using symmetric KCl solutions.

Table 4. Kinetics of depolarization induced current relaxations are not influence by changes in permeant ions.		
Normal Int. & Ext. Solutions	τ_{fast} (ms)	τ_{slow} (ms)
-65 to 35 mV	0.22 ± 0.04	6.71 ± 2.37
-65 to 95 mV	0.25 ± 0.07	4.96 ± 2.98
Symmetric KCl	τ_{fast} (ms)	τ_{slow}(ms)
-65 to 35 mV	0.19 ± 0.02	6.64 ± 1.14
-65 to 95 mV	0.18 ± 0.01	5.15 ± 1.13
Depolarizing voltage jumps were applied after the NR1/2B receptor current response had reached a steady-state level. Amplitudes of the exponential components are reported in Figure 14b. For all experiments $n > 4$ cells.		

3.4.2 Inherent voltage dependence of NR2 subunit gating

The results presented thus far are consistent with the hypothesis that, upon depolarization, NMDA receptors enter a higher P_{open} mode. Voltage-dependent alterations of any one of a number of steps which lead to NMDA receptor activation would predict a higher P_{open} at depolarized membrane potentials. For example, faster channel opening, or slower channel closure, upon membrane depolarization would lead to an increase in P_{open} . In an attempt to determine which NMDA receptor characteristics are augmented by membrane voltage, we utilized a combination of whole-cell recording and simulations to develop a model of NR1/2B receptor activation.

There have been several recent advances in the understanding of NMDA receptor gating (Gibb, 2004). Models in which multiple gating steps precede a final open, conducting state have been shown to reproduce many receptor properties (Banke and Traynelis, 2003; Popescu and Auerbach, 2003; Erreger et al., 2005; Schorge et al., 2005). We have chosen to use a model first proposed by Banke and Traynelis (2003) to explain activation of NR1/2B receptors. The Banke and Traynelis model was developed using heterologous expression of recombinant NR1/2B receptors in a similar mammalian expression system to the one employed here. In the Banke and Traynelis model, shown in **Figure 15**, the closed NMDA receptor (R) binds two agonist molecules (A). Once two glutamate molecules are bound (RA_2), the receptor can enter one of two desensitized states (RA_{2d_1} and RA_{2d_2}), or proceed to the open state. The novel feature of the model is that two pre-opening gating steps must occur before the receptor enters a single open, conducting state (RA_2^*). Banke and Traynelis (2003) provided evidence that these two pre-opening gating steps represent independent conformational changes within the NR1 ($RA_2 \rightarrow RA_{2f}$ and $RA_{2s} \rightarrow RA_2^*$) and NR2 ($RA_2 \rightarrow RA_{2s}$ and $RA_{2f} \rightarrow RA_2^*$) subunits. In previous experiments (Banke and Traynelis, 2003), and here, binding of the co-agonist glycine was ignored because all recordings were performed in the continuous presence of a saturating concentration of this amino acid. Thus, the glycine binding site on the NR1 subunit can be assumed to always be occupied because glycine binding is assumed to be voltage independent and not dependent on glutamate binding.

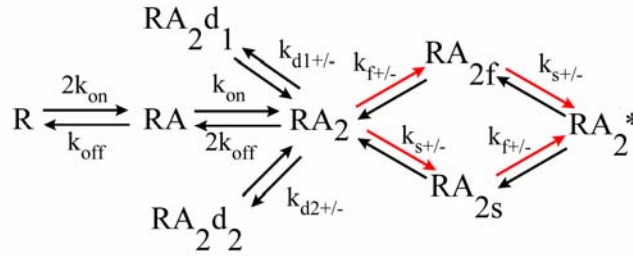


Figure 15. Kinetic scheme used to model NR1/2B receptor activation. Kinetic model used to simulate NR1/2B receptor activation based on Banke and Traynelis (2003). Red arrows indicate rates which were altered to be sensitive to membrane voltage (k_{f+} and k_{s+}).

Table 5. Rates used for NR1/2B receptor model fitting and current simulations.		
	<u>Unit</u>	<u>Rate Constant</u>
k_{on}	$\mu\text{M}^{-1} \text{s}^{-1}$	2.83
k_{off}	s^{-1}	38.1
k_{s+}	s^{-1}	48
k_{s-}	s^{-1}	230
k_{f+}	s^{-1}	2836
k_{f-}	s^{-1}	175
k_{d1+}	s^{-1}	Determined by fitting
k_{d1+}	s^{-1}	Determined by fitting
k_{d1-}	s^{-1}	Determined by fitting
k_{d2+}	s^{-1}	Determined by fitting
k_{d2-}	s^{-1}	Determined by fitting

The rates were taken from Erreger *et al.* (2005) in which the rates were determined from NR1/2B recordings performed at a constant holding potential of -100 mV. Where indicated in text, certain rates were modified to change exponentially with membrane voltage. All rates were fixed during model fitting and current simulations except desensitization rates. Desensitization rates were determined by fitting of macroscopic currents (see Fig. 17-19). The corresponding rates in the unblocked and blocked arms were equivalent.

Simulations from a model in which voltage-dependence was added to the forward rate constant representing the NR1 pre-gating conformational change (k_{f+}) predict a slow component of current relaxation that is sensitive to the amplitude of depolarization (**Fig. 16a**). For simulations, all rates were taken from Erreger *et al.* (2005) (see **Table 5**). The rate constant k_{f+} was modified to change exponentially with membrane voltage based on the following equation:

$$k_{f+} = k_{f+,100\text{mV}} * \exp[(V_m + 100 \text{ mV})/V_{\text{dep}}] \quad (3)$$

where $k_{f+,100\text{mV}}$ is the rate at -100 mV as reported in Erreger *et al.* (2005) (2836 s^{-1}), V_m is the membrane voltage, and V_{dep} is the sensitivity to membrane voltage. Simulations from a model in which the forward rate constant of the NR2 pre-gating conformational change (k_{s+}) changed exponentially with membrane voltage also predicted a slow component of current relaxation in response to depolarization (**Fig. 16b**). The rate constant k_{s+} was modified to change exponentially with membrane voltage based on the following equation:

$$k_{s+} = k_{s+,100\text{mV}} * \exp[(V_m + 100 \text{ mV})/V_{\text{dep}}] \quad (4)$$

where $k_{s+,100\text{mV}}$ is the rate at -100 mV as reported in Erreger *et al.* (2005) (48 s^{-1}) and V_m and V_{dep} are as described in equation 3.

The magnitude of the slow components, and the non-linearity of the current response, mirrored the strength of the voltage sensitivity (V_{dep}), becoming greater with steeper voltage sensitivity (**Fig. 16c**). We have shown previously that slow current relaxations in response to rapid depolarizations are dependent on the identity of the NR2 subunit (Clarke and Johnson, 2006). Thus, we proceeded with the model in which k_{s+} depended exponentially on membrane voltage. We also tested models in which the backwards rate constant of the NR2 pre-gating conformational change (k_{s-}) changed exponentially with membrane voltage (see below).

To determine the strength of the voltage sensitivity of k_{s+} , we measured I-V curves using brief (25 ms) depolarizations from -100 mV to a wide range of voltages (**Fig. 17a**). As expected, NR1/2B receptor currents displayed an initial fast (sub-ms τ) component, followed by a much slower relaxation (τ of several ms) in response to depolarization. The fast and slow components of current relaxations were measured using double exponential fits. When considered separately, the fast component yielded a linear I-V plot (**Fig. 17b**). In contrast, the slow component became larger as the amplitude of the voltage jump increased, which caused the total current I-V plot to display outward rectification (**Fig. 17b**). The fast and slow components were converted to conductances (see Methods), termed g_{fast} and g_{slow} , and normalized to the g_{fast} associated with the

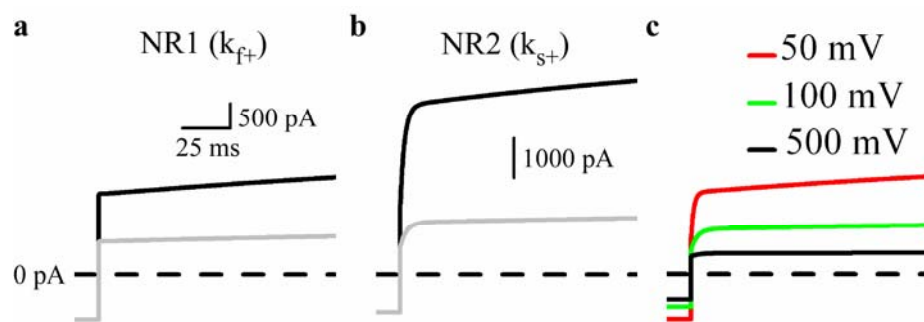


Figure 16. Models containing voltage dependence of the conformational change associated with either the NR1 or NR2 subunit predict a slow component of current relaxation in response to depolarization. (a) Current simulations from a model incorporating voltage dependence (e-fold per 100 mV) of k_{f+} (Fig. 15). Current simulations were run in response to depolarizations from -65 to 35 mV (grey) and -65 to 95 mV (black). (b) As in (a) except k_{s+} changed exponentially with membrane voltage (c) Current simulations in response to depolarization from -65 to 35 mV with varying levels (e-fold per 50, 100, and 500 mV) of voltage sensitivity of k_{s+} . In all parts the dashed line represents the 0 current level.

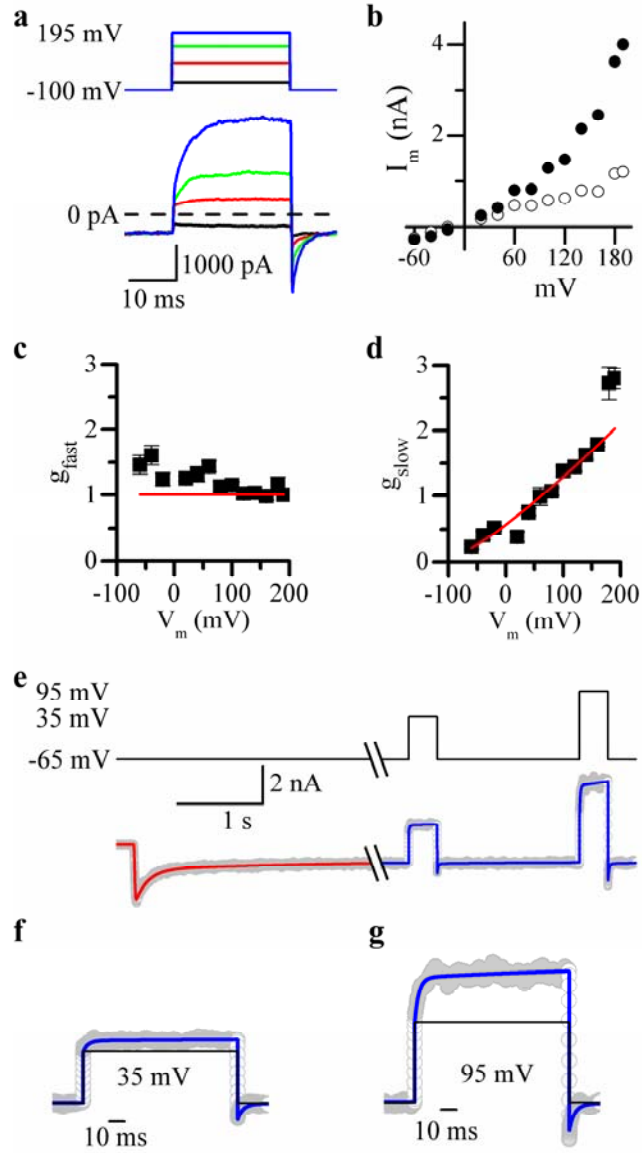


Figure 17. Slow current relaxation in response to depolarization can be reproduced with a model containing voltage dependence of NR2B subunit gating. (a) Current traces (bottom trace) during 25 ms depolarizations from -100 mV to several depolarized voltages (top trace). (b) I-V curve from the cell shown in (a) is linear when the fast component is considered alone (open circles). Addition of the slow component (total current) results in an outwardly rectifying I-V curve (closed circles). (c) g_{fast} had a constant value of ~ 1 across the voltage range, while (d) g_{slow} increased with depolarization. Red lines represent output from a model containing an e-fold per 175 mV acceleration of $k_{\text{s+}}$ (**Fig. 15**). (e) Receptor number and desensitization parameters were determined by fitting the NR1/2B Model (bottom trace, red line) to the first 5 s of a whole-cell current response (bottom trace, grey trace) to application of 1 mM glutamate at -65 mV. Before the break in the x-axis, receptor number and desensitization rates were allowed to vary. Once receptor number and desensitization rates had been determined, all rates were fixed and the NR1/2B Model was used to simulate currents (bottom trace, blue line) in response to depolarizations from -65 to 35 and 95 mV. Membrane voltage is indicated by the top trace. (f, g). Expanded view of current simulations using the NR1/2B Model (blue lines) or a voltage-independent model (black lines). Current simulations are overlaid onto experimental data (grey traces).

largest depolarization (-100 to 195 mV). Normalization accounted for cell to cell variations in receptor number and allowed the data to be averaged across cells ($n = 7$). g_{fast} was linear and had a value near 1 for all voltages (**Fig. 17c**). g_{fast} did decrease slightly upon depolarization with an e-fold change per ~ 520 mV. This decrease in g_{fast} is likely too small to be physiologically relevant and will not be considered further here. In contrast, g_{slow} became larger with increasing depolarization (**Fig. 17d**).

I-V curves were also generated from models which contained varying levels of voltage sensitivity of k_{s+} based on equation (4). Double exponential fits were used to determine the amplitudes of the fast and slow components of simulated current relaxation. The fast and slow components were converted to conductances and normalized as described above. We found that the output from a model in which the V_{dep} of k_{s+} was 175 mV (termed the NR1/2B Model) was in the best agreement with the experimental data over a wide voltage range (**Fig. 17f-h**). The NR1/2B Model and experimental data showed some disagreement at the most depolarized voltages (185 and 195 mV). The divergence between model and experimental data at these extreme voltages may represent a separate phenomenon that only occurs only well outside of the physiological range.

We next set out to determine if the NR1/2B Model also accurately reproduced the time course of slow relaxation. Because desensitization varies greatly from cell-to-cell, we determined desensitization rates and receptor number by fitting the NR1/2B Model to a whole-cell response to 1 mM glutamate that preceded depolarizations from -65 to 35 and 95 mV. During fitting, only the rates into and out of the two desensitized states and the receptor number were allowed to vary. All other rates were taken directly from Erreger *et al.* (2005) (see **Table 5**). As seen previously (Banke and Traynelis, 2003; Erreger *et al.*, 2005), adequate fits required a model containing two desensitized states (data not shown). After receptor number and desensitization rates were determined by fitting, all rates were fixed and the NR1/2B Model was used to simulate currents in response to depolarizations from -65 to 35 and 95 mV (**Fig. 17g, h**). NR1/2B Model simulations, performed with zero free parameters, were in excellent agreement with the experimental data. In contrast, current simulations from a model lacking voltage dependence (**Fig. 17g, h**), or a model in which the backwards rate constant of the NR2 pre-opening conformational change (k_{s-}) changed exponentially with membrane voltage (**Fig. 18**) did not yield fits of as high quality.

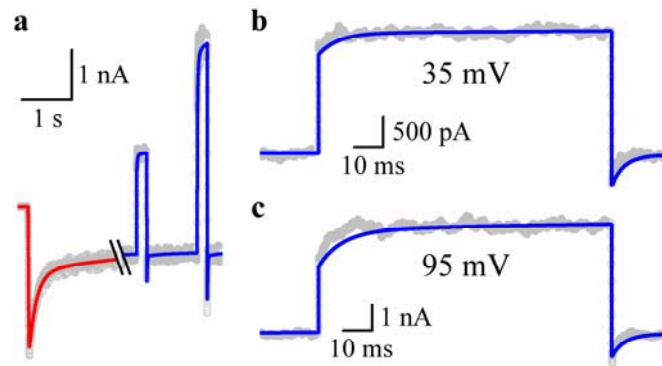


Figure 18. Voltage dependent modification of k_s . predicts slightly slower kinetics of current relaxation in response to membrane depolarization. Current simulations and model fitting were performed using a model in which k_s changed exponentially with membrane voltage (e-fold per 175 mV), such that k_s became slower with depolarization. **(a)** To determine receptor number and desensitization parameters, the model (red trace) was fitted to the first 5-s of a whole-cell current response (grey trace) to an application of 1 mM glutamate at -65 mV. Only desensitization rates and receptor number were allowed to vary before the break in the current. Once desensitization rates and receptor number were determined, all rates in the model were fixed and current simulations (blue trace) were run in response to depolarizations from -65 to 35 and 95 mV. **(b, c)** Enlargements of current simulations (blue trace) overlaid onto experimental data (grey traces) from **(a)** in response to depolarizations from -65 to 35 mV **(b)** and 95 mV **(c)**.

3.4.3 Voltage-dependent gating predicts slow Mg^{2+} unblock

The initial observations of slow Mg^{2+} unblock (Spruston et al., 1995; Vargas-Caballero and Robinson, 2003; Kampa et al., 2004) were surprising due to the rapid kinetics of Mg^{2+} block and unblock measured at the single channel level (Mayer et al., 1984; Nowak et al., 1984). The similarity between the kinetics of slow relaxation in the absence and presence of Mg^{2+} (**Table 3**) suggests that these two phenomena may share a common molecular mechanism. We next determined if the NR1/2B Model could account for the slow phase of Mg^{2+} unblock.

To account for block by Mg^{2+} , a second, “blocked arm” was added to the NR1/2B Model (**Fig. 19a**). The blocked arm followed a trapping-block scheme, in which the NMDA receptor channel is able to close and agonists can dissociate while blocked by Mg^{2+} (Benveniste and Mayer, 1995; Sobolevsky and Yelshansky, 2000). Unlike previous models developed to explain slow Mg^{2+} unblock (Kampa et al., 2004; Vargas-Caballero and Robinson, 2004), we assumed that the rate constants are symmetric, meaning that corresponding rates in the blocked and unblocked arms have equal values (**Table 5**). Previous data suggest that a symmetric model is appropriate to describe block by Mg^{2+} (Sobolevsky and Yelshansky, 2000; Qian et al., 2002; Qian and Johnson, 2002). Simulations using a symmetric trapping block model containing no voltage dependence predicts that Mg^{2+} unblock will be very rapid in response to depolarization (**Fig. 19b**, dashed grey line) (Vargas-Caballero and Robinson, 2004). Surprisingly, the NR1/2B Model, which contained weak voltage sensitivity (e-fold per 175 mV) of k_{s+} , predicts a slow component of current relaxation that is larger in the presence of Mg^{2+} (**Fig. 19b**).

NR1/2B Model simulations were next compared with experimental data. To determine desensitization rates and receptor number, the NR1/2B Model was fit to whole-cell currents in response to application of 1 mM glutamate at -65 mV in the presence of 1 mM Mg^{2+} . During fitting, only receptor number and desensitization rates were allowed to vary, with all other parameters set to values shown in **Table 5**. For simplicity, the desensitized states were omitted from **Figure 19a**, but were present during the fitting procedure. Two unblocked desensitized states were accessible from RA_2 and two blocked desensitized states were accessible from RA_2Mg . Once desensitization rates and receptor number were determined, current simulations in response to voltage jumps from -65 mV to -25, 35, and 95 mV were run with zero free

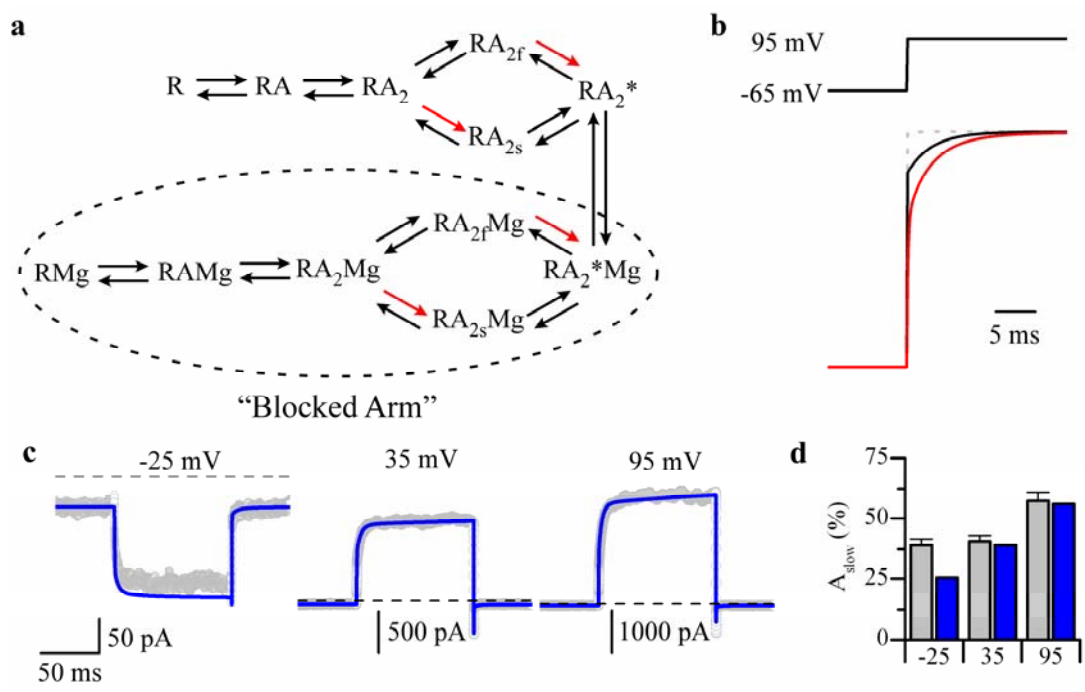


Figure 19. NR1/2B Model accurately predicts the kinetics of Mg^{2+}_o unblock in response to depolarization. (a) To account for block by Mg^{2+}_o , a “blocked arm” was added to the NR1/2B Model. All the corresponding rates in the blocked and unblocked arms were equivalent (**Table 5**). (b) Addition of voltage-dependence to k_{s+} predicts a slow component of current relaxation in response to depolarization in the absence (black line) which is not present in simulations lacking voltage-dependence (dashed grey line). The size of the slow component is enhanced by the addition of Mg^{2+}_o (red line). Voltage during simulations is indicated by the top trace. (c) NR1/2B Model simulations (blue lines) are overlaid onto experimental current traces (grey circles) during depolarization from -65 mV to -25, 35, and 95 mV. Receptor number and desensitization rates were determined by fitting the NR1/2B Model to a whole-cell current response to 1 mM glutamate application at -65 mV in the presence 1 mM Mg^{2+}_o as shown in **Figure 17e**. After receptor number and desensitization rates were determined, all rates were fixed and current simulations were run. Dotted black line represents 0 current level. (d) A_{slow} values determined from multi-exponential fits of both model simulations (blue) and experimental data (grey) are in reasonable agreement.

parameters. Current simulations were in reasonable agreement with experimental data, especially in response to depolarization from -65 to 35 and 95 mV (**Fig. 19c**).

The results from multi-exponential fits of NR1/2B Model output and the averaged results of fits of experimental data collected across several cells ($n = 3$) were compared. Because the NR1/2B Model is complex, current simulations contained many exponential components. However, NR1/2B Model simulations contained a prominent slow component ($\tau_{\text{sim}} = \sim 3$ ms) in response to all depolarizations. The prominent slow component from fits to experimental data (termed τ_{slow}) showed good agreement with τ_{sim} : τ_{slow} had values of $2.80 \pm .78$ ms, $2.69 \pm .44$ ms, and $3.50 \pm .37$ ms in response to depolarizations from -65 to -25, 35, and 95 mV respectively. The sum of the amplitudes of all of the components with τ 's > 1 ms from NR1/2B Model simulations were in good agreement with the A_{slow} measured from experimental data (**Fig. 19d**).

We next determined how well the NR1/2B Model was able to reproduce currents in response to more complex voltage protocols. NR1/2B receptor currents were evoked by application of 1 mM glutamate in the continuous presence of 10 μ M glycine and 0 or 1 mM Mg^{2+}_o . Once a steady-state response at -65 mV was reached, the cell was depolarized to 35 mV for 200 ms. After 200 ms at 35 mV, the cell was repolarized to -65 mV for varying durations before being stepped back to 35 mV (**Fig. 20a**). Following brief repolarizations, the current response to a voltage step back to 35 mV was very rapid. However, with prolonged repolarization, a larger fraction of the response to membrane depolarization was slow (**Fig. 20b, c**). The recovery of the slow component was well fit by a single exponential with τ 's of 2.7 and 3.4 ms in 0 and 1 mM Mg^{2+}_o , respectively. These values are close to that previously measured in native NMDA receptors (Vargas-Caballero and Robinson, 2004). The NR1/2B Model was able to reproduce reasonably well the experimental results collected in 0 (**Fig. 20b**) and 1 mM Mg^{2+}_o (**Fig. 20c**).

3.4.4 NR1/2B currents during stimulation with AP waveforms

To determine if the NR1/2B Model can also predict currents in response to physiological waveforms, we compared experimental data and model simulations in response to

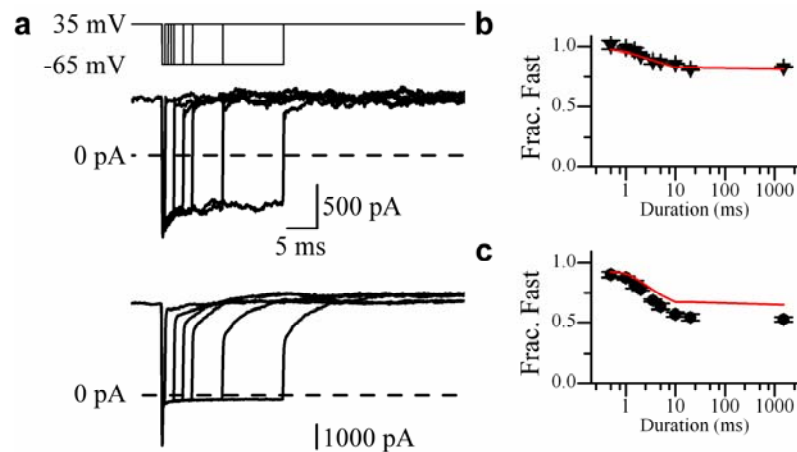


Figure 20. The NR1/2B Model reproduced NR1/2B receptor currents during a complex voltage paradigm. (a) NR1/2B current traces in the absence (middle) and presence (bottom) of 1 mM Mg²⁺_o during protocol used to measure the recovery of slow current relaxation following repolarization from 35 to -65 mV of varying durations (membrane voltage indicated by top trace). (b, c) Summary data of the fraction of current that relaxes rapidly (Frac. Fast, $\tau < 1$ ms) in response to depolarization to 35 mV plotted as a function of the duration of a repolarizing pulse from 35 to -65 mV. Model predictions are overlaid (red lines) from the NR1/2B Model in the absence (b) and presence of 1 mM Mg²⁺_o (c).

depolarizations provided by action potential (AP) waveforms. NR1/2B receptor currents were elicited from HEK 293T cells by application of 1 mM glutamate and saturating (10 μ M) glycine in the continuous presence of 1 mM Mg^{2+}_o . Once the whole-cell current had reached a steady-state level, three AP waveforms collected at the soma or two locations (240 and 280 μ m) on the dendrite of a CA1 pyramidal cell (waveforms courtesy of D. Johnston) were played into the cell. To account for variations in receptor number, the whole-cell current was normalized to the steady-state response at rest (-65 mV) and averaged across cells ($n = 7$).

Model simulations were also carried out using identical AP waveforms. Three models were employed: a voltage-independent model assuming instantaneous Mg^{2+}_o block and unblock, a voltage-independent model with previously published Mg^{2+}_o blocking and unblocking rates (Antonov and Johnson, 1999), and the NR1/2B Model. Because the AP waveforms are brief in duration, models lacking desensitized states yielded similar results as models containing desensitized states (data not shown). Thus, for simplicity, models without desensitized states were used.

NR1/2B Model simulations showed excellent agreement with experimental data in response to all three AP waveforms (**Fig. 21d-f**, red lines). In contrast, current simulations from a instantaneous Mg^{2+}_o unblock model showed poor agreement with experimentally recorded NR1/2B receptor currents in response to the somatic and 240 μ m AP waveforms (**Fig. 21a,b**, blue lines). The instantaneous Mg^{2+}_o unblock models predicted substantial NR1/2B receptor current during the upstroke of the AP waveforms which was not observed experimentally. The instantaneous Mg^{2+}_o unblock model also underestimated the NR1/2B receptor inward currents during the repolarization phase of the AP waveforms.

These results are in agreement with previous models of slow Mg^{2+}_o unblock, which suggest that slow Mg^{2+}_o unblock results in a strong contribution of NMDA receptor current during repolarization (Vargas-Caballero and Robinson, 2004). However, most of the differences between the NR1/2B Model and the instantaneous Mg^{2+}_o unblock model are due to the rates of Mg^{2+}_o block and unblock from open channels and not inherent voltage dependence. Simulations from a model containing no voltage dependence, but with the previously published Mg^{2+}_o blocking and unblocking rates (Antonov and Johnson, 1999), showed good agreement with the experimentally recorded NR1/2B receptor currents (**Fig. 21g-i**, grey lines). The NR1/2B Model

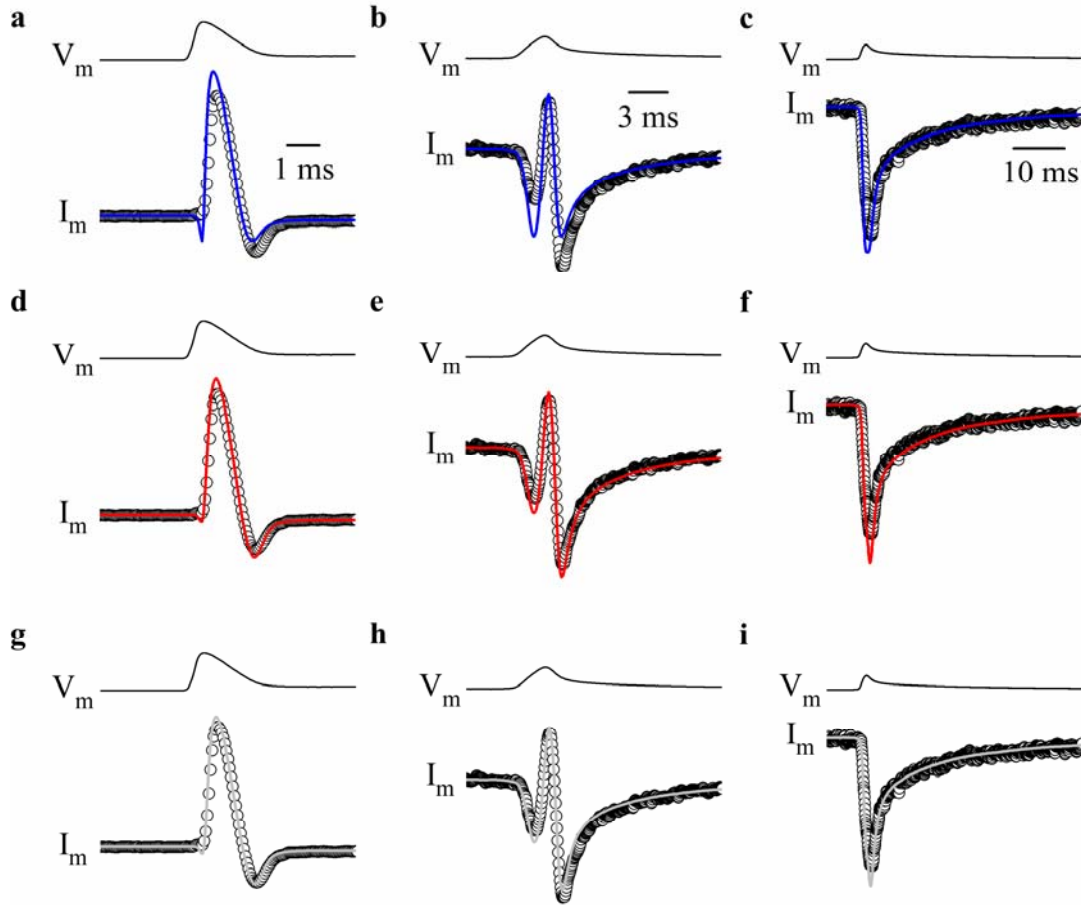


Figure 21. Inherent voltage dependence does not enhance NR1/2B receptor currents in response to depolarizations by AP waveforms. (a, b, c) Experimentally recorded NR1/2B receptor currents (bottom traces) were recorded in the presence of 1 mM glutamate, 10 mM glycine and 1 mM Mg^{2+}_o . Once a steady-state response was achieved, AP waveforms (top trace) recorded at the soma (a), or 240 μm (b) and 280 μm (c) out on the dendrite of a CA1 pyramidal cell were played into the HEK 293T cell. Current simulations from a model assuming instantaneous Mg^{2+}_o block and unblock (blue traces) are overlaid onto experimentally recorded currents (black traces). (d, e, f) As in a, b, c except that the overlaid current simulations are from the NR1/2B Model (red traces). The experimentally recorded NR1/2B receptor currents (black traces) are the same as in (a, b, c). (g, h, i) As in a, b, c except that the overlaid current simulations are from a model containing published rates for block and unblock of Mg^{2+}_o (Antonov and Johnson, 1999), but no voltage sensitivity of k_{S^+} (grey traces). The experimentally recorded NR1/2B receptor currents (black traces) are the same as in (a, b, c).

did predict a slight increase in the peak of inward current in response to both the somatic and 240 μm AP waveform: the peak was 17.3 and 14.9% larger in NR1/2B Model simulations than the voltage-independent model simulations in response to the somatic and 240 μm AP waveforms, respectively. However, this change was not large enough to be detected within experimental data as the experimental data was consistent with either model (**Fig. 21**).

Current simulations from all three models were similar in response to the smallest and slowest depolarization (280 μm AP waveform), and all showed reasonable agreement with the experimental data (**Fig. 21c, f, i**). These data support the previous observations that instantaneous unblock models can account for NMDA receptor currents in response to small depolarizations (Vargas-Caballero and Robinson, 2003).

3.4.5 Voltage-dependent kinetics of NMDA-EPSCs

The decay of NMDA-EPSCs has been shown to be voltage dependent, becoming slower with depolarization (Konnerth et al., 1990; Keller et al., 1991; D'Angelo et al., 1994). In the presence of Mg^{2+}_o , the voltage sensitivity of the NMDA-EPSC decay becomes more marked (Konnerth et al., 1990; Keller et al., 1991; D'Angelo et al., 1994). To determine if the voltage-dependent model can account for these observations, we simulated NR1/2B receptor currents in response to a synaptic glutamate waveform at various membrane potentials. The simulated synaptic glutamate waveform reached a peak concentration of 1.1 mM and decayed with a τ of 1.2 ms (Clements et al., 1992). **Figure 22A** shows the current responses of 100 NR1/2B receptors to the synaptic glutamate waveform at the indicated membrane potentials in 0 and 1 mM Mg^{2+}_o . To determine if the current decay was voltage dependent, the responses at 40 mV were inverted and all responses were normalized to the largest peak response. The normalized NMDA-EPSCs show that the decay of NR1/2B receptor currents is weakly voltage dependent in the absence of Mg^{2+}_o , decaying more slowly at depolarized voltages (**Fig. 22b**). The addition Mg^{2+}_o slightly increased the voltage dependence of the current decay (**Fig. 22b**). These simulation results are qualitatively similar to that previously described; NMDA-EPSCs decay more slowly at depolarized membrane potentials (Konnerth et al., 1990; Keller et al., 1991; D'Angelo et al., 1994). However, the magnitude of the change in current decay with depolarization is far greater in previous experiments than in our simulations. There may be

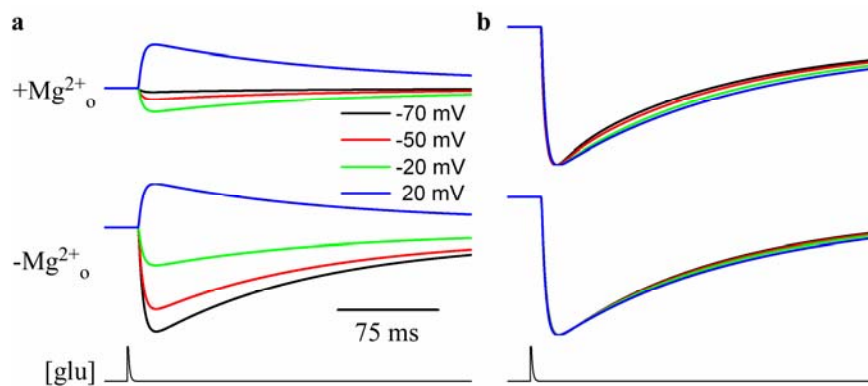


Figure 22. The NR1/2B Model predicts a small increase in the decay of synaptic-like NR1/2B receptor currents at depolarized membrane potentials. (a) Current simulations in response to a 1 ms synaptic-like application of glutamate (bottom trace) in the presence (top traces) and absence (middle traces) of 1 mM Mg²⁺_o at several membrane potentials. Simulations were performed using the rates in **Table 5** along with the desensitization rates as determined in **Figure 19**. (b) Normalization of the peaks from the simulations shown in (a). Upon depolarization, the decay of the simulated synaptic NR1/2B receptor responses slowed slightly. In the presence of Mg²⁺_o (top traces), the depolarization-induced slowing of the current decay was slightly greater than in the absence of Mg²⁺_o (middle traces).

additional effects of membrane voltage on NMDA receptor gating, desensitization, and/or agonist binding characteristics which are models do not include. These uncharacterized effects could further augment the decay of NMDA-EPSCs upon depolarization.

3.5 DISCUSSION

The fundamental physiological significance of voltage-dependent channel block by Mg^{2+}_o has long been appreciated (Mayer et al., 1984; Nowak et al., 1984; Ascher and Nowak, 1988). However, several observations (Keller et al., 1991; Hestrin, 1992; Benveniste and Mayer, 1995; Spruston et al., 1995) suggest that NMDA receptors display an additional, inherent form of voltage sensitivity. Our data reveal that NR1/2B receptor currents are enhanced at positive membrane potentials, which is consistent with the hypothesis that the P_{open} of NR1/2B receptors is higher at depolarized voltages. Based on this observation, we developed a model of NR1/2B receptor activation that incorporates weak voltage dependence of the pre-opening conformational change associated with the NR2B subunit (the NR1/2B Model). The NR1/2B Model accounts for depolarization induced current enhancement in 0 Mg^{2+}_o , slow Mg^{2+}_o unblock, and voltage dependent decay of NMDA-EPSCs.

3.5.1 Voltage-dependent modulation of ligand-gated receptors

In a classic study, Magleby and Stevens (1972) showed that voltage-dependent gating of nicotinic acetylcholine receptors was able to account for the voltage-dependent decay of endplate potentials. Since this pioneering study, voltage-dependent alterations in the kinetics of glycine receptors (Legendre, 1999) and several AMPA receptor subtypes (Raman and Trussell, 1995; Tour et al., 1998), have also been reported. The mechanism by which membrane voltage influences the gating machinery of ligand-gated receptors is not entirely clear. Two mechanisms have been proposed to account for voltage-dependent alterations in nicotinic acetylcholine receptor channel closure. One involves voltage dependent occupation of a permeant ion binding

site (Ascher et al., 1978; Marchais and Marty, 1979), while the other suggests that charged moieties moving through the membrane voltage field play a critical role (Auerbach et al., 1996).

The data presented here suggest that permeant ions do not play a critical role in the observed voltage dependence of NR1/2B activity (**Fig. 14**). The role of gating associated movements of charged moieties cannot be ruled out and may underlie the observed voltage sensitivity of NR1/2B receptors. The degree of voltage sensitivity (e-fold per 175 mV) in the NR1/2B Model is consistent with a single charge moving only 14% of the way through the membrane voltage field during gating-associated conformational changes. Within the rat NR2B amino acid sequence there are several charged amino acids that lie near the intracellular and extracellular faces of transmembrane regions, along with a lysine in the re-entrant P-loop. Slow Mg^{2+}_o unblock is only present from NR1/2A and NR1/2B receptors (Clarke and Johnson, 2006), suggesting that a charged amino acid present only in the NR2A and NR2B sequences would be an attractive candidate to confer inherent voltage-dependence of gating. However, none of the aforementioned amino acids meet this requirement, leaving no obvious targets for site-directed mutagenesis. A long list of alternative arguments could be made, including that there are NR2 subunit dependent differences in the movement of a conserved charged amino acid. Studies investigating the impact of amino acid substitutions on the voltage sensitivity of NR1/2B receptor activation will be needed to directly test the hypothesis that charged amino acids participate in conferring NR1/2B receptors with inherent voltage sensitivity.

3.5.2 Interactions between Mg^{2+}_o and NR1/2B receptor gating

Previous models developed to account for slow Mg^{2+}_o unblock suggested that block by Mg^{2+}_o influences NMDA receptor channel gating (Kampa et al., 2004; Vargas-Caballero and Robinson, 2004). In these models slow Mg^{2+}_o unblock arises from slow egress of the channel from one, or more, closed blocked states. These models accurately predict the slow phase of Mg^{2+}_o unblock under many experimental conditions and are supported by the previous observation of a reduction in single-channel burst duration of cortical NMDA receptors in the presence of Mg^{2+}_o (Ascher and Nowak, 1988). However, these models do not predict slow relaxation in 0 Mg^{2+}_o (**Fig. 12**). In addition, several previous studies have concluded that Mg^{2+}_o does not influence NMDA receptor gating (Sobolevsky and Yelshansky, 2000; Qian et al., 2002). Finally, the

organic NMDA receptor channel blocker amantadine was demonstrated to moderately accelerate channel closure (Blanpied et al., 2005). The degree to which amantadine accelerates channel closure is similar to that proposed for Mg^{2+}_o (Vargas-Caballero and Robinson, 2004). However, upon depolarization, amantadine exhibits a significantly slower component of unblock than Mg^{2+}_o (Blanpied et al., 2005), suggesting that the degree of interaction between amantadine and NMDA receptor gating is more prominent than that of Mg^{2+}_o .

Here, the NR1/2B Model was developed to account for the inherent voltage-dependence of NR1/2B receptors. However, we found that without any further alterations, the NR1/2B Model also accounted for slow Mg^{2+}_o unblock (**Fig. 18**). The simplicity of this explanation is attractive, particularly when the alternative hypothesis that Mg^{2+}_o block alters NMDA receptor channel gating is in conflict with previous data. It should be noted that excellent agreement with experimental data could also be obtained with models containing a combination of weak voltage dependence and small changes in channel gating in the presence of Mg^{2+}_o (data not shown). Thus, these observations leave open the possibility that block by Mg^{2+}_o does cause subtle changes in gating. However, it seems unlikely that Mg^{2+}_o block impacts NMDA receptor gating to the extent previously proposed (Kampa et al., 2004; Vargas-Caballero and Robinson, 2004).

3.5.3 Impact of inherent voltage dependence on NMDA receptor mediated currents

The nature of the inherent voltage dependence we propose suggests that significant alterations in NR1/2B receptor currents will only occur in response to depolarizations that are both large in amplitude and long in duration. The 280 μ m AP waveform has a long half-width (3.55 ms) (Bernard and Johnston, 2003), but the peak depolarization only reaches -20 mV, which is not depolarized enough to significantly alter NR1/2B receptor currents (**Fig. 20c, f**).

Model simulations did suggest that the addition of voltage-sensitivity of k_{s+} would result in a small increase in the peak of inward current induced by the somatic and 240 μ m AP waveforms. However, the predicted increase was small, leaving current simulations from both a voltage-independent model and the NR1/2B Model showing reasonable agreement with experimental data. These data suggest that inherent voltage sensitivity, and thus slow Mg^{2+}_o unblock, will not result in a significant alteration of NR1/2B receptor currents during most back-

propagating APs (but see(Kampa et al., 2004)). It is possible that long duration and large amplitude depolarizations, such as dendritic Ca^{2+} or NMDA spikes (Larkum et al., 1999; Schiller et al., 2000), would result in significant enhancement of NR1/2B receptor currents. NR1/2B receptor currents enhancement by prolonged depolarizations is consistent with experimental data showing that extending the duration of the somatic AP waveform leads to an enhancement of NR1/2B receptor currents (Clarke and Johnson, 2006).

The most striking difference between current simulations and experimental data in response to AP waveforms are the poor fits from models assuming instantaneous Mg^{2+}_o block and unblock. Only in response to the 280 μm AP waveform, which has both slow rising and falling phases, does the model assuming instantaneous Mg^{2+}_o block and unblock provide a reasonable fit to the experimental data (**Fig. 20c**, green lines). These data are in agreement with previous work showing that an instantaneous Mg^{2+}_o unblock models can adequately predict native NMDA receptor currents in response to small depolarizations (Vargas-Caballero and Robinson, 2003). It is important to recognize that while the interaction between Mg^{2+}_o and the open NMDA receptor channel is fast, it is not fast enough to be at equilibrium during rapid depolarizations, such as many AP waveforms.

One physiologically relevant prediction of the voltage dependent model is that the decay of NMDA-EPSCs will become slower with depolarization (**Fig. 21**). This prediction is supported by previous studies on native NMDA receptors (Konnerth et al., 1990; Keller et al., 1991; D'Angelo et al., 1994; Kampa et al., 2004; Vargas-Caballero and Robinson, 2004). Current simulations show that the voltage dependence of decay is weak in 0 Mg^{2+}_o , but upon addition of Mg^{2+}_o the decay of NMDA-EPSCs becomes slightly slower at 40 mV than at -70 mV (**Fig. 21b**). Slower decay of NMDA-EPSCs results in greater charge transfer, and hence Ca^{2+} influx, via NR1/2B receptors.

Enhancement of NMDA receptor mediated currents upon depolarization is normally associated with relief of Mg^{2+}_o block. Here, we show that voltage dependent gating can provide an additional mechanism by which membrane depolarization enhances signaling via the NR1/2B receptor. Thus, inherent voltage dependence, working in concert with Mg^{2+}_o block, imbues NR1/2B receptors with the ability to serve as powerful coincident detectors, signaling pre-synaptic glutamate release and membrane depolarization.

4.0 INHERENCE OF NMDA RECEPTOR ACTIVATION: NR2 SUBUNIT DEPENDENCE AND SLOW MAGNESIUM UNBLOCK

4.1 ABSTRACT

NMDA receptors are heterotetrameric proteins composed of NR1 and NR2 subunits. In many brain regions, including the cortex, the composition of NMDA receptors changes during development. Early in development the NR2B subunit predominates, whereas later in development the NR2A subunit shows higher expression levels. Previous work has suggested that NR1/2B receptor activity displays inherent voltage dependence, beyond that provided by Mg^{2+} block. Here, we show that NR1/2A receptor activity also displays inherent voltage dependence such that NR1/2A receptor currents are enhanced upon membrane depolarization. A model assuming voltage dependence of the NR2A pre-gating conformational change (NR1/2A Model) was able to reproduce NR1/2A receptor currents in both the absence and presence of Mg^{2+} . Both the NR1/2A and the previously described voltage-dependent NR1/2B Models contained identical voltage sensitivities of the NR2 subunit pre-gating conformational change. However, the unique gating kinetics of the NR2A subunit (Erreger *et al.*, 2005) accurately predicted that the NR1/2A receptor currents are less sensitive to changes in membrane voltage than NR1/2B receptor currents. Thus, although pre-gating steps of both NR1/2A and NR1/2B receptors seem to be equally sensitive to membrane voltage, the physiological impact of the inherent voltage sensitivity is predicted to be more prominent for NR1/2B than NR1/2A receptors.

4.2 INTRODUCTION

NMDA receptors are a subtype of ionotropic glutamate receptor found throughout the CNS. NMDA receptor activation has been linked a number of physiological processes, including neuronal migration (Komuro and Rakic, 1993), synapse formation (Constantine-Paton and Cline, 1998), long-term changes in synaptic efficacy (Bliss and Collingridge, 1993), and several forms of learning (Tang et al., 1999; Tsien, 2000; Shapiro, 2001). Excessive activation of NMDA receptors has also been linked to cell death in several pathological states, including stroke, schizophrenia, and Alzheimer's disease (Meldrum, 1992; Cull-Candy et al., 2001; Tsai and Coyle, 2002; Moghaddam and Jackson, 2003; Lleo et al., 2006).

NMDA receptors are heterotetrameric proteins, most commonly composed of NR1 and NR2 subunits. There are eight NR1 subunit isoforms due to alternative splicing of a single gene product (Nakanishi, 1992; Hollmann et al., 1993). In contrast, there are 4 NR2 subunit gene products, termed NR2A-D (Moriyoshi et al., 1991; Monyer et al., 1992; Ishii et al., 1993). Native NMDA receptors display a wide range of pharmacological and biophysical properties, depending on the isoforms of the NR1 and NR2 expressed (Dingledine et al., 1999; Cull-Candy and Leszkiewicz, 2004). The identity of the NR2 subunit within a functional NMDA receptor plays a particularly important role in determining many channel properties, including gating kinetics (Erreger et al., 2005) and affinity for Mg^{2+} (Monyer et al., 1992).

Near typical resting membrane potentials, all NMDA receptor subtypes are powerfully inhibited by Mg^{2+} . However, the percentage of inhibition by Mg^{2+} depends on the NR2 subunit present; NR1/2A and NR1/2B receptors are roughly 5-fold more potently inhibited by Mg^{2+} than NR1/2C and NR1/2D receptors (Monyer et al., 1992; Kuner and Schoepfer, 1996; Qian et al., 2005). Upon depolarization, Mg^{2+} block of all NMDA receptor subtypes is relieved. The speed with which Mg^{2+} unblocks from the NMDA receptor in response to membrane depolarization is also influenced by the NR2 subunit. In response to depolarization, Mg^{2+} unblocks from NR1/2C and NR1/2D receptors very rapidly, while Mg^{2+} unblock from NR1/2A and NR1/2B receptors displays a prominent slow component (Clarke and Johnson, 2006).

A slow component of Mg^{2+} unblock from NR1/2A and NR1/2B receptors was unexpected based on the rapid kinetics with which Mg^{2+} interacts with open NMDA receptor channels (Nowak et al., 1984; Ascher and Nowak, 1988). Two models have recently been

proposed in which slow Mg^{2+}_o unblock arises because Mg^{2+}_o block increases occupancy of Mg^{2+}_o bound, closed states (Kampa et al., 2004; Vargas-Caballero and Robinson, 2004). In these models, Mg^{2+}_o block stabilizes the closed state of the receptor by altering receptor gating alone (Vargas-Caballero and Robinson, 2004), or in addition to altering desensitization and agonist unbinding rates (Kampa et al., 2004). However, other work has suggested that there is little interaction between Mg^{2+}_o and the gating machinery of the NMDA receptor (Sobolevsky and Yelshansky, 2000; Qian et al., 2002; Blanpied et al., 2005).

In an attempt to reconcile these results, we proposed a model in which the inherent voltage dependent properties of NR1/2B receptor activation result in slow Mg^{2+}_o unblock (NR1/2B Model, Chapter 2). Because Mg^{2+}_o unblock from NR1/2A receptors displays a slow component (Clarke and Johnson, 2006), we set out to determine if NR1/2A receptor activity also displays inherent voltage dependence. We find that NR1/2A receptor currents recorded in 0 Mg^{2+}_o are consistent with inherent voltage dependence of NR1/2A receptor activation. We incorporated the recent work describing the kinetics of NR1/2A receptor activation (Erreger et al., 2005) into the previously described NR1/2B Model, leaving the strength of inherent voltage sensitivity of the model unchanged. The voltage dependent NR1/2A model predicted a slow component of depolarization induced current relaxation in 0 and 1 mM Mg^{2+}_o . Even though the NR1/2A and NR1/2B models contained identical voltage sensitivity (e-fold per 175 mV), model simulations predicted more rapid relaxation kinetics of NR1/2A receptor currents. These model simulations are consistent with previous data showing that Mg^{2+}_o unblock proceeds more rapidly from NR1/2A than NR1/2B receptors (Clarke and Johnson, 2006).

4.3 MATERIALS AND METHODS

4.3.1 Cell culture and transfection

The culture and transfection methods used in this study are described in section 2.3.1.

4.3.2 Solutions

Solutions were prepared and applied according to the procedures described in section 2.3.2. Currents were activated by the indicated concentration of NMDA or glutamate either in 0 or 1 mM Mg^{2+} . 10 μ M glycine was added to all solutions. Osmolality and pH were adjusted as described in section 2.3.2. The junction potential between the pipette and bath solution was 5 mV and all holding potentials were corrected for junction potentials.

4.3.3 Whole-cell recording

Whole-cell recordings were performed as described in section 2.3.3.

4.3.4 Data analysis and Curve Fitting

Whole-cell currents were leak and capacitance corrected as described in section 2.3.4. NR1/2A receptor currents were then fit with multi-exponential equations as described in section 2.3.4. The number of exponential components was adjusted as necessary to provide high quality fits, as determined visually. For experiments shown in **Figure 28**, I_{repol} was quantified using a multi-step procedure. First, two responses to glutamate application at -65 mV were collected and averaged. The two -65 mV responses were collected before and after the glutamate application during which the voltage jumps were applied to account for current run-down due to sequential glutamate applications. The averaged -65 mV response was then fit with a double exponential equation. The fits had τ 's of 42.3 ± 7.9 ms and 272.5 ± 83.9 ms ($n = 3$). The fits were used to give a noiseless estimate of the inward current at a given time-point. The I_{repol} stimulated by each 2.5 ms depolarization was then measured. To account for desensitization, each I_{repol} was normalized to the inward current estimate from the double exponential fit to the averaged -65 mV response. In other words, the I_{repol} was expressed as a fraction of the inward current level at the time of membrane repolarization.

4.3.5 Kinetic Modeling

All model fitting and current simulations were done using SCoP 4.0 (Simulation Resources, Inc., Berrien Springs, MI). The model used was based on the NR1/2B Model (**Fig. 15**). Rates were adapted to represent NR1/2A receptors based on Erreger et al. (2005) (see **Table 7**). The only rates that differed from Erreger et al. (2005) were the forward rate of the NR2A subunit conformational change (k_{s+}) and the entry into and recovery from desensitized states. The rate k_{s+} depended exponentially on membrane voltage (Hille, 2001) with the same sensitivity as that used previously in the NR1/2B Model (e-fold per 175 mV, **Fig. 17**). Because desensitization rates and channel number vary from cell to cell, these parameters were determined by fitting the NR1/2A Model whole-cell current responses. The NR1/2A model was fitted to whole-cell currents in response to applications of 1 mM glutamate in the continuous presence of 10 μ M glycine +/- 1 mM Mg^{2+}_o with desensitization rates and receptor number as free parameters. In 0 Mg^{2+}_o , whole-cell currents in response to applications of 1 mM glutamate at -65 mV were fitted with the model depicted in **Figure 24a**. In 1 mM Mg^{2+}_o , whole-cell currents elicited by the application of 1 mM glutamate at 35 mV were fitted with the model depicted in Figures 25a. All others rate constants were fixed (**Table 7**). After desensitization rates and receptor number were determined, all rates were fixed and model simulations were run in response to depolarizations from -65 mV to the indicated depolarized voltage.

4.4 RESULTS

4.4.1 NR1/2A receptor currents are enhanced at positive membrane potentials

Several observations suggest that NMDA receptor activity is inherently modulated by membrane voltage (Konnerth et al., 1990; Keller et al., 1991; D'Angelo et al., 1994; Benveniste and Mayer, 1995; Spruston et al., 1995). As described in Chapter 2, a slow (τ of several ms) component of NR1/2B receptor current relaxation in response to membrane depolarization results from voltage-dependent gating of NR1/2B receptors. The slow component of NR1/2B

receptor current relaxations was present in 0 Mg^{2+}_o and was greatest in response to large amplitude depolarizations. We first set out here to determine if NR1/2A receptor currents also display a slow component of relaxations in response to large amplitude depolarizations in 0 Mg^{2+}_o .

Currents were elicited from HEK 293T cells expressing NR1/2A receptors by application of 30 μM NMDA or 1 mM glutamate in the continuous presence of 10 μM glycine (termed “NMDA” and “Glu”, respectively) and 0 or 1 mM Mg^{2+}_o . NR1/2A receptor currents displayed marked desensitization, reaching a steady-state value after ~15 seconds of continuous agonist application (**Fig. 23a**). Once a steady-state current level was reached, the cell was depolarized from -65 mV to either 55 or 95 mV in NMDA experiments and from -65 mV to either 35 or 95 mV in Glu experiments. A slow component of the current relaxation in response to depolarization was reliably observed in 1 mM Mg^{2+}_o , indicating a slow phase of Mg^{2+}_o unblock (**Fig. 23**, right). However, a slow component of current relaxation in response to large amplitude depolarizations was also observed in 0 Mg^{2+}_o (**Fig. 23**, left).

Depolarization-induced current relaxations in both 0 and 1 mM Mg^{2+}_o were well fit by a triple (NMDA) or double (Glu) exponential equation. The time constants of the fast and first slow component (τ_{fast} and τ_{slow} , respectively) did not depend significantly on the amplitude of the depolarization or on the presence of Mg^{2+}_o (**Table 6**). The value of τ_{slow} was significantly faster in Glu than NMDA for all depolarizations. These data are consistent with previous work (Clarke and Johnson, 2006) describing an acceleration of the slow component of Mg^{2+}_o unblock at high agonist concentrations. The second slow component, $\tau_{\text{slow}2}$, was highly variable, present only in NMDA experiments, and accounted for less than 5% of the total current relaxation (**Table 6**).

In experiments utilizing NMDA, the amplitude of τ_{slow} (A_{slow}) in 0 Mg^{2+}_o was significantly larger in response to depolarizations to 95 than to 55 mV (**Table 6**). In experiments utilizing Glu, a slow component of current relaxation in 0 Mg^{2+}_o was reliably observed only in response to depolarization from -65 to 95 mV. The -65 to 35 mV depolarization may have been too small to induce a prominent slow component of NR1/2A receptor current relaxation. This is contrast to results from NR1/2B receptors, which display a slow component of current relaxation in Mg^{2+}_o in response to depolarizations as small as -65 to 15 mV (**Fig. 12c**). In both NMDA and Glu experiments, A_{slow} was significantly larger in 1 mM than 0 mM Mg^{2+}_o in response to all depolarizations (**Table 6**).

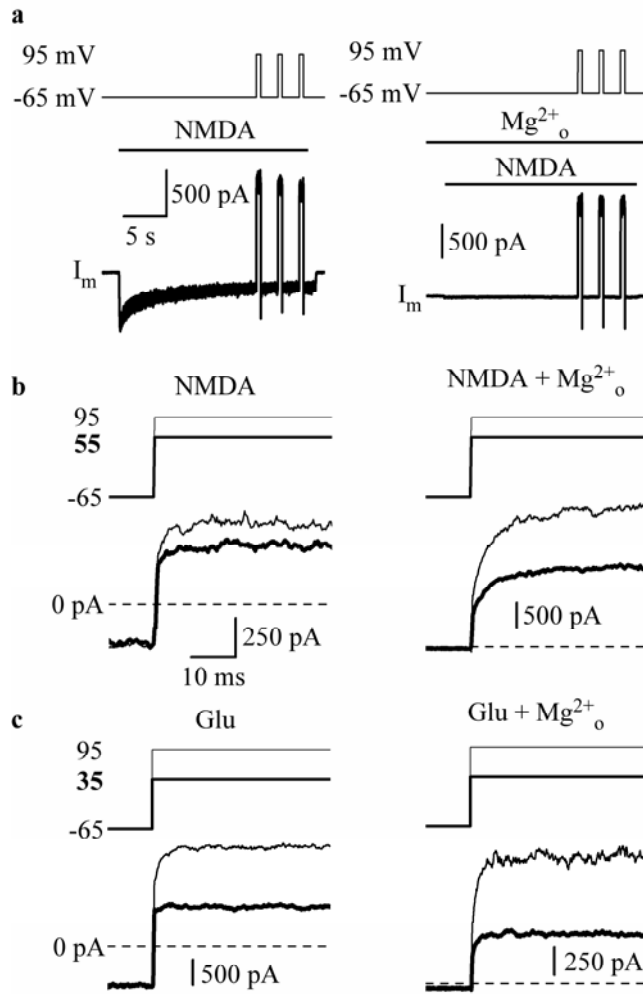


Figure 23. NR1/2A receptor currents display a slow component of relaxation in response to depolarization in both 0 and 1 mM Mg²⁺. (a) 30 μM NMDA and 10 μM glycine (“NMDA”) was applied in 0 (left) and 1 mM Mg²⁺ (right) during whole-cell recordings from an HEK 293T cell expressing NR1/2A receptors. Once the current (bottom trace) had reached a stationary level, three depolarizing voltage jumps (here, -65 to 95 mV) were applied (top trace). NR1/2A receptor currents were leak and capacitive subtracted prior to multi-exponential fitting (See Methods, section 2.3.4). (b) Currents (bottom trace) elicited by NMDA displayed a slow component of relaxation in response to depolarizations (top trace) from -65 to 55 and 95 mV. The slow relaxation was observed in experiments performed in the presence of 0 (left) and 1 mM (right) Mg²⁺. (c) Similar experimental protocol as in (b), except that NR1/2A receptor currents were elicited by application of 1 mM glutamate in the continuous presence of 10 μM glycine (“Glu”). In 0 Mg²⁺ (left), a slow component of current relaxation was only reliably observed in response to depolarizations from -65 to 95 mV. In contrast, currents recorded in 1 mM Mg²⁺ (right) displayed a clear slow component of relaxation in response to depolarizations from -65 to 35 and 95 mV.

Table 6. Depolarization induced current relaxations in 0 and 1 mM Mg²⁺_o

NMDA				
0 Mg²⁺_o	τ_{fast} (ms)	τ_{slow} (ms)	τ_{slow2} (ms)	A_{slow} (%)
-65 to 55 mV	0.34 ± 0.11	4.66 ± 0.31	139 ± 24.1	13.8 ± 2.4 *
-65 to 95 mV	0.50 ± 0.06	4.60 ± 0.95	42 ± 13.1	27.9 ± 2.9
1 mM Mg²⁺_o	τ_{fast} (ms)	τ_{slow} (ms)	τ_{slow2} (ms)	
-65 to 55 mV	0.66 ± 0.22	5.89 ± 0.88	571 ± 276	36.5 ± 5.7 *, #
-65 to 95 mV	0.67 ± 0.11	6.49 ± 0.58	162 ± 3.5	46.2 ± 2.9 #
Glu				
0 Mg²⁺_o	τ_{fast} (ms)	τ_{slow} (ms)	τ_{slow2} (ms)	A_{slow} (%)
-65 to 35 mV	0.17 ± 0.02	—	—	—
-65 to 95 mV	0.20 ± 0.04	2.56 ± 1.06	—	23.67 ± 5.2
1 mM Mg²⁺_o	τ_{fast} (ms)	τ_{slow} (ms)	τ_{slow2} (ms)	A_{slow} (%)
-65 to 35 mV	0.23 ± 0.03	1.90 ± 0.31	—	30.6 ± 4.0 *
-65 to 95 mV	0.32 ± 0.03	2.14 ± 0.25 \$	—	46.3 ± 0.9 #

Membrane voltage was changed during the steady-state response of NR1/2A receptors to application of NMDA or Glu. Experiments were performed in 0 and 1 mM Mg²⁺_o. Leak and capacitive subtracted currents were fit with multi-exponential equations. * indicates a significant (p < .01) difference between the amplitude of τ_{slow} (A_{slow}) in response to depolarizations from -65 to 35 (Glu) or 55 (NMDA) and 95 mV in the same concentration of Mg²⁺_o. # indicates a significant (p < .01) difference between the A_{slow} values in response to the same voltage jump applied in 0 or 1 mM Mg²⁺_o. \$ indicates a significant (p < .001) difference between the τ_{slow} value in NMDA and Glu experiments in response to identical depolarizations. Values are expressed as mean ± SEM.

Depolarization-induced slow relaxation of NR1/2B receptor currents was attributed to a slow rise in P_{open} upon membrane depolarization. In response to repolarization, NR1/2B receptor currents displayed a tail current which slowly returned to baseline as the P_{open} of the NR1/2B receptor returned to a lower value. NR1/2A receptors also displayed a tail current upon repolarization to -65 mV from several depolarized voltages (**Fig. 24a**). In experiments using NMDA, the repolarization induced inward current peak (I_{peak}) depended on the amplitude of the previous depolarization, having a significantly larger value following repolarization to -65 from 95 than from 55 mV (**Fig. 24b**). Similar results were seen in experiments using Glu; I_{peak} was significantly larger following repolarization to -65 mV from 95 than from 35 mV (**Fig. 24b**).

Following the I_{peak} , the current returned to the baseline level over several ms. The return to baseline was well fit with a single exponential equation. In NMDA experiments, the time constant of the current return to baseline (τ_{ret}) was 3.26 ± 0.43 and 3.90 ± 0.24 ms following repolarization to -65 from 55 and 95 mV, respectively. In Glu experiments, τ_{ret} was 1.62 ± 0.08 and 1.83 ± 1.51 ms following repolarization to -65 from 35 and 95 mV, respectively. Taken together, these data suggest that NR1/2A receptors, like NR1/2B receptors, display inherent voltage dependence such that the P_{open} of NR1/2A receptors is enhanced at depolarized membrane potentials.

4.4.2 Model of inherent voltage dependence of NR1/2A receptors

Previous work has shown that a model containing voltage dependence of the NR2B pre-gating conformational change can account for NR1/2B receptor current responses to changes in membrane voltage in 0 and 1 mM Mg^{2+} (see Chapter 2). We next set out to determine if a similar voltage-dependent model would predict NR1/2A receptor currents accurately. As a starting point, we augmented the previously described NR1/2B Model to represent NR1/2A receptor activation based on Erreger *et al.* (2005), in which the unique activation kinetics of NR1/2A receptors are described (the NR1/2A Model, **Fig. 25a**). For all model fitting and simulations, rates were set to those describe in **Table 7**. The rate constant representing the pre-gating conformational change of the NR2A subunit (k_{s+}) was modified to change exponentially

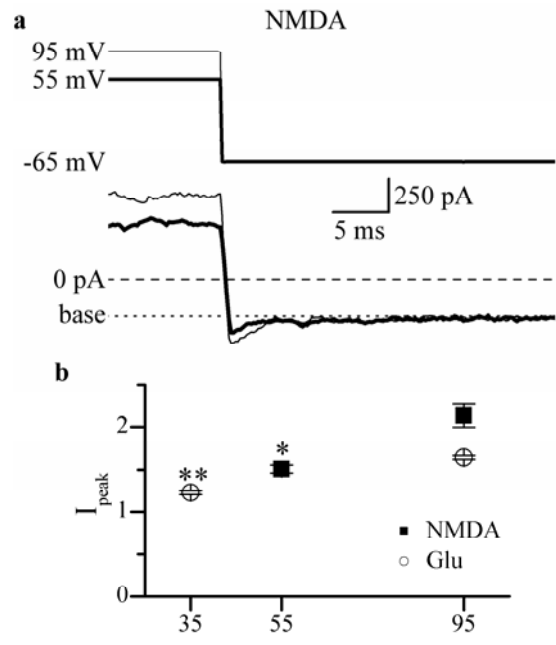


Figure 24. Tail currents following return to -65 mV from several depolarized voltages.

(a) Currents elicited by application of NMDA (bottom trace) during repolarization from 55 mV (thick) or 95 mV (thin) to -65 mV. Immediately following repolarization to -65 mV, the current exceeds the steady-state current measured at -65 mV (base, dotted line). Membrane voltage is indicated by the top trace. (b) I_{peak} values depend significantly on the amplitude of the initial membrane depolarization and become larger following return to -65 mV from more depolarized voltages. Similar results were obtained in experiments utilizing NMDA (black squares) or Glu (open circles). * $p < .01$ and ** $p < .001$.

with membrane voltage based on the following equation:

$$k_{s+} = k_{s+,100mV} * \exp[(V_m + 100 \text{ mV})/V_{dep}] \quad (1)$$

where $k_{s+,100mV}$ is the rate at -100 mV (230 s^{-1}), V_m is the membrane voltage, V_{dep} is the voltage sensitivity of k_{s+} . As a first attempt, we set V_{dep} to the same level as in the NR1/2B model (e-fold per 175 mV). We reasoned that similar voltage dependence of k_{s+} may impact NR1/2A and NR1/2B currents differently because NR1/2A receptors undergo pre-opening conformational changes more rapidly than NR1/2B receptors (Erreger et al., 2005).

Before current simulations were run, receptor number and desensitization rates were determined because these parameters vary widely from cell to cell. To determine receptor number and desensitization rates, the NR1/2A model was fitted to whole-cell currents in response to an application of 1 mM glutamate at -65 mV in 0 mM Mg^{2+}_o (**Fig. 25b**). During fitting, receptor number and desensitization rates were the only free parameters, with all other rates fixed to the values in **Table 7**. Consistent with previous reports (Erreger et al., 2005), NR1/2A receptor currents were well fit by a model containing two desensitized states (**Fig. 25b, d**). Once receptor number and desensitization rates were determined, all rates were fixed and the NR1/2A model was used to simulate currents in response to depolarizations from -65 to 35 and 95 mV. The current simulations showed reasonable agreement with experimentally recorded NR1/2A receptor currents (**Fig. 25c, e**). In contrast, current simulations from a model containing the rates in **Table 7**, but no voltage dependence, underestimated outward current levels in response to each depolarization (**Fig. 25c, e**, black lines).

A similar set of experiments were carried out in the presence of 1 mM Mg^{2+}_o . To account for block by Mg^{2+}_o , an additional “blocked arm” was added to the NR1/2A model (**Fig. 26a**). The blocked arm followed a trapping block scheme in which the NMDA receptor channel was able to close while bound by Mg^{2+}_o , trapping the Mg^{2+}_o ion within the pore. The NR1/2A model was assumed to be symmetric, meaning that the corresponding rates in the blocked and unblocked arms were equivalent. This is in contrast to previous models developed to explain slow Mg^{2+}_o unblock (Kampa et al., 2004; Vargas-Caballero and Robinson, 2004), which proposed asymmetric models (see Discussion). Due to the strong inhibition of NR1/2A receptor currents

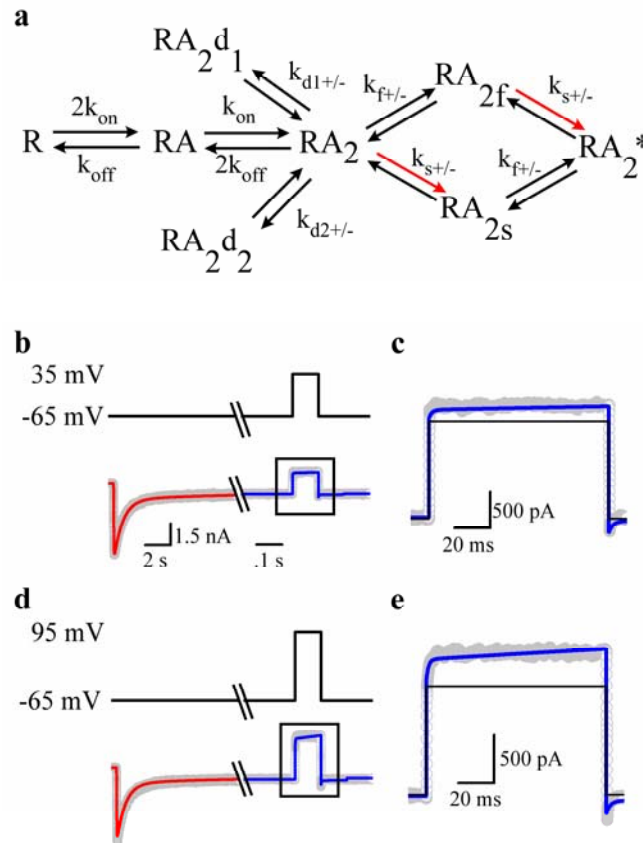


Figure 25. Depolarization induced slow relaxation can be reproduced by a model containing inherent voltage dependence of NR1/2A receptor activation. (a) Kinetic model used to simulate NR1/2A receptor activation based on Erreger et al. (2005). Red arrows indicate rates (k_{s+}) which were voltage dependent (e-fold change per 175 mV). The voltage dependence was such that k_{s+} became more rapid with depolarization. (b) Current traces (bottom grey trace) during application of 1 mM glutamate at -65 mV. Model fits are overlaid (red traces). Fitting was performed on the first 8-s of the current response (prior to hatch marks) with desensitization rates and receptor number allowed to vary. Once the receptor number and desensitization rates were determined, all rates were fixed and the NR1/2A model was used to simulate currents (blue traces) in response to depolarization from -65 to 35 mV. Membrane voltage is indicated by the top trace. (c) Enlarged view of the current trace (grey) and current simulation (blue) in response to a depolarization from -65 to 35 mV. Current simulations from a model containing no voltage dependent rates are overlaid (black trace). (d, e) As in (b & c), except the depolarization was from -65 to 95 mV.

Table 7. Rates used for NR1/2A receptor model fitting and current simulations.

	<u>Unit</u>	<u>Rate Constant</u>
k_{on}	$\mu\text{M}^{-1} \text{s}^{-1}$	31.6
$k_{B_{off}}$	s^{-1}	1010
k_{s+}	s^{-1}	230
k_{s-}	s^{-1}	178
k_{f+}	s^{-1}	3140
k_{f-}	s^{-1}	174
k_{d1+}	s^{-1}	Determined by fitting
k_{d1+}	s^{-1}	Determined by fitting
k_{d1-}	s^{-1}	Determined by fitting
k_{d2+}	s^{-1}	Determined by fitting
k_{d2-}	s^{-1}	Determined by fitting

Where indicated, rates were determined by fitting the NR1/2A Model to macroscopic currents as described in the text (see **Fig. 24, 25**). The remaining rates were taken directly from Erreger *et al.* (2005). # indicates that this rate was modified to change exponentially with membrane voltage as described in the text. During current simulations (indicated by blue traces) all rates were fixed. Corresponding rates in the unblocked and blocked arms were equivalent.

by 1 mM Mg^{2+}_o at -65 mV, receptor number and desensitization rates were determined by fitting the NR1/2A Model to whole-cell currents in response to an application of 1 mM glutamate at 35 mV. As seen above, excellent fits were obtained using a model which contained two desensitized states (**Fig. 26b**). The desensitized states were omitted from **Figure 26a** for clarity, but were present during fitting. The desensitized states were accessible from the RA_2 state in the unblocked arm and the RA_2Mg state in the blocked arm. Once receptor number and desensitization rates were determined, all rates were fixed and current simulations were generated in response to voltage jumps from -65 to -25, 35, and 95 mV. The NR1/2A Model provided reasonable fits to the experimental data, accounting for the slow component of Mg^{2+}_o unblock (**Fig. 26d-f**). In contrast, a model containing no voltage dependence provided poor estimates of the current responses to all three depolarizations (**Fig. 26d-f**).

4.4.3 Kinetics of slow relaxation of NR1/2A currents

Thus far, we have shown that the NR1/2A model can reasonably reproduce slow NR1/2A receptor current relaxations in 0 and 1 mM Mg^{2+}_o . We have shown previously that the slow component of depolarization-induced current relaxation in 1 Mg^{2+}_o is larger and displays faster kinetics from NR1/2A than NR1/2B receptors (**Table 7** and (Clarke and Johnson, 2006)). Is the NR1/2A model able to reproduce these results? A direct comparison of NR1/2A and NR1/2B Model simulations in 1 mM Mg^{2+}_o shows a more rapid initial relaxation of NR1/2A currents, but overall a larger enhancement of NR1/2B currents in response to membrane depolarization (**Fig. 27a,b**). The current simulations contained a large slow component with a tau (τ_{slow}) of 1.81 ms for NR1/2A simulations and 3.57 ms for NR1/2B simulations. These values are very similar to the values obtained from multi-exponential fits of experimental data (**Fig. 27c**). The voltage-sensitivity of k_{s+} in the NR1/2A Model was identical to the voltage-sensitivity of k_{s+} in the previously described NR1/2B Model. These results suggest that differences in gating kinetics (Erreger et al., 2005) can at least partially account for the NR2 subunit differences in the kinetics of Mg^{2+}_o unblock.

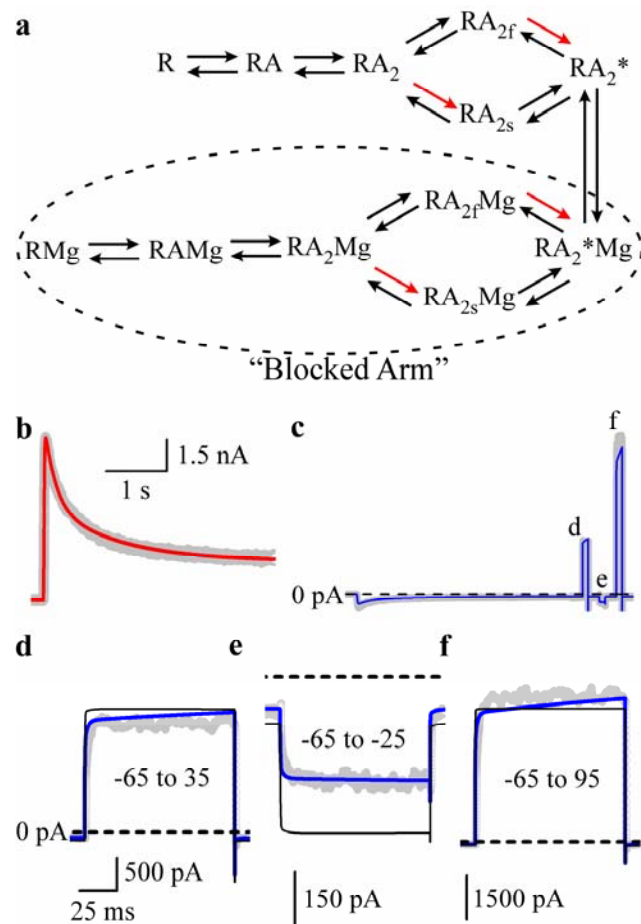


Figure 26. Slow Mg^{2+}_o unblock can be explained by voltage dependent gating of NR1/2A receptors. (a) A schematic of the kinetic model used to simulate NR1/2A receptor currents. An additional arm (termed the “blocked arm”) was added to the NR1/2A Model to account for block by Mg^{2+}_o . Red arrows indicate rates (k_{s+}) which were voltage sensitive (e-fold per 175 mV) (b) Current traces (grey trace) during application of 1 mM glutamate in the presence of 10 μ M glycine and 1 mM Mg^{2+}_o while the cell was held at 35 mV. The NR1/2A Model was fitted (red trace) to the current response to 1 mM glutamate at 35 with desensitization rates and channel number as free parameters. (c) Current simulations (red trace) and experimental data (grey trace) during application of 1 mM glutamate and 1 mM Mg^{2+}_o at -65 mV. Once a steady state response was reached the cell was depolarized from -65 to 35, -25 and 95 mV. Model parameters were fixed as those determined from the fit in (a). (d, e, f) Expanded views of current traces (grey) and simulations (red) in response to a depolarization from -65 to 35 (d), -25 (e), and 95 mV (f). Current simulations from a model containing no voltage dependence are overlaid (black traces).

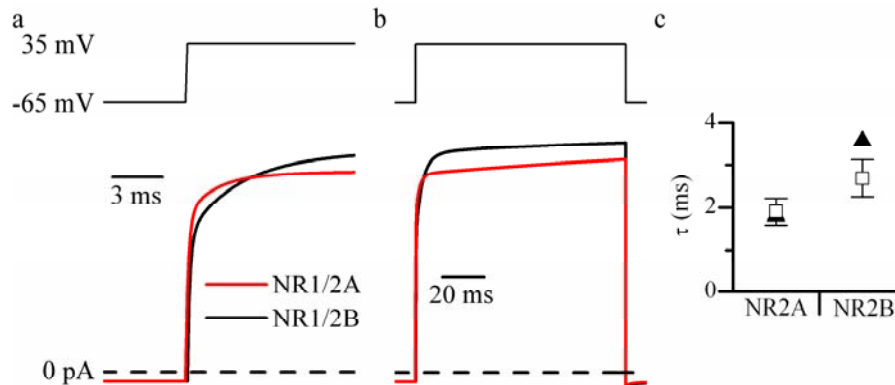


Figure 27. NR2 subunit specific gating kinetics lead to differences in Mg^{2+}_o unblocking kinetics. (a, b) Current simulations from the NR1/2A (red) and NR1/2B (black) Models in response to a voltage jump from -65 to 35 mV. Simulations are taken directly from Figure 25b (NR1/2A) and **Figure 19c** (NR1/2B). (c) Current simulations (black triangles) contain a prominent exponential component which is similar to that obtained from multi-exponential fits to experimental data (open squares). Even though the NR1/2A and NR1/2B Models contain identical voltage sensitivity, the NR1/2A Model predicts more rapid depolarization-induced Mg^{2+}_o unblock.

4.4.4 Mg^{2+}_o unblock and desensitization

In NR1/2A Model simulations there was an additional slow component of current relaxation with a time constant of several hundred ms (**Fig. 27b**). This second slow component accounted for as much as 28% of the total relaxation of NR1/2A Model simulations. The additional slow component arose due to slow egress of channels from Mg^{2+}_o -bound, desensitized states (data not shown). Because the additional slow component developed as desensitization proceeded, simulations in which voltage-jumps are applied shortly following receptor activation do not display the second slow component (**Fig. 28a, b**).

These simulation results suggest depolarizations occurring long after receptor activation would be less effective at stimulating Mg^{2+}_o unblock from NR1/2A receptors than depolarizations occurring shortly after receptor activation. We next set out to determine if, in recombinant NR1/2A receptors, depolarizations occurring shortly after receptor activation stimulate faster Mg^{2+}_o unblock than depolarizations occurring long after receptor activation. To this end, we applied brief (2.5 ms) depolarizations from -65 to 35 mV at various time points during a 600 ms application of 1 mM glutamate in the continuous presence of 10 μ M glycine and 1 mM Mg^{2+}_o (**Fig. 28c**). We then measured the peak of inward current upon repolarization to -65 mV (I_{repol}), prior to re-block by Mg^{2+}_o . The repolarization-induced peak reflects the number of unblocked NR1/2A receptors and is the point at which maximum Ca^{2+} influx occurs. The I_{repol} values were normalized to remove effects of desensitization (see Methods). Regardless of the time post-agonist application at which the depolarization occurred, the normalized I_{repol} values were not statistically different (**Fig. 28d**). These data suggest that the kinetics of depolarization-induced Mg^{2+}_o unblock from NR1/2A receptors do not depend critically on the timing between agonist application and membrane depolarization (Clarke and Johnson, 2006), but see (Kampa et al., 2004).

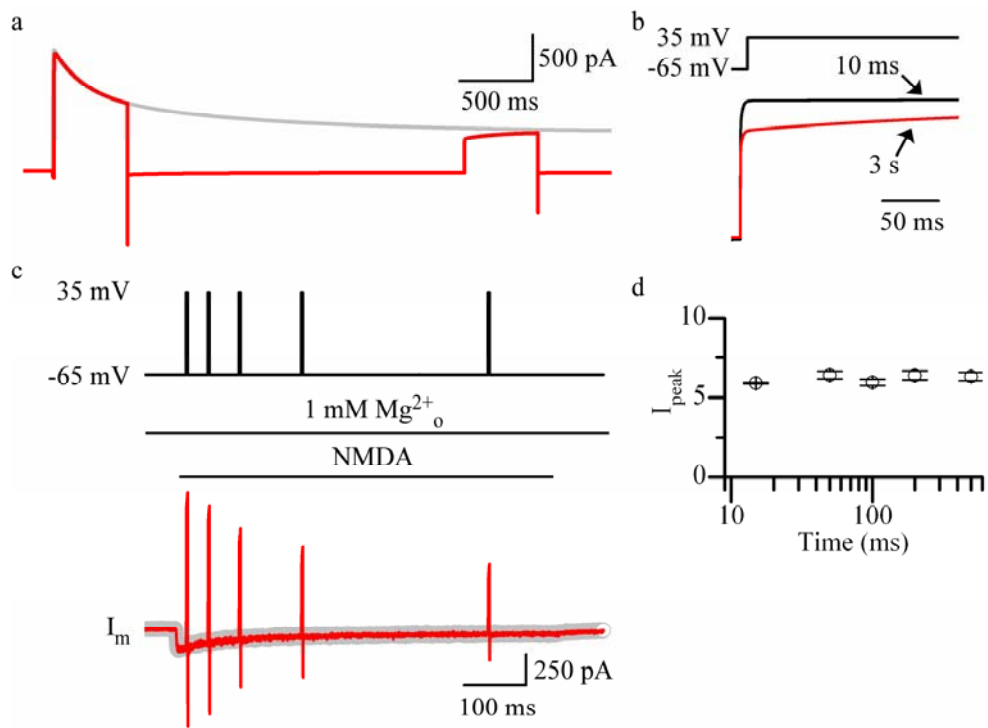


Figure 28. Depolarization induced inward currents do not depend on the timing between receptor activation and membrane depolarization. (a) Current simulations from the NR1/2A Model in response to application of 1 mM glutamate at 35 mV (grey) or at -65 mV (red). During the current simulation to glutamate application at -65 mV, 500 ms depolarizing voltage steps from -65 to 35 mV were applied either 10 ms or 3.0 s after receptor activation. Current simulations were performed in the presence of 1 mM Mg^{2+} . (b) Current simulations from (a) are enlarged around the region of membrane depolarization. To allow comparisons, current simulations in response to depolarizations from -65 to 35 mV applied either 10 ms (black) or 500 ms (red) after receptor activation are shifted so that the time of depolarization is identical. To remove effects of desensitization, the depolarization-induced simulated currents were normalized to currents from a simulated response to glutamate application at a constant membrane potential of 35 mV. A second slow component with a τ of several hundred ms is only present in response to the voltage jump occurring 3 s following receptor activation. (c) NR1/2A receptor currents (bottom traces) recorded in response to application of 1 mM glutamate at -65 mV in the continuous presence of 1 mM Mg^{2+} . Currents are shown either just in response to glutamate application (grey traces), or in response to glutamate application during which several 2.5 ms depolarizations to 35 mV were applied (red traces). Depolarizations (top trace) were applied at various time points (15, 50, 100, 200, 500 ms) following receptor activation. (d) Pooled I_{peak} values induced by 2.5 ms depolarizations occurring at various time points following NR1/2A receptor activation. All recordings were done in the continuous presence of 1 mM Mg^{2+} .

4.5 DISCUSSION

Here, we report a slow relaxation of NR1/2A receptor currents in response to membrane depolarization in 0 Mg^{2+}_o . The kinetics of the slow current relaxation are nearly identical to the kinetics of slow Mg^{2+}_o unblock (**Table 6**), suggesting a common molecular mechanism. A kinetic model of NR1/2A receptor activation containing weak inherent voltage dependence of the NR2A subunit pre-opening conformational change (the NR1/2A Model) reasonably reproduced NR1/2A receptor currents in response to depolarizations in 0 and 1 mM Mg^{2+}_o . These data suggest that gating of the NR1/2A receptor, like the NR1/2B receptor, is modulated by membrane voltage.

4.5.1 Inherent voltage dependence of NMDA receptors

A number of observations in the literature suggest that NMDA receptors display inherent voltage dependence. A slow component of current relaxation in response to membrane depolarization has been reported previously from native hippocampal NMDA receptor currents recorded in 0 Mg^{2+}_o (Benveniste and Mayer, 1995; Spruston et al., 1995). The slow current relaxation accounted for as much as 23% of the total response to a depolarization from -100 to 60 mV and was well fit by an exponential component with a τ of 2.5 ms (Benveniste and Mayer, 1995). These results are consistent with expression of NR1/2A receptors, which is plausible based on previous studies showing high expression of the NR2A subunit in the hippocampus (Monyer et al., 1994). Several studies have also shown that NMDA-EPSC decay becomes slower with depolarization (Konnerth et al., 1990; Keller et al., 1991; D'Angelo et al., 1994). Finally, the NMDA receptor open probability (P_{open}) has been reported to increase with membrane depolarization (Nowak and Wright, 1992; Li-Smerin and Johnson, 1996; Li-Smerin et al., 2000)

The previous data suggesting that NMDA receptors display inherent voltage dependence led us to investigate if voltage dependent gating could also explain the slow NR1/2A receptor current relaxations we observed in response to membrane depolarization. Using kinetic

modeling, we were able to show that a voltage-dependent NR1/2A model (the NR1/2A Model) reasonably reproduced NR1/2A receptor currents in response to membrane depolarization in 0 and 1 mM Mg^{2+}_o . The NR1/2A Model was adapted from the NR1/2B Model (**Fig. 15**) based on previous work describing the gating kinetics associated with NR1/2A receptor activation (Erreger et al., 2005). Erreger *et al.* (2005) hypothesized that NR1/2A receptors undergo pre-gating conformational changes more rapidly than NR1/2B receptors (Erreger et al., 2005). Thus, we reasoned that identical voltage sensitivity (e-fold per 175 mV) of the forward rate (k_{s+}) of NR2 subunit pre-opening conformational change may differentially impact NR1/2A and NR1/2B currents. Indeed, in model simulations the NR2 subunit differences in gating lead to more rapid relaxation of NR1/2A than NR1/2B receptor currents in response to membrane depolarization (**Fig. 27**). A similar trend was also seen in experimental recordings (**Table 7**). These data suggest that NR2 subunit differences in gating kinetics can explain the NR2 subunit-dependent differences in depolarization induced current relaxations (Clarke and Johnson, 2006).

4.5.2 Desensitization and Mg^{2+}_o unblock

An interesting discrepancy between current simulations and experimental data is that the NR1/2A model predicts a large, very slow second slow component (τ of several hundred ms) Mg^{2+}_o unblock. In our hands, a very slow component of Mg^{2+}_o unblock is only seen under certain experimental conditions (**Table 6**, and (Clarke and Johnson, 2006)), although the very slow component never accounted for more than 10% of the total current relaxation. This is in contrast to NR1/2A Model simulations in which the very slow component of Mg^{2+}_o unblock accounts for as much as 23% of the total current relaxation in response to depolarization. These simulation results agree with the previous observation of a large very slow component of Mg^{2+}_o unblock from native NMDA receptors ((Kampa et al., 2004), but see (Vargas-Caballero and Robinson, 2004)). In Kampa *et al.* (2004), and in NR1/2A Model simulations here, there is relationship between the very slow component of Mg^{2+}_o unblock and desensitization (**Fig. 28**). The experimental variability of the very slow component of Mg^{2+}_o unblock may, at least in part, arise because NMDA receptor desensitization varies both with the duration of recording and the experimental preparation (Sather et al., 1990; Sather et al., 1992)

The characteristics of the very slow component of Mg^{2+} unblock in NR1/2A Model simulations and experimental data presented here are significantly different, suggesting that the arrangement of the desensitized states in the NR1/2A model may be inappropriate. In the current NR1/2A Model, the desensitized states are accessible from the A2R state, as has been previously proposed (Banke and Traynelis, 2003; Erreger et al., 2005). However, the exact location of the desensitized states is difficult to determine and remains unclear (Gibb, 2004). For example, in a recent study from Schorge, Elenes, & Colquhoun (2005), a model of NR1/2A receptor activation is proposed which contains a single desensitized state accessible only once the receptor is fully bound by both glutamate and glycine and the NR1 subunit has undergone pre-gating conformational changes (Schorge et al., 2005).

The very slow component of Mg^{2+} unblock has been suggested to play a role in shaping the time-window for STDP by rendering depolarizations occurring long after receptor activation less effective at stimulating Mg^{2+} unblock than depolarizations occurring shortly after receptor activation (Kampa et al., 2004). Here, in experimental conditions in which the very slow component of Mg^{2+} unblock is negligible, we find no relationship between the kinetics of Mg^{2+} unblock and the timing between receptor activation and membrane depolarization (**Fig. 28c, d**). These results suggest that in the absence of a very slow component of unblock, the kinetics of Mg^{2+} unblock do not alter the time-window for STDP mediated by NR1/2A receptors. Thus, in future studies it will be important to determine under which conditions the very slow component of Mg^{2+} unblock is present.

4.5.3 Functional implications for synaptic currents

The NR1/2B Model predicts voltage-dependent decay of synaptic-like NR1/2B receptor currents (**Fig. 22**). To determine if the NR1/2A Model predicts similar voltage-dependent decay we used the NR1/2A Model to simulate NR1/2A receptor currents in response to a synaptic-like glutamate waveform. To eliminate any potential complications from receptor desensitization, all simulations were performed using models lacking desensitized states. All other rates were set to those shown in **Table 7**. **Figure 29a** shows the current responses of 100 NR1/2A receptors to a synaptic glutamate waveform at membrane potentials of -70, -30, -10 and 30 mV in the presence of 1 mM Mg^{2+} . Similar to the results observed using the NR1/2B Model (**Fig. 22**), the decay of

the simulated NR1/2A synaptic-like currents is voltage dependent (**Fig. 29b**). Voltage-dependent changes in the kinetics of NMDA receptor mediated EPSCs may be an important mechanism by which depolarization enhances NMDA receptor mediated currents, beyond relief of Mg^{2+} block.

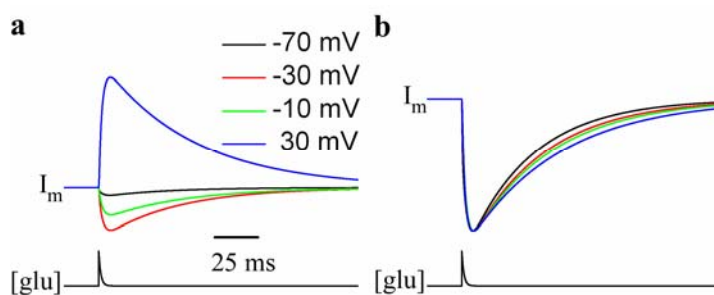


Figure 29. Decay of NR1//2A synaptic-like current simulations is only modestly influenced by membrane voltage. (a) Simulations of NR1//2A receptor currents (top traces) in response to a synaptic-like glutamate application (bottom trace) in the presence of 1 mM Mg^{2+} . Simulations were performed at a variety of membrane potentials using the rates from **Table 7** and no desensitized states. (b) The response at 30 mV was inverted (blue trace) and the peak current from each simulation in (a) was normalized to ease comparisons of decay time. The decay slowed modestly with depolarization from -70 to 30 mV.

5.0 GENERAL DISCUSSION

The research presented in this dissertation focused on the relationship between NMDA receptor gating, membrane voltage, and block by Mg^{2+}_o . In addition, we investigated how these characteristics are modified based on the type of NR2 subunit present within a functional NMDA receptor. The main conclusions were that NR1/2A and NR1/2B receptor activation displays inherent voltage dependence, while NR1/2C and NR1/2D receptor activation does not. The voltage dependence of NR1/2A and NR1/2B receptor activation led to a slow component of Mg^{2+}_o unblock that was not observed from NR1/2C and NR1/2D receptors. In the following discussion I will address some of the broader mechanistic and physiological implications of the research.

5.1 SLOW UNBLOCK VERSUS SLOW POTENTIALIAION

One of the main conclusions of this dissertation is that the inherent voltage dependent characteristics of NR1/2A and NR1/2B receptors can account for slow relaxations in response to depolarizations in both the absence and presence of Mg^{2+}_o . We were drawn to the potential relationship between slow current relaxations in the absence and presence of Mg^{2+}_o because they shared similar kinetics and NR2 subunit dependence. Slow current relaxations in 0 and 1 mM Mg^{2+}_o were observed in response to membrane depolarization in experiments from NR1/2A and NR1/2B receptors. In contrast, NR1/2C and NR1/2D receptor currents relaxed very rapidly in response to membrane depolarization in the 0 and 1 mM Mg^{2+}_o . Even large amplitude depolarizations did not elicit a slow component of NR1/2D receptor current relaxation (**Fig. 30**).

To account for slow current relaxation in response to membrane depolarization in 0 Mg^{2+}_o , we proposed two models in which the open state of NR1/2A and NR1/2B receptors are

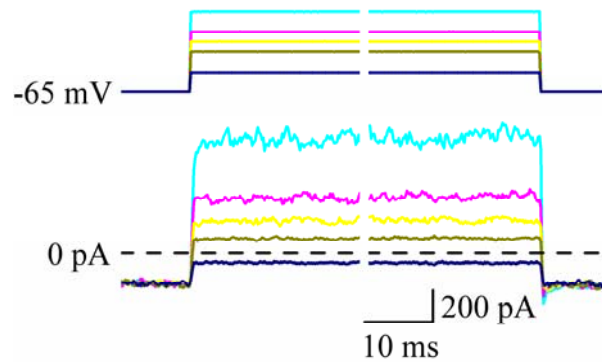


Figure 30. NR1/2D receptor currents do not display a slow component in response to depolarization in 0 Mg^{2+} . NR1/2D receptor currents (bottom traces) were activated by application of 30 μM NMDA in the continuous presence of 10 μM glycine and 0 Mg^{2+} . Once a steady-state current was reached, the voltage was changed from -65 to -25 (blue), 15 (olive), 35 (yellow), 55 (magenta), and 95 mV (cyan). In response to membrane depolarization, NR1/2D receptor currents relaxed from inward to outward currents very rapidly, with the outward current reaching a steady-state level within 2 ms of the end of the voltage jump.

stabilized at depolarized voltages. These models are consistent with the previous observation that the P_{open} of NMDA receptors is higher at depolarized membrane potentials (Nowak and Wright, 1992; Li-Smerin and Johnson, 1996; Li-Smerin et al., 2001). In the presence of Mg^{2+}_o the proposed models become more complicated. A portion of the slow relaxation upon membrane depolarization in the presence of Mg^{2+}_o reflects stabilization of the open state similar to that seen in the absence of Mg^{2+}_o . However, the addition of Mg^{2+}_o increased the amplitude of the slow relaxation (**Fig. 19b**). The slow component is exaggerated in the presence of Mg^{2+}_o because of slow exit of receptors from the blocked arm. In this discussion, slow current relaxation in the presence of Mg^{2+}_o will be functionally defined as slow Mg^{2+}_o unblock, even though a portion of the relaxation reflects higher occupation of the open state by channels which have already unblocked Mg^{2+}_o .

It is important to note that the models described in this dissertation differ from previous models that suggest slow Mg^{2+}_o arises from alterations of one, or more, NMDA receptor characteristics when the receptor is blocked by Mg^{2+}_o (Kampa et al., 2004; Vargas-Caballero and Robinson, 2004). It is entirely possible that a truly accurate model would contain a combination of voltage dependent activation and slightly different gating kinetics in the presence of Mg^{2+}_o . However, in this general discussion only models containing inherent voltage dependence are discussed.

5.2 INTERACTIONS BETWEEN BLOCKERS AND CHANNEL GATING

Several NMDA receptor channel blockers have been shown to alter channel gating to some extent while blocking (Blanpied et al., 1997; Dilmore and Johnson, 1998; Sobolevsky et al., 1999; Sobolevsky and Yelshansky, 2000; Blanpied et al., 2005). The impact of block by Mg^{2+}_o on channel gating remains controversial. The NR1/2A and NR1/2B Models presented in this dissertation assume that Mg^{2+}_o block does not impact any aspects of NMDA receptor channel gating. In contrast, two models previously proposed to account for the slow component of Mg^{2+}_o unblock suggest that Mg^{2+}_o block enhances channel closure alone (Vargas-Caballero and Robinson, 2004), or in concert with alterations in the rates of desensitization and agonist unbinding (Kampa et al., 2004).

Data relevant to the issue of how Mg^{2+}_o block affects channel gating come from experiments using the open channel blocker amantadine. Amantadine has recently been shown to increase occupancy of the closed state of the NMDA receptor when blocking by accelerating the rate of channel closure (Blanpied et al., 2005). The degree to which amantadine block accelerates channel closure (~3-fold) is very similar to that proposed for Mg^{2+}_o block (Vargas-Caballero and Robinson, 2004). If block by amantadine and Mg^{2+}_o both accelerate channel closure, and acceleration of channel closure leads to the slow component of Mg^{2+}_o unblock, then unblock of amantadine would be expected to display a slow component. Indeed, depolarization-induced amantadine unblock does display a prominent slow component (**Fig. 31a**). However, depolarization induced unblock of amantadine proceeds significantly slower than unblock of Mg^{2+}_o (**Fig. 31b, Table 8**), even though amantadine unblocks from open NMDA receptor channels even faster than Mg^{2+}_o (Blanpied et al., 2005). These data suggest that any influence of Mg^{2+}_o block on NMDA receptor gating must be less than that observed during amantadine block.

The interactions between channel blockers and gating can provide information regarding the conformational changes associated with channel activation. Because amantadine is trapped by NMDA receptor channels (Blanpied et al., 1997), the site at which amantadine binds must be deep within the channel pore, at, or near, the narrowest constriction of the channel. The binding site for Mg^{2+}_o has also been proposed to lie at narrowest constriction of the NMDA receptor channel (Wollmuth et al., 1998). If the only gating-associated conformational changes occurred near the narrowest constriction of the channel, block by both amantadine and Mg^{2+}_o could be expected to alter channel gating equally. However, amantadine impacts channel gating more than Mg^{2+}_o , suggesting that portions of the NMDA receptor protein other than the narrowest constriction undergo gating associated conformational changes.

Previous data suggest that the external vestibule changes conformation upon channel gating (Sobolevsky et al., 2002). Amantadine, because it is larger than Mg^{2+}_o , would be able to better interact with gating associated conformational changes of the external vestibule. Because amantadine block accelerates channel closure, there must be interactions between the external vestibule and amantadine which stabilize the closed state of the NMDA receptor channel. This hypothesis suggests that the size of a blocker should correlate with the degree to which the blocker interacts with channel gating, with larger blockers having a more profound impact on channel gating. However, not all interactions between channel blockers and gating lead to more

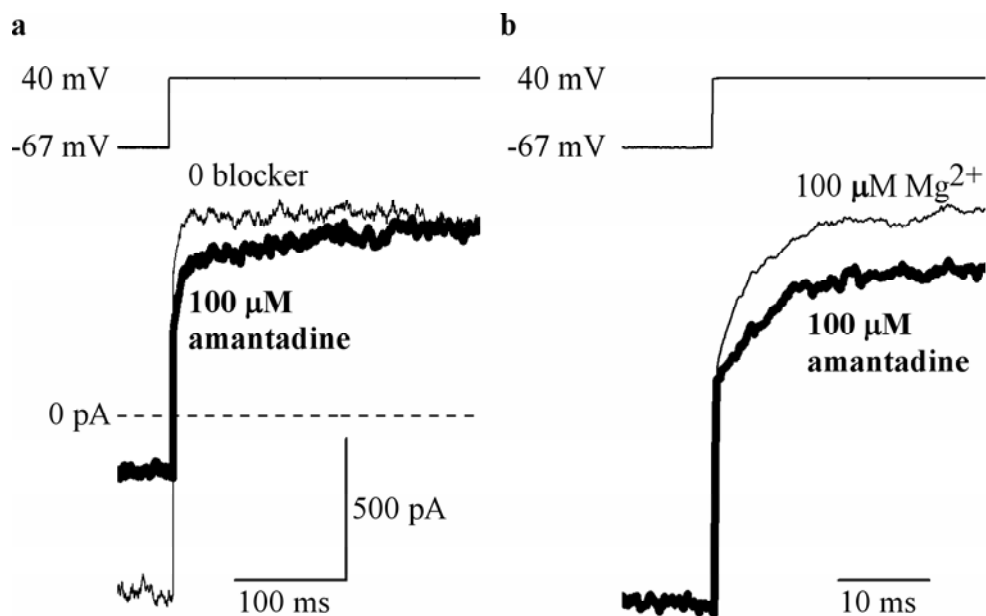


Figure 31. Following a rapid depolarizing step, unblock of amantadine contains a prominent slow component. (a) Whole-cell current records during a voltage step from -67 mV to 40 mV in the presence of 30 μM NMDA + 10 μM glycine (thin trace) and the indicated concentration of amantadine (thick trace). (b) An expanded time scale of whole-cell current records during a voltage step from -67 mV to 40 mV in the presence of 30 μM NMDA + 10 μM glycine and the indicated concentration of the extracellular channel blocker Mg²⁺ (thin trace) or amantadine (thick trace). The same concentration of blocker (100 μM) was used for amantadine and Mg²⁺ because at this voltage (-67 mV) amantadine and Mg²⁺ have similar IC₅₀ values, ~40 μM (Blanpied et al., 1997; Qian et al., 2002; Blanpied et al., 2005; Qian et al., 2005). Currents are normalized to the steady state level before the voltage step and the steady state level following the voltage jump to remove potentiation by Mg²⁺ present in NR1/2B receptors (Paoletti et al., 1995). Lines above the current traces indicate the time of voltage change.

Table 8. Current relaxations following rapid depolarizing voltage steps.

NMDA / glycine +	τ_{fast} (ms)	amp _{fast} (%)	τ_{slow} (ms)	amp _{slow} (%)	$\tau_{\text{slow 2}}$ (ms)	amp _{slow 2} (%)
0 blocker	.338 ± .016	88.46 ± 1.63	14.48 ± 6.85	11.5 ± 1.63		
100 μM amantadine	.279 ± .027	53.09 ± 3.32	5.17 ± .51	27.54 ± 1.86	153.04 ± 5.91	19.37 ± 1.58
100 μM Mg ²⁺	.399 ± .031	71.31 ± 1.47	8.51 ± .42	28.69 ± 1.47		

The membrane voltage of an HEK 293T cell expressing NR1/2B receptors was stepped from -67 mV to +40 mV in the presence of 30 μM NMDA/10 μM glycine + 0 blocker, 100 μM amantadine, or 100 μM Mg²⁺. The resulting current traces were fit using either a double (NMDA/glycine + 0 blocker and 100 μM Mg²⁺) or a triple (NMDA/glycine + 100 μM amantadine) exponential equation. Mean ± SEM.

rapid channel closure; sequential blockers prevent NMDA receptor channel closure (Benveniste and Mayer, 1995; Antonov and Johnson, 1996; Sobolevsky et al., 1999). Thus, characteristics other than size alone must determine the functional consequences of interactions between channel blockers and gating associated conformational changes of the NMDA receptor. It is important to note that these data do not rule out the possibility that the activation gate lies at the narrowest constriction of the channel. Instead, they only suggest that other portions of the NMDA receptor protein must change conformation in response to channel gating.

5.3 MUTATIONS INFLUENCING VOLTAGE DEPENDENT CHARACTERISTICS

Experiments investigating the NR2 subunit dependence of Mg^{2+}_o blocking characteristics have provided some insight into the molecular mechanisms underlying inherent voltage dependence of NMDA receptor activation. A single amino acid mutation has recently been identified that changes the NR1/2A receptor Mg^{2+}_o IC_{50} to that observed for NR1/2D receptors (Gao et al., 2004). The amino acid is located close to the intracellular end of M3 (**Fig 32a**). In NR2A and NR2B, the residue is a serine, while in NR2C and NR2D the residue is a lysine. When the mutant NR2A subunit (NR2AS632L) is expressed with wild-type NR1, the Mg^{2+}_o IC_{50} measured at -65 mV is 211 μ M, which is much closer to that of wild-type NR1/2D receptors (191 μ M) than wild-type NR1/2A receptors (40 μ M) (Gao et al., 2004). Surprisingly, this mutation also eliminates slow Mg^{2+}_o unblock; depolarization induced Mg^{2+}_o unblock from S632L mutant receptors is extremely rapid (**Fig 32b, c**).

Potential mechanistic explanations for the impact of the S632L mutation can be gleaned from previous work on the voltage-dependent modulation of ligand-gated receptors. To account for the voltage dependence of the rate of nicotinic acetylcholine receptor channel closure (Magleby and Stevens, 1972), two separate, but not mutually exclusive, mechanisms have been proposed. The first mechanism proposes that occupation of a permeant ion binding site alters channel closure (Ascher et al., 1978; Marchais and Marty, 1979). Occupation of the site was proposed to be favored at hyperpolarized voltages, and when occupied, inhibit channel closure. The second mechanism suggests that gating associated rearrangements of charged moieties in the nicotinic acetylcholine receptor protein influence channel closure (Auerbach et al., 1996). The

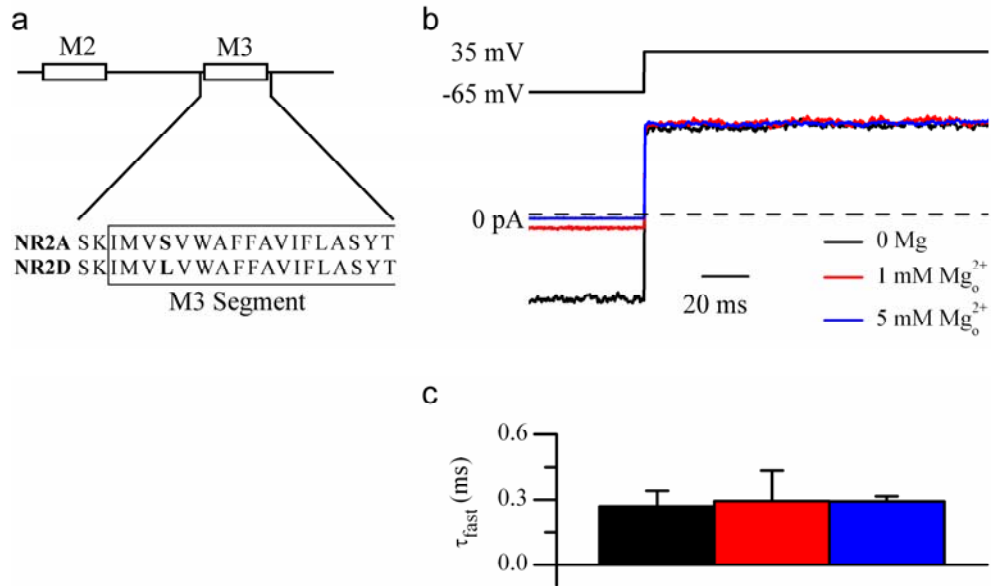


Figure 32. Elimination of slow Mg²⁺_o unblock by a single amino acid substitution. (a) Schematic representation of the NMDA receptor subunits (above). The amino acid sequence near the intracellular face of M3 has been blown up and the sequences for the NR2A and NR2D subunits are aligned. There is high conservation of this region between subunits, except for residue 632, which is a serine (S) in NR2A and a leucine (L) in NR2D. (b) Representative whole cell current traces (bottom) from NR1/2AS632L receptors in response to a depolarization from -65 to 35 mV (top trace). Depolarizations were applied during a steady state response to 30 μM NMDA and 10 μM glycine in the presence of 0, 1, or 5 mM Mg²⁺_o. (c) Pooled results from single exponential fits of current responses to a depolarization from -65 to 35 mV in the presence of 0 (black), 1 (red), or 5 mM Mg²⁺_o (blue).

later of these two mechanisms has also been suggested to underlie the voltage dependence of glycine receptor channel closure (Legendre, 1999). Below is a discussion of how these mechanisms may contribute to the voltage dependence of NMDA receptor activation.

5.3.1 Voltage dependence and permeant ions

One plausible explanation for the impact of the NR2A(S632L) substitution is that the mutation disrupts a permeant ion binding site involved in NR1/2A and NR1/2B receptor voltage sensitivity. The location of the S632L mutation suggests that the amino acid would participate in forming an intracellular binding site (**Fig. 32a**). In order to be consistent with the data presented in this dissertation, the site would need to display one of two characteristics: 1. Occupation of the site encourages channel opening and is favored at depolarized potentials. 2. Occupation of the site discourages channel opening and is favored at hyperpolarized potentials.

To test the validity of the hypothesis that an intracellular permeant ion binding site is involved in voltage dependent gating, we performed voltage jump experiments using an intracellular solution containing zero permeant ions (intracellular solution composed of the impermeant ion NMDG). The results showed that upon repolarization from 35 to -65 mV, a significant tail current was still observed (data not shown). The tail current is indicative of the NMDA receptor entering a higher P_{open} mode upon depolarization to 35 mV even though little ion flux occurs at this voltage. These data argue against the hypothesis that occupation of an intracellular permeant ion binding site influences NMDA receptor channel opening.

It is possible that the S to L mutation induced a shift in M3 that altered a permeant ion binding site located in another section of the protein. To explore this possibility we assessed the depolarization induced current relaxation in altered extracellular permeant ions. We found that the slow component of current relaxation in 0 Mg^{2+}_o persisted in a wide variety of extracellular permeant ion concentrations (data not shown). We were particularly hopeful that extracellular Ca^{2+} may play a role in inherent voltage dependence. Yet the slow component of NR1/2B receptor current relaxation induced by membrane depolarization was present in symmetric KCl, which contains nominally 0 extracellular Ca^{2+} (see Chapter 2).

An extremely high affinity Ca^{2+} binding site exists near the extracellular mouth of NMDA receptors (Premkumar and Auerbach, 1996; Sharma and Stevens, 1996). This high

affinity site may be saturated even in nominally 0 extracellular Ca^{2+} solutions (such as the symmetric KCl solution used in Chapter 2), which can still contain several μM of free Ca^{2+} . To truly lower free extracellular Ca^{2+} to near zero, solutions must include a Ca^{2+} buffer such as EGTA. Preliminary results using an extracellular solution containing 0 Ca^{2+} and 1 mM EGTA have shown little impact of the removal of Ca^{2+} on the kinetics of NR1/2B receptor current relaxations in response to depolarization (**Fig. 33**). There was a modest reduction of the amplitude of the slow component of current relaxation in depolarization from -65 to 35 and 95 mV in 0 and 1 mM Mg^{2+}_o , although the reduction does not appear to be significant (**Fig. 33c**). Taken together, these data suggest that binding of permeant ions to the NMDA receptor channel cannot fully explain the inherent voltage dependence of NR1/2A and NR1/2B receptor activity.

The data presented in this dissertation suggest that an intracellular ion binding site is not critical for the voltage sensitivity of NR1/2A and NR1/2B receptor activation. However, the observation that block by internal Mg^{2+} (Mg^{2+}_i) stabilizes the NMDA receptor open state (Li-Smerin and Johnson, 1996; Li-Smerin et al., 2001) would be consistent with voltage-dependent occupation of an intracellular ion binding site. These seemingly contradictory results could be resolved if NMDA receptors contained a super-high affinity binding site on the intracellular entrance to the channel. The affinity of this hypothetical site would have to be so great that even in our attempt to reduce intracellular permeant ions to 0, the site was still saturated. Another possibility is that the intracellular binding site is so readily accessible from the internal solution that the impermeant ion NMDG, which was the major intracellular ion during the 0 intracellular permeant ion experiments described above, was able to bind to the site. These alternative hypotheses will need to be addressed by future research before the relationship between permeant ions and voltage-dependent NMDA receptor gating can be determined.

5.3.2 Gating associated movement of charged amino acids

Another potential mechanism to achieve inherent voltage sensitivity of channel activity would be to have charged amino acids move in relation to the membrane voltage field upon channel gating. Because neither the NR2A/B nor NR2C/D subunits contain a charged amino acid at position 632, it seems unlikely that this amino acid is directly involved in inherent voltage sensitivity. It is possible that the mutation induces a shift in the position of the M3 segment in

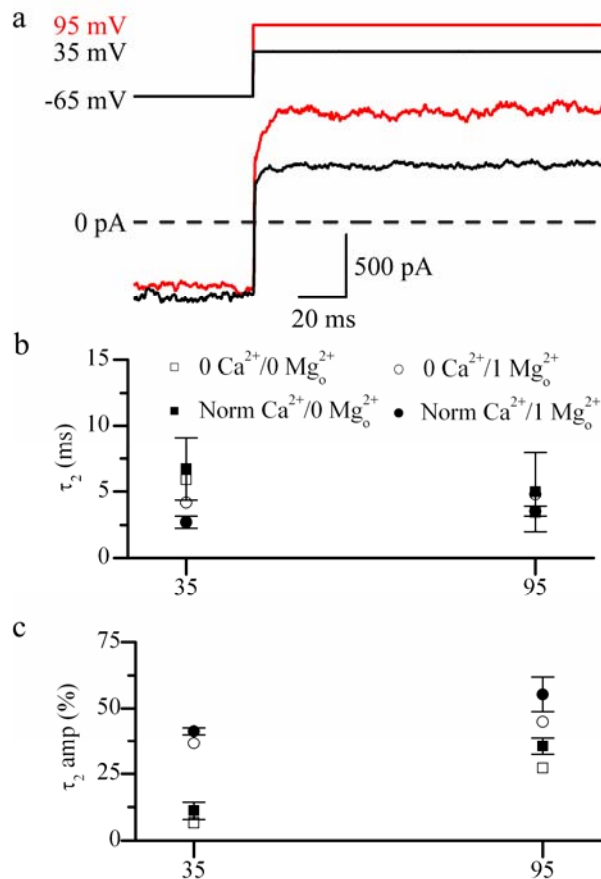


Figure 33. Elimination of free extracellular Ca^{2+} does not have a large impact on NR1/2B receptor current response to depolarization. (a) Representative whole-cell NR1/2B current traces (bottom) in response to depolarizations from -65 to 35 mV (black) or 95 mV (red) in the presence of 0 free extracellular Ca^{2+} (1 mM EGTA). Depolarizations were applied once the current response to application of 1 mM glutamate and 10 μ M glycine had reached a steady state response. Membrane voltage indicated by top trace. (b, c) Pooled results from double exponential fits of NR1/2B receptor current relaxations in response to 500 ms voltage steps from -65 to 35 mV or 95 mV. Experiments were performed in normal extracellular solutions (closed symbols) or in 0 extracellular Ca^{2+} solutions (open symbols). Depolarizations were applied during a steady state current response in 0 (squares) or 1 mM Mg^{2+} (circles).

the membrane and alters the location of a charged amino acid in another section of the protein. However, no amino acids are obvious targets for site-directed mutagenesis studies. Further research, both at the single channel level and utilizing structural modeling, may provide insight into the molecular mechanisms underlying inherent voltage sensitivity of NR1/2A and NR1/2B receptors.

5.4 VOLTAGE DEPENDENT ENHANCEMENT OF NMDA RECEPTOR CURRENTS

Some of my initial experiments led to the conclusion that rapid depolarizations, such as somatic AP waveforms, stimulate Mg^{2+} unblock from only a fraction of NR1/2B receptors (**Fig. 11**). These data seem to conflict with later experiments showing that models with and without voltage dependent can reproduce NR1/2B currents in response to AP waveforms equally well (**Fig. 21**). Some insight into the source of the discrepancy can be gleaned from NR1/2B model simulations during depolarizations provided by the three AP waveforms used in **Figure 11**. Simulations were generated using two NR1/2B models, one with and one without voltage dependence. Both the voltage dependent and the voltage independent NR1/2B models lacked desensitized states. All other rates were set to those shown in **Table 5**. In agreement with **Figure 21**, simulated current responses to the somatic AP waveform are similar from models with and without voltage dependence (**Fig. 34**). However, as the duration of the most depolarized voltage was increased to 5 and then 25 ms, the current simulations from the two models diverge. The inward peaks (I_{peaks}) from the voltage independent NR1/2B model simulations are similar in response to all three AP waveforms (**Fig. 34**). In contrast, the I_{peaks} from the voltage dependent NR1/2B model increase as the duration of the most depolarized voltage increased (**Fig. 34**). The I_{peaks} were normalized to the I_{peak} in response to the 25 ms extended AP waveform, as was done in **Figure 11**. The voltage-dependent NR1/2B model predicted that the unaltered somatic AP waveform will induce an I_{peak} that is ~70% of the I_{peak} induced by the 25 ms extended AP waveform. In contrast, the voltage independent NR1/2B model predicted a near constant I_{peak} value (**Fig. 34**). The results from the voltage-dependent model show excellent agreement with the experimental data shown in **Figure 11**.

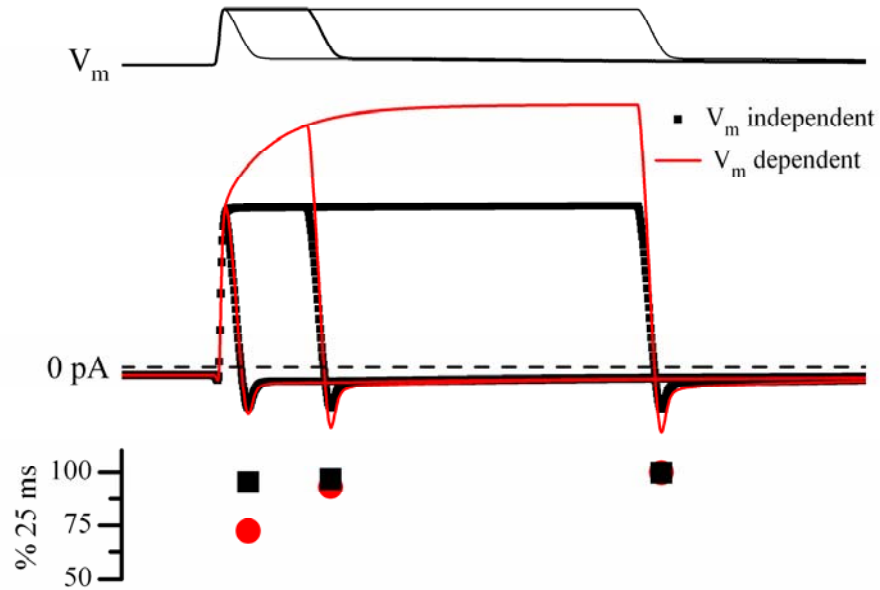


Figure 34. NR1/2B Model simulations in response to AP waveforms of varying duration.

Two NR1/2B models were used for simulations, one with and one without voltage dependent modulation of the NR2B pre-gating conformation change (k_{s+}). Both models contained no desensitized states and all rates were fixed to those describe in **Table 5**. For the voltage dependent model, k_{s+} changed exponentially with membrane voltage as described in Chapter 2. Current simulations (middle traces) were run in response to a 5 s application of 1 mM glutamate in the continuous presence of 1 mM Mg^{2+}_o . After 3 s of glutamate application, one of the three APs used in **Figure 11** were applied as a voltage signal (top trace). The three APs were: somatic AP, 5 ms extended somatic AP, and 25 ms extended somatic AP. Simulations were generated using a voltage dependent (red) and a voltage independent (black) model. The repolarization induced peak of inward current (I_{peak}) was measured and expressed as a percentage of the I_{peak} induced by the 25 ms extended somatic AP (bottom graph).

The NR1/2B model simulations described above (**Fig. 34**) somewhat alter the interpretation of the data presented in **Figure 11**. When the experiments in **Figure 11** were first performed, it was assumed that the single underlying cause of the reduction in the I_{peak} in response to the somatic AP was due to a population of receptors never unblocking Mg^{2+}_o . Based on this interpretation, we expected models which do not predict slow Mg^{2+}_o unblock to predict larger currents in response to a somatic AP waveform than models which do predict slow Mg^{2+}_o unblock. Instead, it seems that in addition to slow Mg^{2+}_o unblock, another reason for the small I_{peak} in response to the somatic AP is an enhancement of the current response to the 25 ms extended AP. These data would suggest that for a given brief depolarization, such as a back-propagating AP, the difference in the amount of Mg^{2+}_o unblock from NR1/2A and NR1/2B receptors may be overestimated by **Figure 11**.

Despite the small change in the interpretation of the data in **Figure 11**, one physiological implication remains the same: longer, and larger, depolarizations will enhance NR1/2A and NR1/2B receptor currents. Do such depolarizations occur physiologically? Data showing that NR1/2B receptor currents in response to several back propagating AP waveforms can be equally well reproduced by models with and without voltage suggest that they may not (**Fig. 21**). However, I would argue that with all of the variability in the characteristics of depolarizations occurring within neurons, there are bound to be conditions under which inherent voltage dependence of NMDA receptors is relevant. For example, cortical neurons can fire several APs in a burst at frequencies up to 250 Hz (Tang et al., 1999). Within a critical frequency, back-propagating APs during a burst can induce a regenerative Ca^{2+} spike that greatly increases the duration of dendritic depolarization (Larkum et al., 1999). During these long duration depolarizations, the data presented in this dissertation would predict a significant enhancement of NMDA receptor current. In addition the enhancement of NR1/2B receptor currents would be predicted to be larger than NR1/2A receptor currents. Interestingly, recent data has suggested that dendritic Ca^{2+} spikes play a crucial role in STDP (Kampa et al., 2004).

Long duration dendritic depolarization can also be observed during so-called “NMDA spikes”. NMDA spikes occur upon co-activation of several closely spaced synapses on a dendritic segment and result in highly superlinear summation of the individual excitatory post-synaptic potentials (Schiller et al., 2000; Ariav et al., 2003; Polsky et al., 2004). In the dendrite, a NMDA spike causes sustained dendritic depolarization, which simulations predict can

depolarized the membrane to ~ 0 mV for tens of ms (Rhodes, 2006). Such large amplitude and long duration depolarizations are likely to lead to a significant enhancement of the NMDA receptor P_{open} , resulting in enhanced NMDA receptor mediated currents in the region of the dendrite in which the NMDA spike was initiated.

5.5 PHYSIOLOGICAL ROLES OF NMDA RECEPTOR SUBTYPES

In several places I have alluded to the notion that NR2 subunit specific properties may allow different NMDA receptor subtypes to serve unique roles within the CNS. The developmental and regional differences in NR2 subunit expression would provide a means by which the NR2 subunit specific properties of NMDA receptors could be fit with the needs of certain neuronal connections. This hypothesis is supported by the description of NR2 subunit specific trafficking of NMDA receptors within some neurons (Ito et al., 2000; Kumar and Huguenard, 2003).

5.5.1 The role of NMDA receptors as coincidence detectors

One of the most recognized physiological functions of the NMDA receptor is to serve as a coincidence detector, signaling coordinated presynaptic glutamate release and postsynaptic depolarization. Coincidence detection, along with high Ca^{2+} permeability, have lead to the notion that NMDA receptor activity is a critical component in many forms of long-term synaptic plasticity (Bliss and Collingridge, 1993; Bear and Abraham, 1996; Malenka and Bear, 2004). When the requirements for plasticity induction are discussed, NMDA receptors are often viewed as a homogenous population of receptors. However, this is clearly not the case. The affinity for Mg^{2+} depends on the NR2 subunit present within a functional NMDA receptor (Monyer et al., 1994). In addition, we have shown for the first time in this dissertation that the properties of depolarization-induced Mg^{2+} unblock from NMDA receptors are also NR2-subunit dependent: Mg^{2+} unblocks from NR1/2C and NR1/2D receptors rapidly, while Mg^{2+} unblock from NR1/2A and NR1/2B receptors displays a prominent slow component.

Slow Mg^{2+}_o unblock and high Mg^{2+}_o affinity make NR1/2A and NR1/2B receptors better coincident detectors than NR1/2C and NR1/2D receptors. To illustrate this point, we played three hippocampal AP waveforms (collected from the soma and 240 μm or 280 μm out on the dendrite) into an HEK 293T expressing either NR1/2A or NR1/2D receptors (**Fig. 35a**). The AP waveforms were applied during a steady-state response to 1 mM glutamate in the presence of 10 μM glycine and 1 mM Mg^{2+}_o . The ratio of the peak inward current elicited by the AP waveform (I_{peak}) to the steady-state response to glutamate at -65 mV (I_{ss}) was significantly ($p < .001$) larger from NR1/2A than NR1/2D receptors in response to all three AP waveforms (**Fig. 35b**). The I_{peak} values from NR1/2A receptors scaled with the size of the depolarization, having the largest value in response to the somatic AP waveform and the smallest value in response to the 280 μm AP waveform. In contrast, the I_{peak} values from NR1/2D receptors were similar in response to all AP waveforms (**Fig. 35b**). Taken together, these data illustrate that depolarization induced currents, as compared to baseline currents, are far greater via NR1/2A than NR1/2D receptors. Better coincidence detection, along with higher Ca^{2+} permeability (Burnashev et al., 1995), suggests that NR1/2A and NR1/2B receptors are more likely to be involved in such processes as long term changes in synaptic efficacy than NR1/2C and/or NR1/2D receptors. However, it should be noted that NR1/2C and NR1/2D receptor activation has been implicated in LTD (Hrabetova et al., 2000).

5.5.2 Differential roles of NR1/2A and NR1/2B receptors in synaptic plasticity

Even though both NR1/2A and NR1/2B receptors appear to be equipped to mediate long-term changes in synaptic strength, the exact role of NR1/2A and NR1/2B receptors remains controversial. In many brain regions, there is a developmental rise in NR2A subunit expression. In both the barrel and visual cortices, the switch from high NR2B expression to high NR2A expression has been correlated with the end of critical periods for LTP induction (Barth and Malenka, 2001; Erisir and Harris, 2003). The involvement of the NR2B subunit in LTP has also been supported by the observation that transgenic overexpression of the NR2B subunit leads to mice that display enhanced LTP (Tang et al., 1999).

More recently, the role of NR1/2A and NR1/2B receptors in plasticity has been investigated using subunit specific antagonists. Several studies have found evidence that, within

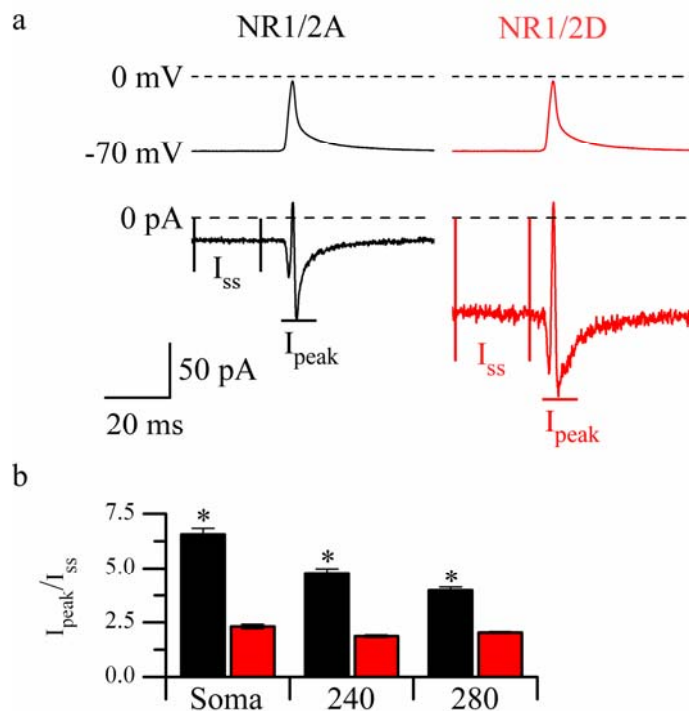


Figure 35. NR1/2A receptors are better equipped to act as coincidence detectors than NR1/2D receptors. (a) Examples of whole-cell currents (bottom traces) elicited from HEK 293T cells expressing NR1/2A (black) or NR1/2D (red) receptors. An AP waveform (top trace) recorded previously from 240 μm out on the dendrite of a CA1 pyramidal cell was applied as a voltage command (AP waveform provided by Xixi Chen and Dan Johnston). The steady state current at -65 mV (I_{ss}) and the peak of inward current induced by the AP waveform (I_{peak}) were both measured. (b) Pooled results (NR1/2A, $n = 5$; NR1/2D, $n = 4$) of the I_{peak}/I_{ss} ratio in response to AP waveforms collected from the soma and 240 or 280 μm out on the dendrite of a CA1 pyramidal cell. For all AP waveforms the I_{peak}/I_{ss} ratio was significantly ($p < .0001$) larger from NR1/2A than NR1/2D receptors.

the adult animal, LTP induction depends on NR1/2A receptor activation, while LTD induction requires activation of NR1/2B receptors (Liu et al., 2004; Massey et al., 2004). Consistent with these findings, Kim *et al.* (2005) found that in mature hippocampal cultures (30 days *in vitro*), NR1/2A receptor activation promotes, while NR1/2B receptor activation inhibits, surface expression of AMPA receptors. These studies are supported by model simulations which suggest that LTD-like induction paradigms induce more charge transfer via NR1/2B receptors, while LTP-like induction paradigms induce greater charge transfer via NR1/2A receptors (Erreger et al., 2005). However, several groups have reported contradictory results, suggesting that NR1/2A and NR1/2B receptors participate in both LTP and LTD (Berberich et al., 2005; Toyoda et al., 2005; Weitlauf et al., 2005). One major source of discrepancy regarding the NR2 subunit dependence of plasticity may rest on how well the NR2 subunit specific antagonists differentiate between NR1/2A and NR1/2B receptors. While the NR1/2B receptor antagonist ifenprodil has reliably been shown to selectively inhibit NR1/2B receptors (Williams, 1993), the specificity of the NR1/2A receptor antagonist, NVP-AAM077, has recently been called into question (Neyton and Paoletti, 2006).

The mechanism by which distinct NMDA receptor subtypes could support different forms of plasticity remains unknown. The kinetics and amount of Ca^{2+} influx via different NMDA receptor subtypes may play a key role. The results described in Chapter 1 suggested that rapid depolarizations, such as AP waveforms, are more effective at stimulating Mg^{2+} unblock from NR1/2A than NR1/2B receptors. These data support the notion that, during periods of coincident pre and postsynaptic activity, Ca^{2+} influx via NR1/2A receptors may be greater than via NR1/2B receptors. However, these results must be tempered by the possibility that most back-propagating APs may not provide the necessary depolarization to augment currents via NR1/2A or NR1/2B receptors. In addition, it is not clear how inherent voltage dependence would impact NR1/2A and NR1/2B receptor currents during low- and high-frequency stimulation paradigms, as those typically used to induce LTD and LTP, respectively.

Although not investigated in this dissertation, it is important to acknowledge that another potential mechanism by which different NMDA receptor subtypes may support different forms of plasticity is via coupling to distinct intracellular signaling pathways. The C-terminus of each NR2 subunit allows unique interactions with different signaling and scaffolding molecules (Sprengel et al., 1998; Sheng and Pak, 2000). For example, CAMKII binds much more tightly to

the NR2B C-terminus than the NR2A C-terminus (Strack and Colbran, 1998; Leonard et al., 1999; Mayadevi et al., 2002). Regulation of synaptic levels of CAMKII, due to varying expression levels of the NR2A and NR2B subunit, has been proposed to regulate LTP induction (Barria and Malinow, 2005).

From this discussion, it is clear that assessing the differential contributions of NR1/2A and NR1/2B receptors to LTP and LTD is a difficult task. At this point the relationship between NR1/2A and NR1/2B receptor activity and LTP and LTD remains unclear. However, based on the available data it seems that the situation is far more complex than a simple association of NR1/2A receptor activity with LTP and NR1/2B receptor activity with LTD.

5.5.3 The physiological significance of low Mg^{2+}_o affinity

Remarkably, there is a paucity of information regarding the functional significance of the low Mg^{2+}_o affinity of NR1/2C and NR1/2D receptors. In addition to low Mg^{2+}_o affinity, we have shown in this dissertation that NR1/2C and NR1/2D receptors display very rapid Mg^{2+}_o unblocking kinetics. Less powerful inhibition by Mg^{2+}_o , and rapid Mg^{2+}_o unblocking kinetics, reduces the ability of NR1/2C and NR1/2D receptors to serve as coincident detectors (**Fig. 35**). So, if not to serve the canonical role assigned to NMDA receptors, what is the physiological role of the NR1/2C and NR1/2D receptors?

The unique properties of Mg^{2+}_o block and unblock of NR1/2C and NR1/2D receptors should allow them to participate more readily in synaptic activity occurring at, or near, typical resting membrane potentials. The NR2C subunit is highly expressed in the adult cerebellum, most notably in granule cells (which also express the NR2A subunit). The NR2D subunit is highly expressed throughout the embryonic brain and in some brain regions in the adult, including the hindbrain, midbrain, and to a lesser extent the cortex (Monyer et al., 1994; Wenzel et al., 1996; Dunah et al., 1998). If NR1/2C and NR1/2D receptors were important for synaptic transmission, then NR1/2C- and NR1/2D-knockout mice would be expected to show significant deficits, particularly in brain regions in which they are highly expressed. However, mice lacking NR2C expression in the cerebellum appear remarkably normal (Kadotani et al., 1996). If expression of both the NR2A and NR2C subunits is eliminated in the cerebellum, mice do have reduced

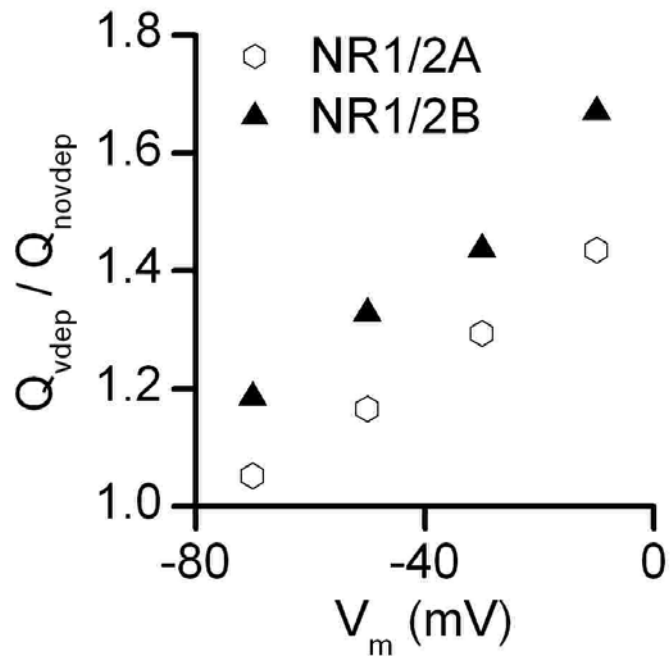


Figure 36. Voltage-dependent increase of simulated NMDA-EPSCs is NR2 subunit dependent. NR1/2A and NR1/2B receptor responses to a synaptic like application of glutamate (Clements et al., 1992) were generated using Models containing the rates listed in **Tables 5** and **8**. Responses were generated at several voltages (-70, -50, -30, and -10 mV). The total charge transfer (Q) was compared between models with (Q_{vdep}) and without (Q_{novdep}) voltage dependence. There was a larger impact of the inherent voltage dependence on NR1/2B responses, resulting in a larger Q_{vdep}/Q_{novdep} ratio for NR1/2B (closed symbols) than NR1/2A (open symbols) receptors. The total charge transfer was calculated as the area under the current curve from the start of the response until the response had decayed to 5% of the peak value. The amount of Ca^{2+} entry is proportional to the total charge transfer because NR1/2A and NR1/2B receptors display similar fraction Ca^{2+} currents (Schneppenburger, 1996).

NMDA-EPSCs measured in granule cells and display motor discoordination (Kadotani et al., 1996). NR2D knockout mice are also viable and by many accounts are not significantly different than wild-type mice, although the NR2D knockout mice do display a reduction in spontaneous activity (Ikeda et al., 1995). The observation that NR2D knockout mice are viable is particularly surprising because the high expression of the NR2D subunit in the embryonic brain suggests that this subunit plays a particularly important role in development.

The data from knockout mice suggest that neither the NR2C nor the NR2D subunit play a critical physiological role in the CNS. However, data from knockout experiments can be difficult to interpret because the absence of either NR2C or NR2D subunit expression could be overcome through compensation by other NR2 subunits. In wild-type animals, brain regions in which NR2D subunits participate in synaptic transmission should be easy to identify because NR1/2D receptors display unusually slow deactivation kinetics (τ_{decay} of several seconds). However, slowly decaying synaptic currents typical of NR1/2D receptors have yet to be identified in the adult brain even though single-channel studies have provided evidence that NR2D containing NMDA receptors are expressed by several cell types (Momiya et al., 1996; Cull-Candy et al., 1998; Misra et al., 2000; Brickley et al., 2003). These data suggest that in the adult brain NR2D containing NMDA receptors may be located primarily, if not exclusively, at extrasynaptic sites. However, the existence of synaptic triheteromeric receptors containing the NR2D subunit cannot be ruled out.

NR2C and NR2D receptors may play a particularly important role in inhibitory interneurons. The NR2D subunit is highly expressed by interneurons in several brain regions, including the striatum, cortex, and hippocampus (Monyer et al., 1994; Standaert et al., 1996). NR2C subunit expression has also been identified in striatal and hippocampal interneurons (Monyer et al., 1994; Standaert et al., 1999). Electrophysiological recordings support the hypothesis that interneurons express high levels of NR2C and/or NR2D containing NMDA receptors. Inhibitory transmission is reduced upon application of the NMDA receptor antagonist APV (Grunze et al., 1996). Application of MK-801, an open NMDA receptor channel blocker, disproportionately inhibits NMDA receptors located on interneurons as opposed to pyramidal neurons (Li et al., 2002). Both of these observations are consistent with interneurons containing NMDA receptors which are active near typical resting membrane potentials.

The physiological role of NR2C and/or NR2D expression by certain subtypes of interneurons is not clear. It is interesting to note that NMDA receptor hypofunction has been implicated in schizophrenia (Coyle et al., 2003). Data supporting this hypothesis come from experiments showing that NMDA receptor blockers, such as PCP, can reproduce many symptoms of schizophrenia (Morris et al., 2005). Because NR1/2C and NR1/2D receptors are more active than NR1/2A and NR1/2B receptors at hyperpolarized membrane potentials, the main result of MK-801 application may be blockade of NR1/2C and/or NR1/2D receptors. This hypothesis suggests that NR1/2C and NR1/2D receptors play a critical role in controlling cortical excitability via activity in interneurons, and that dysregulation of NR1/2C and NR1/2D receptors may be involved in the etiology of schizophrenia.

5.6 SIGNALING VIA SYNAPTIC AND EXTRASYNAPTIC NMDA RECEPTORS

NMDA receptors are expressed across the entire surface of neurons, and not just clustered at sites of synaptic contact. Patches pulled from almost any surface of a neuron yield NMDA receptor mediated currents, although NMDA receptors are clustered at a higher density at synaptic as compared to extrasynaptic sites. Once within a synapse, NMDA receptors are connected to a huge network of proteins within the post-synaptic density (Husi et al., 2000). The close proximity of synaptic NMDA receptors to many signaling molecules may allow Ca^{2+} influx via synaptic NMDA receptors to activate separate signaling pathways than Ca^{2+} influx via extrasynaptic receptors (Hardingham et al., 2002).

In addition to differential effects on signaling cascades, the amount of Ca^{2+} influx through synaptic and extrasynaptic NMDA receptors may differ. Glutamate in the synaptic cleft can reach concentrations of 1.1 mM (Clements et al., 1992). As glutamate diffuses away from the synapse, it is quickly taken up by high-affinity glutamate transporters located on astrocytes which surround the synaptic cleft. In some cases, the glutamate transporters can become overwhelmed allowing glutamate to spill out of the synapse (Asztely et al., 1997; Diamond, 2001; Clark and Cull-Candy, 2002; Scimemi et al., 2004). Glutamate spillover will result in activation of extrasynaptic NMDA receptors, although the concentration of glutamate sensed by

extrasynaptic NMDA receptors is much lower than the concentration of glutamate sensed by synaptic NMDA receptors.

Exposure to different glutamate concentrations due to synaptic release versus spillover may alter the kinetics of Mg^{2+}_o unblock from synaptic and extrasynaptic receptors. In this dissertation I have provided evidence that the kinetics of Mg^{2+}_o unblock become slower as the concentration of agonist used to activate the receptors is lowered. These results suggest that during a given depolarization, synaptic NMDA receptors would display faster Mg^{2+}_o unblock than extrasynaptic NMDA receptors because they are exposed to a higher concentration of glutamate (**Fig. 37**). This hypothesis must be tempered by the results suggesting that slow Mg^{2+}_o unblock may have limited impact on NR1/2B receptor currents during back-propagating AP waveforms (**Fig. 21**). However, during dendritic depolarization that might be expected to induce significant enhancement of NMDA receptor currents, such as Ca^{2+} or NMDA spikes, enhancement could be expected to preferentially influence synaptic NMDA receptors.

5.7 THE PESKY TRIHETEROMERIC CHANNELS

There is significant evidence that many, if not most, native NMDA receptors contain more than one type of NR2 subunit (triheteromeric receptors). In the adult rat cortex, immunoprecipitation of native NMDA receptors has provided direct evidence for triheteromeric NR1/2A/2B receptors (Sheng et al., 1994; Chazot and Stephenson, 1997; Luo et al., 1997). Quantification of immunoprecipitation data suggests that over 50% of native cortical NMDA receptors are NR1/2A/NR2B receptors (Luo et al., 1997). Triheteromeric channels have also been identified in several other brain regions, including channels containing NR2A or NR2B along with either the NR2C or NR2D subunit (Chazot et al., 1994; Sundstrom et al., 1997; Dunah et al., 1998; Cathala et al., 2000; Brickley et al., 2003; Jones and Gibb, 2005).

It has long proved difficult to isolate and study triheteromeric NMDA receptors within recombinant systems. Expression of NR1 along with both the NR2A and NR2D subunits in *Xenopus* oocytes yields a novel channel type that has been proposed to represent NR1/2A/2D receptors (Cheffings and Colquhoun, 2000). In many respects, the proposed NR1/2A/2D receptors display properties that are intermediate between pure NR1/2A and pure NR1/2D

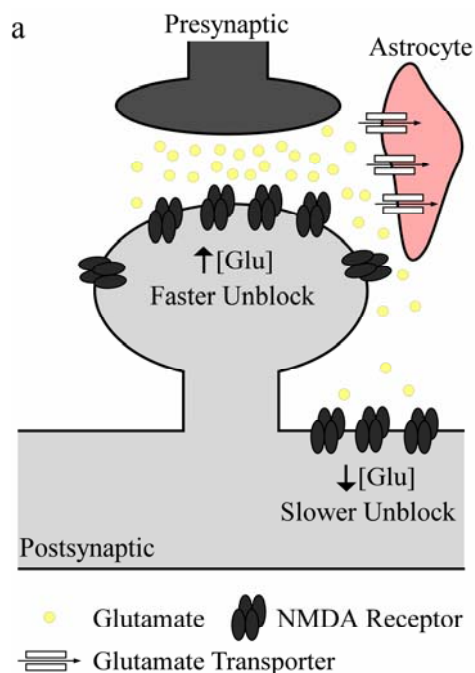


Figure 37. Mg^{2+} unblocking kinetics may differ between synaptic and extrasynaptic NMDA receptors. Schematic representation of glutamate release at a prototypical central synapse. NMDA receptors are clustered at synaptic sites, but are also found at perisynaptic and extrasynaptic regions. Upon release from the presynaptic terminal, glutamate reaches a very high concentration in the synaptic cleft (~ 1.1 mM). High affinity glutamate transporters located on astrocytes prevent significant glutamate spillover from the cleft into the extrasynaptic space. Because synaptic NMDA receptors are activated by a higher concentration of glutamate than extrasynaptic receptors, Mg^{2+} unblock will proceed more rapidly from synaptic than extrasynaptic NMDA receptors.

receptors. Expression of NR1, NR2A, and NR2B in HEK 293T cells yields NMDA receptors that display Mg^{2+}_o unblocking kinetics between those observed for pure NR1/2A and pure NR1/2B receptors (data not show). It is tempting to speculate that these results represent Mg^{2+}_o unblock from triheteromeric NR1/2A/2B receptors. However, it is difficult to distinguish whole-cell currents mediated by NR1/2A/2B receptors from those mediated by two independent populations of pure NR1/2A and pure NR1/2B receptors. Recent strides have been made using serial mutations to isolate NR1/2A/NR2B receptors within *Xenopus* oocytes (Hatton and Paoletti, 2005). The NR1/2A/NR2B receptors still bound NR2A and NR2B specific antagonists with high affinity, although the percent inhibition was reduced (Hatton and Paoletti, 2005).

These data further support the notion that the characteristics of triheteromeric NMDA receptors lie somewhere between the characteristics of the two NR2 subunits contained within the functional receptors. Unfortunately, one of the mutations utilized by Hatton and Paoletti (2005) to isolate NR1/2A/NR2B receptors greatly reduced block by Mg^{2+}_o . Thus, this technique would not be useful to study the kinetics of Mg^{2+}_o unblock. Hopefully, further research will provide tools to isolate triheteromeric NMDA receptors, allowing their functional contribution to synaptic transmission finally to be determined. In future studies it will be important to characterize the kinetics of Mg^{2+}_o unblock from NR1/2A/2B triheteromeric channels as well as triheteromeric channels which include one NR2A or NR2B subunit along with one NR2C or NR2D subunit.

5.8 GENERAL CONCLUSIONS

The research presented in this dissertation addressed the NR2 subunit dependence of Mg^{2+}_o unblocking kinetics and inherent voltage dependence. The work was intended to extend our knowledge of the relationship between NMDA receptor activation, Mg^{2+}_o block, and membrane voltage. The general conclusions were as follows:

- Depolarization-induced Mg^{2+}_o unblock from NMDA receptors is NR2 subunit dependent. Mg^{2+}_o unblock from NR1/2A and NR1/2A receptors is multi-phasic,

containing both fast ($\tau < 1$ ms) and slow (τ of many ms) components. In contrast, Mg^{2+}_o unblock from NR1/2C and NR1/2D receptors contains only a fast component.

- The slow component of Mg^{2+}_o unblock from NR1/2B receptors is larger and slower than the slow component of Mg^{2+}_o unblock from NR1/2A receptors.
- NR1/2A and NR1/2B receptor activity displays inherent voltage sensitivity, such that NR1/2A and NR1/2B receptor currents are enhanced at depolarized membrane potentials. The enhancement is consistent with an increase in the P_{open} of the receptors at depolarized membrane potentials.
- A kinetic model of NR1/2B receptor activation in which the NR1/2B receptor opens more rapidly upon depolarization accounts for NR1/2B receptor currents in the absence of Mg^{2+}_o and the slow component of depolarization-induced Mg^{2+}_o unblock.
- Incorporating the kinetics of NR1/2A receptor activation into the voltage-dependent NR1/2B model can account for the differences in the kinetics of slow Mg^{2+}_o unblock from NR1/2A and NR1/2B receptors.
- Inherent voltage dependence provides an additional means by which depolarization enhances currents via NR1/2A and NR1/2B receptors, beyond that provided by relief of Mg^{2+}_o block.

BIBLIOGRAPHY

- Amar M, Perin-Dureau F, Neyton J (2001) High-affinity Zn block in recombinant N-methyl-D-aspartate receptors with cysteine substitutions at the Q/R/N site. *Biophys J* 81:107-116.
- Anis NA, Berry SC, Burton NR, Lodge D (1983) The dissociative anaesthetics, ketamine and phencyclidine, selectively reduce excitation of central mammalian neurones by N-methyl-aspartate. *Br J Pharmacol* 79:565-575.
- Antonov SM, Johnson JW (1996) Voltage-dependent interaction of open-channel blocking molecules with gating of NMDA receptors in rat cortical neurons. *J Physiol* 493:425-445.
- Antonov SM, Johnson JW (1999) Permeant ion regulation of N-methyl-D-aspartate receptor channel block by Mg(2+). *Proc Natl Acad Sci U S A* 96:14571-14576.
- Ariav G, Polsky A, Schiller J (2003) Submillisecond precision of the input-output transformation function mediated by fast sodium dendritic spikes in basal dendrites of CA1 pyramidal neurons. *J Neurosci* 23:7750-7758.
- Armstrong N, Sun Y, Chen GQ, Gouaux E (1998) Structure of a glutamate-receptor ligand-binding core in complex with kainate. *Nature* 395:913-917.
- Ascher P, Nowak L (1988) The role of divalent cations in the N-methyl-D-aspartate responses of mouse central neurones in culture. *J Physiol* 399:247-266.
- Ascher P, Marty A, Neild TO (1978) Life time and elementary conductance of the channels mediating the excitatory effects of acetylcholine in *Aplysia* neurones. *J Physiol* 278:177-206.
- Asztely F, Erdemli G, Kullmann DM (1997) Extrasynaptic glutamate spillover in the hippocampus: dependence on temperature and the role of active glutamate uptake. *Neuron* 18:281-293.
- Auerbach A, Zhou Y (2005) Gating reaction mechanisms for NMDA receptor channels. *J Neurosci* 25:7914-7923.
- Auerbach A, Sigurdson W, Chen J, Akk G (1996) Voltage dependence of mouse acetylcholine receptor gating: different charge movements in di-, mono- and unliganded receptors. *J Physiol* 494 (Pt 1):155-170.
- Avignone E, Frenguelli BG, Irving AJ (2005) Differential responses to NMDA receptor activation in rat hippocampal interneurons and pyramidal cells may underlie enhanced pyramidal cell vulnerability. *Eur J Neurosci* 22:3077-3090.
- Banke TG, Traynelis SF (2003) Activation of NR1/NR2B NMDA receptors. *Nat Neurosci* 6:144-152.
- Barria A, Malinow R (2005) NMDA Receptor Subunit Composition Controls Synaptic Plasticity by Regulating Binding to CaMKII. *Neuron* 48:289-301.
- Barth AL, Malenka RC (2001) NMDAR EPSC kinetics do not regulate the critical period for LTP at thalamocortical synapses. *Nat Neurosci* 4:235-236.

- Bear MF, Colman H (1990) Binocular competition in the control of geniculate cell size depends upon visual cortical N-methyl-D-aspartate receptor activation. *Proc Natl Acad Sci U S A* 87:9246-9249.
- Bear MF, Abraham WC (1996) Long-term depression in hippocampus. *Annu Rev Neurosci* 19:437-462.
- Beck C, Wollmuth LP, Seeburg PH, Sakmann B, Kuner T (1999) NMDAR channel segments forming the extracellular vestibule inferred from the accessibility of substituted cysteines. *Neuron* 22:559-570.
- Benveniste M, Mayer ML (1995) Trapping of glutamate and glycine during open channel block of rat hippocampal neuron NMDA receptors by 9-aminoacridine. *J Physiol* 483 (Pt 2):367-384.
- Benveniste M, Clements J, Vyklicky L, Jr., Mayer ML (1990) A kinetic analysis of the modulation of N-methyl-D-aspartic acid receptors by glycine in mouse cultured hippocampal neurones. *J Physiol* 428:333-357.
- Berberich S, Punnakkal P, Jensen V, Pawlak V, Seeburg PH, Hvalby O, Kohr G (2005) Lack of NMDA receptor subtype selectivity for hippocampal long-term potentiation. *J Neurosci* 25:6907-6910.
- Bernard C, Johnston D (2003) Distance-dependent modifiable threshold for action potential back-propagation in hippocampal dendrites. *J Neurophysiol* 90:1807-1816.
- Bi GQ, Poo MM (1998) Synaptic modifications in cultured hippocampal neurons: dependence on spike timing, synaptic strength, and postsynaptic cell type. *J Neurosci* 18:10464-10472.
- Bienenstock EL, Cooper LN, Munro PW (1982) Theory for the development of neuron selectivity: orientation specificity and binocular interaction in visual cortex. *J Neurosci* 2:32-48.
- Billups D, Liu YB, Birnstiel S, Slater NT (2002) NMDA receptor-mediated currents in rat cerebellar granule and unipolar brush cells. *J Neurophysiol* 87:1948-1959.
- Blanpied TA, Clarke RJ, Johnson JW (2005) Amantadine inhibits NMDA receptors by accelerating channel closure during channel block. *J Neurosci* 25:3312-3322.
- Blanpied TA, Boeckman FA, Aizenman E, Johnson JW (1997) Trapping channel block of NMDA-activated responses by amantadine and memantine. *J Neurophysiol* 77:309-323.
- Bliss TV, Collingridge GL (1993) A synaptic model of memory: long-term potentiation in the hippocampus. *Nature* 361:31-39.
- Bowie D, Mayer ML (1995) Inward rectification of both AMPA and kainate subtype glutamate receptors generated by polyamine-mediated ion channel block. *Neuron* 15:453-462.
- Brickley SG, Misra C, Mok MH, Mishina M, Cull-Candy SG (2003) NR2B and NR2D subunits coassemble in cerebellar Golgi cells to form a distinct NMDA receptor subtype restricted to extrasynaptic sites. *J Neurosci* 23:4958-4966.
- Burnashev N, Zhou Z, Neher E, Sakmann B (1995) Fractional calcium currents through recombinant GluR channels of the NMDA, AMPA and kainate receptor subtypes. *J Physiol* 485 (Pt 2):403-418.
- Burnashev N, Schoepfer R, Monyer H, Ruppersberg JP, Gunther W, Seeburg PH, Sakmann B (1992) Control by asparagine residues of calcium permeability and magnesium blockade in the NMDA receptor. *Science* 257:1415-1419.

- Cathala L, Misra C, Cull-Candy S (2000) Developmental profile of the changing properties of NMDA receptors at cerebellar mossy fiber-granule cell synapses. *J Neurosci* 20:5899-5905.
- Chapman AG (2000) Glutamate and epilepsy. *J Nutr* 130:1043S-1045S.
- Chazot PL, Stephenson FA (1997) Molecular dissection of native mammalian forebrain NMDA receptors containing the NR1 C2 exon: direct demonstration of NMDA receptors comprising NR1, NR2A, and NR2B subunits within the same complex. *J Neurochem* 69:2138-2144.
- Chazot PL, Coleman SK, Cik M, Stephenson FA (1994) Molecular characterization of N-methyl-D-aspartate receptors expressed in mammalian cells yields evidence for the coexistence of three subunit types within a discrete receptor molecule. *J Biol Chem* 269:24403-24409.
- Cheffings CM, Colquhoun D (2000) Single channel analysis of a novel NMDA channel from *Xenopus* oocytes expressing recombinant NR1a, NR2A and NR2D subunits. *J Physiol* 526 Pt 3:481-491.
- Chen GQ, Cui C, Mayer ML, Gouaux E (1999a) Functional characterization of a potassium-selective prokaryotic glutamate receptor. *Nature* 402:817-821.
- Chen HS, Lipton SA (1997) Mechanism of memantine block of NMDA-activated channels in rat retinal ganglion cells: uncompetitive antagonism. *J Physiol* 499 (Pt 1):27-46.
- Chen N, Moshaver A, Raymond LA (1997) Differential sensitivity of recombinant N-methyl-D-aspartate receptor subtypes to zinc inhibition. *Mol Pharmacol* 51:1015-1023.
- Chen N, Luo T, Raymond LA (1999b) Subtype-dependence of NMDA receptor channel open probability. *J Neurosci* 19:6844-6854.
- Ciabarra AM, Sullivan JM, Gahn LG, Pecht G, Heinemann S, Sevarino KA (1995) Cloning and characterization of chi-1: a developmentally regulated member of a novel class of the ionotropic glutamate receptor family. *J Neurosci* 15:6498-6508.
- Clark BA, Cull-Candy SG (2002) Activity-dependent recruitment of extrasynaptic NMDA receptor activation at an AMPA receptor-only synapse. *J Neurosci* 22:4428-4436.
- Clark GD, Clifford DB, Zorumski CF (1990) The effect of agonist concentration, membrane voltage and calcium on N-methyl-D-aspartate receptor desensitization. *Neuroscience* 39:787-797.
- Clarke RJ, Johnson JW (2006) NMDA receptor NR2 subunit dependence of the slow component of magnesium unblock. *J Neurosci* 26:5825-5834.
- Clements JD, Lester RA, Tong G, Jahr CE, Westbrook GL (1992) The time course of glutamate in the synaptic cleft. *Science* 258:1498-1501.
- Cline HT, Constantine-Paton M (1990) NMDA receptor agonist and antagonists alter retinal ganglion cell arbor structure in the developing frog retinotectal projection. *J Neurosci* 10:1197-1216.
- Constantine-Paton M, Cline HT (1998) LTP and activity-dependent synaptogenesis: the more alike they are, the more different they become. *Curr Opin Neurobiol* 8:139-148.
- Cormier RJ, Greenwood AC, Connor JA (2001) Bidirectional synaptic plasticity correlated with the magnitude of dendritic calcium transients above a threshold. *J Neurophysiol* 85:399-406.
- Coyle JT, Tsai G, Goff D (2003) Converging evidence of NMDA receptor hypofunction in the pathophysiology of schizophrenia. *Ann N Y Acad Sci* 1003:318-327.

- Cull-Candy S, Brickley S, Farrant M (2001) NMDA receptor subunits: diversity, development and disease. *Curr Opin Neurobiol* 11:327-335.
- Cull-Candy SG, Leszkiewicz DN (2004) Role of distinct NMDA receptor subtypes at central synapses. *Sci STKE* 2004:re16.
- Cull-Candy SG, Brickley SG, Misra C, Feldmeyer D, Momiyama A, Farrant M (1998) NMDA receptor diversity in the cerebellum: identification of subunits contributing to functional receptors. *Neuropharmacology* 37:1369-1380.
- Curtis DR, Phillis JW, Watkins JC (1960) The chemical excitation of spinal neurones by certain acidic amino acids. *J Physiol* 150:656-682.
- D'Angelo E, Rossi P, Taglietti V (1994) Voltage-dependent kinetics of N-methyl-D-aspartate synaptic currents in rat cerebellar granule cells. *Eur J Neurosci* 6:640-645.
- Del Castillo J, Katz B (1957) Interaction at end-plate receptors between different choline derivatives. *Proc R Soc Lond B Biol Sci* 146:369-381.
- Diamond JS (2001) Neuronal glutamate transporters limit activation of NMDA receptors by neurotransmitter spillover on CA1 pyramidal cells. *J Neurosci* 21:8328-8338.
- Dilmore JG, Johnson JW (1998) Open channel block and alteration of N-methyl-D-aspartic acid receptor gating by an analog of phencyclidine. *Biophys J* 75:1801-1816.
- Dingledine R, Borges K, Bowie D, Traynelis SF (1999) The glutamate receptor ion channels. *Pharmacol Rev* 51:7-61.
- Dudel J (1974) Nonlinear voltage dependence of excitatory synaptic current in crayfish muscle. *Pflugers Arch* 352:227-241.
- Dunah AW, Luo J, Wang YH, Yasuda RP, Wolfe BB (1998) Subunit composition of N-methyl-D-aspartate receptors in the central nervous system that contain the NR2D subunit. *Mol Pharmacol* 53:429-437.
- Erisir A, Harris JL (2003) Decline of the critical period of visual plasticity is concurrent with the reduction of NR2B subunit of the synaptic NMDA receptor in layer 4. *J Neurosci* 23:5208-5218.
- Erreger K, Traynelis SF (2005) Allosteric interaction between zinc and glutamate binding domains on NR2A causes desensitization of NMDA receptors. *J Physiol* 569:381-393.
- Erreger K, Dravid SM, Banke TG, Wyllie DJ, Traynelis SF (2005) Subunit-specific gating controls rat NR1/NR2A and NR1/NR2B NMDA channel kinetics and synaptic signalling profiles. *J Physiol* 563:345-358.
- Evans RH, Francis AA, Hunt K, Oakes DJ, Watkins JC (1979) Antagonism of excitatory amino acid-induced responses and of synaptic excitation in the isolated spinal cord of the frog. *Br J Pharmacol* 67:591-603.
- Fayyazuddin A, Villarroel A, Le Goff A, Lerma J, Neyton J (2000) Four residues of the extracellular N-terminal domain of the NR2A subunit control high-affinity Zn²⁺ binding to NMDA receptors. *Neuron* 25:683-694.
- Furukawa H, Gouaux E (2003) Mechanisms of activation, inhibition and specificity: crystal structures of the NMDA receptor NR1 ligand-binding core. *Embo J* 22:2873-2885.
- Furukawa H, Singh SK, Mancusso R, Gouaux E (2005) Subunit arrangement and function in NMDA receptors. *Nature* 438:185-192.
- Gao W, Qian A, Johnson JW (2004) A Single Amino Acid in the M3 Region of NR2A Modifies Block of NMDA Receptors by External Mg²⁺. In: *Biophysics Society 48th Annual Meeting*, pp 1506-Pos. Baltimore, MD.

- Garaschuk O, Schneggenburger R, Schirra C, Tempia F, Konnerth A (1996) Fractional Ca²⁺ currents through somatic and dendritic glutamate receptor channels of rat hippocampal CA1 pyramidal neurones. *J Physiol* 491 (Pt 3):757-772.
- Gibb AJ (2004) NMDA receptor subunit gating--uncovered. *Trends Neurosci* 27:7-10; discussion 10.
- Gibb AJ, Colquhoun D (1992) Activation of N-methyl-D-aspartate receptors by L-glutamate in cells dissociated from adult rat hippocampus. *J Physiol* 456:143-179.
- Giffard RG, Monyer H, Christine CW, Choi DW (1990) Acidosis reduces NMDA receptor activation, glutamate neurotoxicity, and oxygen-glucose deprivation neuronal injury in cortical cultures. *Brain Res* 506:339-342.
- Green GM, Gibb AJ (2001) Characterization of the single-channel properties of NMDA receptors in laminae I and II of the dorsal horn of neonatal rat spinal cord. *Eur J Neurosci* 14:1590-1602.
- Grunze HC, Rainnie DG, Hasselmo ME, Barkai E, Hearn EF, McCarley RW, Greene RW (1996) NMDA-dependent modulation of CA1 local circuit inhibition. *J Neurosci* 16:2034-2043.
- Hardingham GE, Fukunaga Y, Bading H (2002) Extrasynaptic NMDARs oppose synaptic NMDARs by triggering CREB shut-off and cell death pathways. *Nat Neurosci* 5:405-414.
- Hatton CJ, Paoletti P (2005) Modulation of triheteromeric NMDA receptors by N-terminal domain ligands. *Neuron* 46:261-274.
- Hatton CJ, Shelley C, Brydson M, Beeson D, Colquhoun D (2003) Properties of the human muscle nicotinic receptor, and of the slow-channel myasthenic syndrome mutant epsilonL221F, inferred from maximum likelihood fits. *J Physiol* 547:729-760.
- Hayashi T (1954) Effects of sodium glutamate on the nervous system. *Keio J Med* 3:192-193.
- Hestrin S (1992) Developmental regulation of NMDA receptor-mediated synaptic currents at a central synapse. *Nature* 357:686-689.
- Hestrin S, Nicoll RA, Perkel DJ, Sah P (1990) Analysis of excitatory synaptic action in pyramidal cells using whole-cell recording from rat hippocampal slices. *J Physiol* 422:203-225.
- Heynen AJ, Quinlan EM, Bae DC, Bear MF (2000) Bidirectional, activity-dependent regulation of glutamate receptors in the adult hippocampus in vivo. *Neuron* 28:527-536.
- Hille B (2001) *Ion Channels of Excitable Membranes*, Third Edition. Sunderland, MA: Sinauer Associates, Inc.
- Hodgkin AL, Huxley AF (1952a) A quantitative description of membrane current and its application to conduction and excitation in nerve. *J Physiol* 117:500-544.
- Hodgkin AL, Huxley AF (1952b) The dual effect of membrane potential on sodium conductance in the giant axon of *Loligo*. *J Physiol* 116:497-506.
- Hodgkin AL, Huxley AF (1952c) The components of membrane conductance in the giant axon of *Loligo*. *J Physiol* 116:473-496.
- Hodgkin AL, Huxley AF (1952d) Currents carried by sodium and potassium ions through the membrane of the giant axon of *Loligo*. *J Physiol* 116:449-472.
- Hollmann M, Heinemann S (1994) Cloned glutamate receptors. *Annu Rev Neurosci* 17:31-108.
- Hollmann M, Boulter J, Maron C, Beasley L, Sullivan J, Pecht G, Heinemann S (1993) Zinc potentiates agonist-induced currents at certain splice variants of the NMDA receptor. *Neuron* 10:943-954.

- Honey CR, Miljkovic Z, MacDonald JF (1985) Ketamine and phencyclidine cause a voltage-dependent block of responses to L-aspartic acid. *Neurosci Lett* 61:135-139.
- Hrabetova S, Serrano P, Blace N, Tse HW, Skifter DA, Jane DE, Monaghan DT, Sacktor TC (2000) Distinct NMDA receptor subpopulations contribute to long-term potentiation and long-term depression induction. *J Neurosci* 20:RC81.
- Hu B, Zheng F (2005) Molecular determinants of glycine-independent desensitization of NR1/NR2A receptors. *J Pharmacol Exp Ther* 313:563-569.
- Huettner JE, Bean BP (1988) Block of N-methyl-D-aspartate-activated current by the anticonvulsant MK-801: selective binding to open channels. *Proc Natl Acad Sci U S A* 85:1307-1311.
- Husi H, Ward MA, Choudhary JS, Blackstock WP, Grant SG (2000) Proteomic analysis of NMDA receptor-adhesion protein signaling complexes. *Nat Neurosci* 3:661-669.
- Hynd MR, Scott HL, Dodd PR (2004) Glutamate-mediated excitotoxicity and neurodegeneration in Alzheimer's disease. *Neurochem Int* 45:583-595.
- Ikeda K, Araki K, Takayama C, Inoue Y, Yagi T, Aizawa S, Mishina M (1995) Reduced spontaneous activity of mice defective in the epsilon 4 subunit of the NMDA receptor channel. *Brain Res Mol Brain Res* 33:61-71.
- Ikeda K, Nagasawa M, Mori H, Araki K, Sakimura K, Watanabe M, Inoue Y, Mishina M (1992) Cloning and expression of the epsilon 4 subunit of the NMDA receptor channel. *FEBS Lett* 313:34-38.
- Inanobe A, Furukawa H, Gouaux E (2005) Mechanism of Partial Agonist Action at the NR1 Subunit of NMDA Receptors. *Neuron* 47:71-84.
- Ishii T, Moriyoshi K, Sugihara H, Sakurada K, Kadotani H, Yokoi M, Akazawa C, Shigemoto R, Mizuno N, Masu M, et al. (1993) Molecular characterization of the family of the N-methyl-D-aspartate receptor subunits. *J Biol Chem* 268:2836-2843.
- Ito I, Kawakami R, Sakimura K, Mishina M, Sugiyama H (2000) Input-specific targeting of NMDA receptor subtypes at mouse hippocampal CA3 pyramidal neuron synapses. *Neuropharmacology* 39:943-951.
- Ito I, Futai K, Katagiri H, Watanabe M, Sakimura K, Mishina M, Sugiyama H (1997) Synapse-selective impairment of NMDA receptor functions in mice lacking NMDA receptor epsilon 1 or epsilon 2 subunit. *J Physiol* 500 (Pt 2):401-408.
- Iwasato T, Erzurumlu RS, Huerta PT, Chen DF, Sasaoka T, Ulupinar E, Tonegawa S (1997) NMDA receptor-dependent refinement of somatotopic maps. *Neuron* 19:1201-1210.
- Jahr CE, Stevens CF (1987) Glutamate activates multiple single channel conductances in hippocampal neurons. *Nature* 325:522-525.
- Jahr CE, Stevens CF (1990a) A quantitative description of NMDA receptor-channel kinetic behavior. *J Neurosci* 10:1830-1837.
- Jahr CE, Stevens CF (1990b) Voltage dependence of NMDA-activated macroscopic conductances predicted by single-channel kinetics. *J Neurosci* 10:3178-3182.
- Jin R, Gouaux E (2003) Probing the function, conformational plasticity, and dimer-dimer contacts of the GluR2 ligand-binding core: studies of 5-substituted willardiines and GluR2 S1S2 in the crystal. *Biochemistry* 42:5201-5213.
- Jin R, Banke TG, Mayer ML, Traynelis SF, Gouaux E (2003) Structural basis for partial agonist action at ionotropic glutamate receptors. *Nat Neurosci* 6:803-810.
- Johnson JW, Ascher P (1987) Glycine potentiates the NMDA response in cultured mouse brain neurons. *Nature* 325:529-531.

- Johnson JW, Qian A (2002) Interaction between channel blockers and channel gating of NMDA receptors. *Biological Membranes* 19:17-22.
- Jonas P, Sakmann B (1992) Glutamate receptor channels in isolated patches from CA1 and CA3 pyramidal cells of rat hippocampal slices. *J Physiol* 455:143-171.
- Jones KS, VanDongen HM, VanDongen AM (2002) The NMDA receptor M3 segment is a conserved transduction element coupling ligand binding to channel opening. *J Neurosci* 22:2044-2053.
- Jones S, Gibb AJ (2005) Functional NR2B- and NR2D-containing NMDA receptor channels in rat substantia nigra dopaminergic neurones. *J Physiol* 569:209-221.
- Kadotani H, Hirano T, Masugi M, Nakamura K, Nakao K, Katsuki M, Nakanishi S (1996) Motor discoordination results from combined gene disruption of the NMDA receptor NR2A and NR2C subunits, but not from single disruption of the NR2A or NR2C subunit. *J Neurosci* 16:7859-7867.
- Kampa BM, Clements J, Jonas P, Stuart GJ (2004) Kinetics of Mg²⁺ unblock of NMDA receptors: implications for spike-timing dependent synaptic plasticity. *J Physiol* 556:337-345.
- Kashiwagi K, Masuko T, Nguyen CD, Kuno T, Tanaka I, Igarashi K, Williams K (2002) Channel blockers acting at N-methyl-D-aspartate receptors: differential effects of mutations in the vestibule and ion channel pore. *Mol Pharmacol* 61:533-545.
- Katz B, Miledi R (1972) The statistical nature of the acetylcholine potential and its molecular components. *J Physiol* 224:665-699.
- Keller BU, Konnerth A, Yaari Y (1991) Patch clamp analysis of excitatory synaptic currents in granule cells of rat hippocampus. *J Physiol* 435:275-293.
- Kew JN, Kemp JA (1998) An allosteric interaction between the NMDA receptor polyamine and ifenprodil sites in rat cultured cortical neurones. *J Physiol* 512 (Pt 1):17-28.
- Kim MJ, Dunah AW, Wang YT, Sheng M (2005) Differential Roles of NR2A- and NR2B-Containing NMDA Receptors in Ras-ERK Signaling and AMPA Receptor Trafficking. *Neuron* 46:745-760.
- Kleckner NW, Dingledine R (1988) Requirement for glycine in activation of NMDA-receptors expressed in *Xenopus* oocytes. *Science* 241:835-837.
- Koch K (1999) *Biophysics of Computation*. Oxford: Oxford University Press.
- Kohda K, Wang Y, Yuzaki M (2000) Mutation of a glutamate receptor motif reveals its role in gating and delta2 receptor channel properties. *Nat Neurosci* 3:315-322.
- Kohr G, Jensen V, Koester HJ, Mihaljevic AL, Utvik JK, Kvellø A, Ottersen OP, Seeburg PH, Sprengel R, Hvalby O (2003) Intracellular domains of NMDA receptor subtypes are determinants for long-term potentiation induction. *J Neurosci* 23:10791-10799.
- Komuro H, Rakic P (1993) Modulation of neuronal migration by NMDA receptors. *Science* 260:95-97.
- Konnerth A, Keller BU, Ballanyi K, Yaari Y (1990) Voltage sensitivity of NMDA-receptor mediated postsynaptic currents. *Exp Brain Res* 81:209-212.
- Krupp JJ, Vissel B, Heinemann SF, Westbrook GL (1996) Calcium-dependent inactivation of recombinant N-methyl-D-aspartate receptors is NR2 subunit specific. *Mol Pharmacol* 50:1680-1688.
- Krupp JJ, Vissel B, Heinemann SF, Westbrook GL (1998) N-terminal domains in the NR2 subunit control desensitization of NMDA receptors. *Neuron* 20:317-327.

- Krupp JJ, Vissel B, Thomas CG, Heinemann SF, Westbrook GL (1999) Interactions of calmodulin and alpha-actinin with the NR1 subunit modulate Ca²⁺-dependent inactivation of NMDA receptors. *J Neurosci* 19:1165-1178.
- Kumar SS, Huguenard JR (2003) Pathway-specific differences in subunit composition of synaptic NMDA receptors on pyramidal neurons in neocortex. *J Neurosci* 23:10074-10083.
- Kuner T, Schoepfer R (1996) Multiple structural elements determine subunit specificity of Mg²⁺ block in NMDA receptor channels. *J Neurosci* 16:3549-3558.
- Kuner T, Wollmuth LP, Karlin A, Seeburg PH, Sakmann B (1996) Structure of the NMDA receptor channel M2 segment inferred from the accessibility of substituted cysteines. *Neuron* 17:343-352.
- Kutsuwada T, Kashiwabuchi N, Mori H, Sakimura K, Kushiya E, Araki K, Meguro H, Masaki H, Kumanishi T, Arakawa M, et al. (1992) Molecular diversity of the NMDA receptor channel. *Nature* 358:36-41.
- Larkum ME, Kaiser KM, Sakmann B (1999) Calcium electrogenesis in distal apical dendrites of layer 5 pyramidal cells at a critical frequency of back-propagating action potentials. *Proc Natl Acad Sci U S A* 96:14600-14604.
- Laurie DJ, Seeburg PH (1994) Regional and developmental heterogeneity in splicing of the rat brain NMDAR1 mRNA. *J Neurosci* 14:3180-3194.
- Laurie DJ, Putzke J, Zieglgansberger W, Seeburg PH, Tolle TR (1995) The distribution of splice variants of the NMDAR1 subunit mRNA in adult rat brain. *Brain Res Mol Brain Res* 32:94-108.
- Legendre P (1999) Voltage dependence of the glycine receptor-channel kinetics in the zebrafish hindbrain. *J Neurophysiol* 82:2120-2129.
- Legendre P, Rosenmund C, Westbrook GL (1993) Inactivation of NMDA channels in cultured hippocampal neurons by intracellular calcium. *J Neurosci* 13:674-684.
- Leonard AS, Lim IA, Hemsworth DE, Horne MC, Hell JW (1999) Calcium/calmodulin-dependent protein kinase II is associated with the N-methyl-D-aspartate receptor. *Proc Natl Acad Sci U S A* 96:3239-3244.
- Li-Smerin Y, Johnson JW (1996) Effects of intracellular Mg²⁺ on channel gating and steady-state responses of the NMDA receptor in cultured rat neurons. *J Physiol* 491 (Pt 1):137-150.
- Li-Smerin Y, Aizenman E, Johnson JW (2000) Inhibition by intracellular Mg(2+) of recombinant N-methyl-D-aspartate receptors expressed in Chinese hamster ovary cells. *J Pharmacol Exp Ther* 292:1104-1110.
- Li-Smerin Y, Levitan ES, Johnson JW (2001) Free intracellular Mg(2+) concentration and inhibition of NMDA responses in cultured rat neurons. *J Physiol* 533:729-743.
- Li JH, Wang YH, Wolfe BB, Krueger KE, Corsi L, Stocca G, Vicini S (1998) Developmental changes in localization of NMDA receptor subunits in primary cultures of cortical neurons. *Eur J Neurosci* 10:1704-1715.
- Li Q, Clark S, Lewis DV, Wilson WA (2002) NMDA receptor antagonists disinhibit rat posterior cingulate and retrosplenial cortices: a potential mechanism of neurotoxicity. *J Neurosci* 22:3070-3080.
- Li Y, Erzurumlu RS, Chen C, Jhaveri S, Tonegawa S (1994) Whisker-related neuronal patterns fail to develop in the trigeminal brainstem nuclei of NMDAR1 knockout mice. *Cell* 76:427-437.

- Lisman JE, McIntyre CC (2001) Synaptic plasticity: a molecular memory switch. *Curr Biol* 11:R788-791.
- Liu L, Wong TP, Pozza MF, Lingenhoehl K, Wang Y, Sheng M, Auberson YP, Wang YT (2004) Role of NMDA receptor subtypes in governing the direction of hippocampal synaptic plasticity. *Science* 304:1021-1024.
- Lleo A, Greenberg SM, Growdon JH (2006) Current pharmacotherapy for Alzheimer's disease. *Annu Rev Med* 57:513-533.
- Low CM, Zheng F, Lyuboslavsky P, Traynelis SF (2000) Molecular determinants of coordinated proton and zinc inhibition of N-methyl-D-aspartate NR1/NR2A receptors. *Proc Natl Acad Sci U S A* 97:11062-11067.
- Luo J, Wang Y, Yasuda RP, Dunah AW, Wolfe BB (1997) The majority of N-methyl-D-aspartate receptor complexes in adult rat cerebral cortex contain at least three different subunits (NR1/NR2A/NR2B). *Mol Pharmacol* 51:79-86.
- MacDonald JF, Bartlett MC, Mody I, Pahapill P, Reynolds JN, Salter MW, Schneiderman JH, Pennefather PS (1991) Actions of ketamine, phencyclidine and MK-801 on NMDA receptor currents in cultured mouse hippocampal neurones. *J Physiol* 432:483-508.
- Magee JC, Johnston D (1997) A synaptically controlled, associative signal for Hebbian plasticity in hippocampal neurons. *Science* 275:209-213.
- Magleby KL, Stevens CF (1972) A quantitative description of end-plate currents. *J Physiol* 223:173-197.
- Malenka RC, Bear MF (2004) LTP and LTD; An Embarrassment of Riches. *Neuron* 44:5-21.
- Mallon AP, Auberson YP, Stone TW (2005) Selective subunit antagonists suggest an inhibitory relationship between NR2B and NR2A-subunit containing N-methyl-D-aspartate receptors in hippocampal slices. *Exp Brain Res* 162:374-383.
- Marchais D, Marty A (1979) Interaction of permeant ions with channels activated by acetylcholine in *Aplysia* neurones. *J Physiol* 297:9-45.
- Markram H, Lubke J, Frotscher M, Sakmann B (1997) Regulation of synaptic efficacy by coincidence of postsynaptic APs and EPSPs. *Science* 275:213-215.
- Massey PV, Johnson BE, Moulton PR, Auberson YP, Brown MW, Molnar E, Collingridge GL, Bashir ZI (2004) Differential roles of NR2A and NR2B-containing NMDA receptors in cortical long-term potentiation and long-term depression. *J Neurosci* 24:7821-7828.
- Matsuda K, Kamiya Y, Matsuda S, Yuzaki M (2002) Cloning and characterization of a novel NMDA receptor subunit NR3B: a dominant subunit that reduces calcium permeability. *Brain Res Mol Brain Res* 100:43-52.
- Matsuda K, Fletcher M, Kamiya Y, Yuzaki M (2003) Specific assembly with the NMDA receptor 3B subunit controls surface expression and calcium permeability of NMDA receptors. *J Neurosci* 23:10064-10073.
- Mayadevi M, Praseeda M, Kumar KS, Omkumar RV (2002) Sequence determinants on the NR2A and NR2B subunits of NMDA receptor responsible for specificity of phosphorylation by CaMKII. *Biochim Biophys Acta* 1598:40-45.
- Mayer ML, Armstrong N (2004) Structure and function of glutamate receptor ion channels. *Annu Rev Physiol* 66:161-181.
- Mayer ML, Westbrook GL, Guthrie PB (1984) Voltage-dependent block by Mg²⁺ of NMDA responses in spinal cord neurones. *Nature* 309:261-263.
- Mayer ML, Vyklicky L, Jr., Clements J (1989) Regulation of NMDA receptor desensitization in mouse hippocampal neurons by glycine. *Nature* 338:425-427.

- Mayer ML, MacDermott AB, Westbrook GL, Smith SJ, Barker JL (1987) Agonist- and voltage-gated calcium entry in cultured mouse spinal cord neurons under voltage clamp measured using arsenazo III. *J Neurosci* 7:3230-3244.
- McCulloch RM, Johnston GA, Game CJ, Curtis DR (1974) The differential sensitivity of spinal interneurons and Renshaw cells to Kainate and N-methyl-D-aspartate. *Exp Brain Res* 21:515-518.
- Meldrum BS (1992) Excitatory amino acid receptors and disease. *Curr Opin Neurol Neurosurg* 5:508-513.
- Misra C, Brickley SG, Farrant M, Cull-Candy SG (2000) Identification of subunits contributing to synaptic and extrasynaptic NMDA receptors in Golgi cells of the rat cerebellum. *J Physiol* 524 Pt 1:147-162.
- Moghaddam B (2003) Bringing order to the glutamate chaos in schizophrenia. *Neuron* 40:881-884.
- Moghaddam B, Jackson ME (2003) Glutamatergic animal models of schizophrenia. *Ann N Y Acad Sci* 1003:131-137.
- Momiyama A, Feldmeyer D, Cull-Candy SG (1996) Identification of a native low-conductance NMDA channel with reduced sensitivity to Mg²⁺ in rat central neurones. *J Physiol* 494 (Pt 2):479-492.
- Monyer H, Burnashev N, Laurie DJ, Sakmann B, Seeburg PH (1994) Developmental and regional expression in the rat brain and functional properties of four NMDA receptors. *Neuron* 12:529-540.
- Monyer H, Sprengel R, Schoepfer R, Herb A, Higuchi M, Lomeli H, Burnashev N, Sakmann B, Seeburg PH (1992) Heteromeric NMDA receptors: molecular and functional distinction of subtypes. *Science* 256:1217-1221.
- Mori H, Masaki H, Yamakura T, Mishina M (1992) Identification by mutagenesis of a Mg(2+)-block site of the NMDA receptor channel. *Nature* 358:673-675.
- Mori H, Manabe T, Watanabe M, Satoh Y, Suzuki N, Toki S, Nakamura K, Yagi T, Kushiya E, Takahashi T, Inoue Y, Sakimura K, Mishina M (1998) Role of the carboxy-terminal region of the GluR epsilon2 subunit in synaptic localization of the NMDA receptor channel. *Neuron* 21:571-580.
- Moriyoshi K, Masu M, Ishii T, Shigemoto R, Mizuno N, Nakanishi S (1991) Molecular cloning and characterization of the rat NMDA receptor. *Nature* 354:31-37.
- Morris BJ, Cochran SM, Pratt JA (2005) PCP: from pharmacology to modelling schizophrenia. *Curr Opin Pharmacol* 5:101-106.
- Nahum-Levy R, Tam E, Shavit S, Benveniste M (2002) Glutamate but not glycine agonist affinity for NMDA receptors is influenced by small cations. *J Neurosci* 22:2550-2560.
- Nakanishi S (1992) Molecular diversity of the glutamate receptors. *Clin Neuropharmacol* 15 Suppl 1 Pt A:4A-5A.
- Neyton J, Paoletti P (2006) Relating NMDA receptor function to receptor subunit composition: limitations of the pharmacological approach. *J Neurosci* 26:1331-1333.
- Nishi M, Hinds H, Lu HP, Kawata M, Hayashi Y (2001) Motoneuron-specific expression of NR3B, a novel NMDA-type glutamate receptor subunit that works in a dominant-negative manner. *J Neurosci* 21:RC185.
- Nowak L, Bregestovski P, Ascher P, Herbert A, Prochiantz A (1984) Magnesium gates glutamate-activated channels in mouse central neurones. *Nature* 307:462-465.

- Nowak LM, Wright JM (1992) Slow voltage-dependent changes in channel open-state probability underlie hysteresis of NMDA responses in Mg(2+)-free solutions. *Neuron* 8:181-187.
- O'Hara PJ, Sheppard PO, Thogersen H, Venezia D, Haldeman BA, McGrane V, Houamed KM, Thomsen C, Gilbert TL, Mulvihill ER (1993) The ligand-binding domain in metabotropic glutamate receptors is related to bacterial periplasmic binding proteins. *Neuron* 11:41-52.
- Onodera K, Takeuchi A (1978) Effects of membrane potential and temperature on the excitatory post-synaptic current in the crayfish muscle. *J Physiol* 276:183-192.
- Paoletti P, Neyton J, Ascher P (1995) Glycine-independent and subunit-specific potentiation of NMDA responses by extracellular Mg²⁺. *Neuron* 15:1109-1120.
- Paoletti P, Perin-Dureau F, Fayyazuddin A, Le Goff A, Callebaut I, Neyton J (2000) Molecular organization of a zinc binding n-terminal modulatory domain in a NMDA receptor subunit. *Neuron* 28:911-925.
- Patneau DK, Vyklicky L, Jr., Mayer ML (1993) Hippocampal neurons exhibit cyclothiazide-sensitive rapidly desensitizing responses to kainate. *J Neurosci* 13:3496-3509.
- Perez-Otano I, Schulteis CT, Contractor A, Lipton SA, Trimmer JS, Sucher NJ, Heinemann SF (2001) Assembly with the NR1 subunit is required for surface expression of NR3A-containing NMDA receptors. *J Neurosci* 21:1228-1237.
- Polsky A, Mel BW, Schiller J (2004) Computational subunits in thin dendrites of pyramidal cells. *Nat Neurosci* 7:621-627.
- Popescu G, Auerbach A (2003) Modal gating of NMDA receptors and the shape of their synaptic response. *Nat Neurosci* 6:476-483.
- Popescu G, Robert A, Howe JR, Auerbach A (2004) Reaction mechanism determines NMDA receptor response to repetitive stimulation. *Nature* 430:790-793.
- Premkumar LS, Auerbach A (1996) Identification of a high affinity divalent cation binding site near the entrance of the NMDA receptor channel. *Neuron* 16:869-880.
- Premkumar LS, Qin F, Auerbach A (1997) Subconductance states of a mutant NMDA receptor channel kinetics, calcium, and voltage dependence. *J Gen Physiol* 109:181-189.
- Qian A, Johnson JW (2002) Channel gating of NMDA receptors. *Physiol Behav* 77:577-582.
- Qian A, Antonov SM, Johnson JW (2002) Modulation by permeant ions of Mg(2+) inhibition of NMDA-activated whole-cell currents in rat cortical neurons. *J Physiol* 538:65-77.
- Qian A, Buller AL, Johnson JW (2005) NR2 subunit-dependence of NMDA receptor channel block by external Mg²⁺. *J Physiol* 562:319-331.
- Raman IM, Trussell LO (1995) Concentration-jump analysis of voltage-dependent conductances activated by glutamate and kainate in neurons of the avian cochlear nucleus. *Biophys J* 69:1868-1879.
- Ramoas AS, Mower AF, Liao D, Jafri SI (2001) Suppression of cortical NMDA receptor function prevents development of orientation selectivity in the primary visual cortex. *J Neurosci* 21:4299-4309.
- Rhodes P (2006) The properties and implications of NMDA spikes in neocortical pyramidal cells. *J Neurosci* 26:6704-6715.
- Rosenmund C, Westbrook GL (1993a) Rundown of N-methyl-D-aspartate channels during whole-cell recording in rat hippocampal neurons: role of Ca²⁺ and ATP. *J Physiol* 470:705-729.
- Rosenmund C, Westbrook GL (1993b) Calcium-induced actin depolymerization reduces NMDA channel activity. *Neuron* 10:805-814.

- Sather W, Johnson JW, Henderson G, Ascher P (1990) Glycine-insensitive desensitization of NMDA responses in cultured mouse embryonic neurons. *Neuron* 4:725-731.
- Sather W, Dieudonne S, MacDonald JF, Ascher P (1992) Activation and desensitization of N-methyl-D-aspartate receptors in nucleated outside-out patches from mouse neurones. *J Physiol* 450:643-672.
- Schiller J, Major G, Koester HJ, Schiller Y (2000) NMDA spikes in basal dendrites of cortical pyramidal neurons. *Nature* 404:285-289.
- Schneggenburger R (1996) Simultaneous measurement of Ca²⁺ influx and reversal potentials in recombinant N-methyl-D-aspartate receptor channels. *Biophys J* 70:2165-2174.
- Schneggenburger R, Zhou Z, Konnerth A, Neher E (1993) Fractional contribution of calcium to the cation current through glutamate receptor channels. *Neuron* 11:133-143.
- Schorge S, Colquhoun D (2003) Studies of NMDA receptor function and stoichiometry with truncated and tandem subunits. *J Neurosci* 23:1151-1158.
- Schorge S, Elenes S, Colquhoun D (2005) Maximum likelihood fitting of single channel NMDA activity with a mechanism composed of independent dimers of subunits. *J Physiol*.
- Scimemi A, Fine A, Kullmann DM, Rusakov DA (2004) NR2B-containing receptors mediate cross talk among hippocampal synapses. *J Neurosci* 24:4767-4777.
- Shapiro M (2001) Plasticity, hippocampal place cells, and cognitive maps. *Arch Neurol* 58:874-881.
- Sharma G, Stevens CF (1996) Interactions between two divalent ion binding sites in N-methyl-D-aspartate receptor channels. *Proc Natl Acad Sci U S A* 93:14170-14175.
- Shelley C, Colquhoun D (2005) A human congenital myasthenia-causing mutation (epsilon L78P) of the muscle nicotinic acetylcholine receptor with unusual single channel properties. *J Physiol* 564:377-396.
- Sheng M (2001) Molecular organization of the postsynaptic specialization. *Proc Natl Acad Sci U S A* 98:7058-7061.
- Sheng M, Pak DT (2000) Ligand-gated ion channel interactions with cytoskeletal and signaling proteins. *Annu Rev Physiol* 62:755-778.
- Sheng M, Cummings J, Roldan LA, Jan YN, Jan LY (1994) Changing subunit composition of heteromeric NMDA receptors during development of rat cortex. *Nature* 368:144-147.
- Sobolevsky AI, Yelshansky MV (2000) The trapping block of NMDA receptor channels in acutely isolated rat hippocampal neurones. *J Physiol* 526 Pt 3:493-506.
- Sobolevsky AI, Koshelev SG, Khodorov BI (1999) Probing of NMDA channels with fast blockers. *J Neurosci* 19:10611-10626.
- Sobolevsky AI, Beck C, Wollmuth LP (2002) Molecular rearrangements of the extracellular vestibule in NMDAR channels during gating. *Neuron* 33:75-85.
- Sonkusare SK, Kaul CL, Ramarao P (2005) Dementia of Alzheimer's disease and other neurodegenerative disorders--memantine, a new hope. *Pharmacol Res* 51:1-17.
- Sprengel R, Suchanek B, Amico C, Brusa R, Burnashev N, Rozov A, Hvalby O, Jensen V, Paulsen O, Andersen P, Kim JJ, Thompson RF, Sun W, Webster LC, Grant SG, Eilers J, Konnerth A, Li J, McNamara JO, Seeburg PH (1998) Importance of the intracellular domain of NR2 subunits for NMDA receptor function in vivo. *Cell* 92:279-289.
- Spruston N, Jonas P, Sakmann B (1995) Dendritic glutamate receptor channels in rat hippocampal CA3 and CA1 pyramidal neurons. *J Physiol* 482 (Pt 2):325-352.
- Standaert DG, Landwehrmeyer GB, Kerner JA, Penney JB, Jr., Young AB (1996) Expression of NMDAR2D glutamate receptor subunit mRNA in neurochemically identified

- interneurons in the rat neostriatum, neocortex and hippocampus. *Brain Res Mol Brain Res* 42:89-102.
- Standaert DG, Friberg IK, Landwehrmeyer GB, Young AB, Penney JB, Jr. (1999) Expression of NMDA glutamate receptor subunit mRNAs in neurochemically identified projection and interneurons in the striatum of the rat. *Brain Res Mol Brain Res* 64:11-23.
- Steigerwald F, Schulz TW, Schenker LT, Kennedy MB, Seeburg PH, Kohr G (2000) C-Terminal truncation of NR2A subunits impairs synaptic but not extrasynaptic localization of NMDA receptors. *J Neurosci* 20:4573-4581.
- Stern P, Behe P, Schoepfer R, Colquhoun D (1992) Single-channel conductances of NMDA receptors expressed from cloned cDNAs: comparison with native receptors. *Proc R Soc Lond B Biol Sci* 250:271-277.
- Strack S, Colbran RJ (1998) Autophosphorylation-dependent targeting of calcium/ calmodulin-dependent protein kinase II by the NR2B subunit of the N-methyl- D-aspartate receptor. *J Biol Chem* 273:20689-20692.
- Sundstrom E, Whittemore S, Mo LL, Seiger A (1997) Analysis of NMDA receptors in the human spinal cord. *Exp Neurol* 148:407-413.
- Tang CM, Dichter M, Morad M (1990) Modulation of the N-methyl-D-aspartate channel by extracellular H⁺. *Proc Natl Acad Sci U S A* 87:6445-6449.
- Tang YP, Shimizu E, Dube GR, Rampon C, Kerchner GA, Zhuo M, Liu G, Tsien JZ (1999) Genetic enhancement of learning and memory in mice. *Nature* 401:63-69.
- Toth K, McBain CJ (1998) Afferent-specific innervation of two distinct AMPA receptor subtypes on single hippocampal interneurons. *Nat Neurosci* 1:572-578.
- Tour O, Parnas H, Parnas I (1998) Depolarization increases the single-channel conductance and the open probability of crayfish glutamate channels. *Biophys J* 74:1767-1778.
- Tovar KR, Westbrook GL (1999) The incorporation of NMDA receptors with a distinct subunit composition at nascent hippocampal synapses in vitro. *J Neurosci* 19:4180-4188.
- Toyoda H, Zhao MG, Zhuo M (2005) Roles of NMDA receptor NR2A and NR2B subtypes for long-term depression in the anterior cingulate cortex. *Eur J Neurosci* 22:485-494.
- Traynelis SF, Cull-Candy SG (1990) Proton inhibition of N-methyl-D-aspartate receptors in cerebellar neurons. *Nature* 345:347-350.
- Traynelis SF, Hartley M, Heinemann SF (1995) Control of proton sensitivity of the NMDA receptor by RNA splicing and polyamines. *Science* 268:873-876.
- Traynelis SF, Burgess MF, Zheng F, Lyuboslavsky P, Powers JL (1998) Control of voltage-independent zinc inhibition of NMDA receptors by the NR1 subunit. *J Neurosci* 18:6163-6175.
- Tsai G, Coyle JT (2002) Glutamatergic mechanisms in schizophrenia. *Annu Rev Pharmacol Toxicol* 42:165-179.
- Tsien JZ (2000) Linking Hebb's coincidence-detection to memory formation. *Curr Opin Neurobiol* 10:266-273.
- Vargas-Caballero M, Robinson HP (2003) A slow fraction of Mg²⁺ unblock of NMDA receptors limits their contribution to spike generation in cortical pyramidal neurons. *J Neurophysiol* 89:2778-2783.
- Vargas-Caballero M, Robinson HPC (2004) Fast and Slow Voltage-Dependent Dynamics of Magnesium Block in the NMDA Receptor: The Asymmetric Trapping Block Model. *J Neurosci* 24:6171-6180.

- Vicini S, Wang JF, Li JH, Zhu WJ, Wang YH, Luo JH, Wolfe BB, Grayson DR (1998) Functional and pharmacological differences between recombinant N-methyl-D-aspartate receptors. *J Neurophysiol* 79:555-566.
- Villarroel A, Regalado MP, Lerma J (1998) Glycine-independent NMDA receptor desensitization: localization of structural determinants. *Neuron* 20:329-339.
- Watanabe J, Beck C, Kuner T, Premkumar LS, Wollmuth LP (2002) DRPEER: a motif in the extracellular vestibule conferring high Ca²⁺ flux rates in NMDA receptor channels. *J Neurosci* 22:10209-10216.
- Watkins JC, Evans RH (1981) Excitatory amino acid transmitters. *Annu Rev Pharmacol Toxicol* 21:165-204.
- Weitlauf C, Honse Y, Auberson YP, Mishina M, Lovinger DM, Winder DG (2005) Activation of NR2A-containing NMDA receptors is not obligatory for NMDA receptor-dependent long-term potentiation. *J Neurosci* 25:8386-8390.
- Wenzel A, Villa M, Mohler H, Benke D (1996) Developmental and regional expression of NMDA receptor subtypes containing the NR2D subunit in rat brain. *J Neurochem* 66:1240-1248.
- Williams K (1993) Ifenprodil discriminates subtypes of the N-methyl-D-aspartate receptor: selectivity and mechanisms at recombinant heteromeric receptors. *Mol Pharmacol* 44:851-859.
- Wollmuth LP, Sakmann B (1998) Different mechanisms of Ca²⁺ transport in NMDA and Ca²⁺-permeable AMPA glutamate receptor channels. *J Gen Physiol* 112:623-636.
- Wollmuth LP, Sobolevsky AI (2004) Structure and gating of the glutamate receptor ion channel. *Trends Neurosci* 27:321-328.
- Wollmuth LP, Kuner T, Sakmann B (1998) Adjacent asparagines in the NR2-subunit of the NMDA receptor channel control the voltage-dependent block by extracellular Mg²⁺. *J Physiol* 506 (Pt 1):13-32.
- Wyllie DJ, Behe P, Colquhoun D (1998) Single-channel activations and concentration jumps: comparison of recombinant NR1a/NR2A and NR1a/NR2D NMDA receptors. *J Physiol* 510 (Pt 1):1-18.
- Wyllie DJ, Behe P, Nassar M, Schoepfer R, Colquhoun D (1996) Single-channel currents from recombinant NMDA NR1a/NR2D receptors expressed in *Xenopus* oocytes. *Proc R Soc Lond B Biol Sci* 263:1079-1086.
- Yu XM, Askalan R, Keil GJ, 2nd, Salter MW (1997) NMDA channel regulation by channel-associated protein tyrosine kinase Src. *Science* 275:674-678.
- Yuan H, Erreger K, Dravid SM, Traynelis SF (2005) Conserved structural and functional control of N-methyl-D-aspartate receptor gating by transmembrane domain M3. *J Biol Chem* 280:29708-29716.
- Zeron MM, Hansson O, Chen N, Wellington CL, Leavitt BR, Brundin P, Hayden MR, Raymond LA (2002) Increased sensitivity to N-methyl-D-aspartate receptor-mediated excitotoxicity in a mouse model of Huntington's disease. *Neuron* 33:849-860.
- Zhang S, Ehlers MD, Bernhardt JP, Su CT, Haganir RL (1998) Calmodulin mediates calcium-dependent inactivation of N-methyl-D-aspartate receptors. *Neuron* 21:443-453.
- Zheng F, Erreger K, Low CM, Banke T, Lee CJ, Conn PJ, Traynelis SF (2001) Allosteric interaction between the amino terminal domain and the ligand binding domain of NR2A. *Nat Neurosci* 4:894-901.

- Zhu Y, Auerbach A (2001a) K(+) occupancy of the N-methyl-d-aspartate receptor channel probed by Mg(2+) block. *J Gen Physiol* 117:287-298.
- Zhu Y, Auerbach A (2001b) Na(+) occupancy and Mg(2+) block of the n-methyl-d-aspartate receptor channel. *J Gen Physiol* 117:275-286.